2023

Method Development for the Quantification of Heavy Metals in Biological Matrices and Its Application to Clinical and Environmental Samples

Michelle Catherine Gende

LOYOLA UNIVERSITY CHICAGO

METHOD DEVELOPMENT FOR THE QUANTIFICATION OF HEAVY METALS IN BIOLOGICAL MATRICES AND ITS APPLICATION TO CLINICAL AND ENVIRONMENTAL SAMPLES

A DISSERTATION SUBMITTED TO

THE FACULTY OF THE GRADUATE SCHOOL

IN CANDIDACY FOR THE DEGREE OF

DOCTOR OF PHILOSOPHY

PROGRAM IN CHEMISTRY

BY

MICHELLE GENDE

CHICAGO, IL

MAY 2023

ACKNOWLEDGEMENTS

I would like to thank my research advisor Dr. Martina Schmeling. Thank you for taking me under your wing and allowing me to be a member of your research team. I deeply appreciate all the advice and guidance you have given over the past years that have helped me mature as a chemist.

I would like to thank my committee members throughout the years: Dr. Dali Liu, Dr. Alannah Fitch, and Dr. Graham Moran. The advice that was given to me throughout my time at Loyola from each of you has been incredible and I deeply appreciate the interest taken in my growth as a scientist. I am very grateful to Dr. Bruce Gaynes, my final committee member and collaborator. Thank you for everything you have done over the years to help get this project off the ground and for being a pleasure to work with.

I would like to extend my thanks to everyone who has worked with me during my time at Loyola including Allison Leuders for her assistance with many of the experimentation and Alyssa Tovar. I would also like to thank my Loyola family; Jaina Bhayani and Xiolmara Martinez. I will miss our walks and monthly dinners, but I am so thankful of the bond that has been built between us.

This work would not have been possible without the support of my family and friends. Especially, my husband Brad, whose constant encouragement and faith in me never wavered. You are my biggest cheerleader, and I don't tell you enough how much that means to me. My parents Brian and Kathy Lund who sacrificed so much to help me achieve my goals and instilled in me my work ethic. To my in-laws, Bob and Stacey Gende, who also supported me ever since they met me and welcomed me into their family. To my friends, Andy and Molly Sroka. You have been some of my biggest fans and the feeling is mutual. Thank you for being there.

Finally, I would like to thank Loyola University Chicago, the Department of Chemistry and Biochemistry, for the opportunity it has provided me. I would not have been able to further my education without this support and I am, and will always be, incredibly grateful.

To Brad

TABLE OF CONTENTS

LIST OF TABLES

LIST OF FIGURES

LIST OF ABBREVIATIONS

GFAA	Graphite Furnace Atomic Absorption
E. COLI	*Escherichia coli*
ROS	Reactive Oxygen Species
DNA	Deoxyribonucleic Acid
RNA	Ribonucleic Acid
B.C.	Before Christ
EDTA	Ethylenediaminetetraacetic Acid
IHME	Institute for Health Metrics and Evaluation
BAL	British Anti-Lewisite
PPIS	Proton Pump Inhibitors
EPA	Environmental Protection Agency
OSHA	Occupational Safety and Health Administration
FDA	Federal Drug Administration
ATSDR	Agency for Toxic Substances and Disease Registry
NIOSH	National Institute for Occupational Safety and Health
WHO	World Health Organization
DPV	Differential Pulse Voltammetry
IC	Ion Chromatography

ICP-MS	Inductively Coupled Plasma Mass Spectrometry
IR	Infrared Detection
TXRF	Total Reflection X-ray Fluorescence
FAAS	Flame Atomic Absorption Spectrometry
ppm	Parts Per Million
ppb	Parts Per Billion
PSC	Posterior Subcapsular
ECCE	Extracapsular Cataract Extraction
IOL	Intraocular Lens
OFZ	Organelle Free Zone
ATP	Adenine Triphosphate
SHPS	Small heat shock proteins
SOD	Superoxide Dismutase
GSH	Glutathione
NADPH	Nicotinamide Adenine Dinucleotide Phosphate
MTS	Metallothioneins
EC	Extracellular
BMI	Body Mass Index
ECP	*Escherichia Coli* Cell Pellet
MAAD	Microwave Assisted Acid Digestion
CRM	Certified Reference Material
LB	Luria Broth
HCL	Hollow Cathode Lamp

BSS	Buffer Saline Solution
LUMC	Loyola University Medical Center
CCP	Cataract Cell Pellet
D_2	Deuterium Lamp
PTFE	Polytetrafluoroethylene
H_2SO_4	Sulfuric Acid
HNO_3	Nitric Acid
H_2O_2	Hydrogen Peroxide
HEPES	4-(2-hydroxyethyl)-1-piperazineethanesulfonic acid
W	Watts
$NH_4H_2PO_4$	Ammonium dihydrogen phosphate
$Mg(NO_3)_2$	Magnesium nitrate
Pb	Lead
Cd	Cadmium
Cr	Chromium
Cu	Copper
Zn	Zinc
Na	Sodium
Mg	Magnesium
K	Potassium
Ca	Calcium
Mn	Manganese
Fe	Iron

C	Cobalt
Ni	Nickel
Ga	Gallium
MΩ	Megaohms
g	Gram
ng	Nanogram
mg	Milligram
mL	Milliliter
kg	Kilogram
M	MOLAR
mM	Millimolar
v/v	Volume per Volume
mg/kg	Milligram per Kilogram
µg	Microgram
µg/g	Microgram per Gram
LOD	Limit of Detection
LOQ	Limit of Quantification
SD	Standard Deviation
RSD	Relative Standard Deviation
OVAD	Open Vessel Acid Digestion
MAAD	Microwave Assisted Acid Digestion

ABSTRACT

A three-fold approach was taken to develop a method for the detection of heavy metals in different matrices and had to be performed sequentially. The first was to develop a method capable of quantifying lead in complex matrices by graphite furnace atomic absorption (GFAA). The developed method needed to meet specific analytical requirements, namely, to be robust, sensitive, and accurate. Initially, four different sample preparation methods were explored for the quantification of lead using *Escherichia coli* (*E. coli)* as a sample matrix. The sample preparation procedures attempted were acidic dilution, matrix modification, conventional heating digestion, and microwave assisted acid digestion (MAAD). It was determined that MAAD procedure was the optimal method as it had a percent recovery of 99.01 ± 9.46 and a reasonable relative standard deviation of 15.75%.

The second goal of this study was to apply the developed method for the quantification of other analytes. This was successfully applied for the quantification of cadmium, chromium, copper, and zinc in *E. coli* and the percent recoveries for these elements were 109.8 ± 11.62%, 98.66 ± 9.483%, 99.23 ± 4.79%, and 100.3 ± 11.86%, respectively. The accuracy of these measurements was confirmed by analyzing certified reference materials (CRM). This CRM had cadmium chromium, copper, and zinc quantified by a third party, the European Commission. The percent differences between the experimental values determined in this study compared to the reference value was less than 10% for each analyte. Therefore, the MAAD method was

deemed accurate for the analysis of these analyte.

The third goal of this study was to demonstrate the developed method's versatility for the quantification of the analytes in different matrices, namely clinical and environmental samples. The clinical samples successfully analyzed in this study were human cataract lenses, removed during phacoemulsification at Loyola University Medical Center (LUMC). Cataracts are the leading cause of blindness in the world and are caused when the lifelong proteins within the lens start an opacification process. A total of 57 cataract samples were analyzed finding the following averages, $8.99 \times 10^{-2} \pm 8.20 \times 10^{-2}$ μg/g cadmium, 3.32 ± 6.04 μg/g chromium, 3.16 ± 1.83 μg/g copper, 6.57 ± 10.4 μg/g lead, and 35.1 ± 22.6 μg/g zinc. These results were considered accurate based on the previous analysis of CRM, a secondary analysis by total X-ray fluorescence spectrometry (TXRF) and a comparison to previous studies quantifying heavy metals in either normal or cataract lenses. TXRF determined an average for copper to be 3.19 ± 2.32 μg/g, with a relative percent difference of 1.26%. Indicating the difference between the results determined by GFAA and TXRF to be negligible. This served as an example of how the developed method can be utilized for the quantification of heavy metals in a complex matrix.

The environmental samples analyzed in this study were the plant *Daucus Carota,* or "Queen Ann's Lace." A plant naturally growing in the Midwest. This plant was collected from the Calumet industrial corridor, an area set aside within the city of Chicago for industrial uses and documented heavy metal pollution. *Daucus Carota* was collected from three different locations within the Calumet industrial corridor. It was determined that heavy metal bioaccumulation within *Daucus Carota* was dependent upon the location of its collection. Location 1, which was near a series of railways, had the highest concentrations determined for the analyte's cadmium, copper, lead, and zinc while Location 3, close to a sewage treatment

plant, had the highest chromium content. Following a secondary analysis, the TXRF samples concluded that its results for lead and copper were accurate. However, when examining the results for zinc, it was determined that GFAA overestimated the values or TXRF underestimated the values. Since zinc is not considered an environmental pollutant, it could be concluded that the analysis of heavy metal pollutants in environmental samples was successful.

Overall, this study successfully developed an analytical method that can quantify multiple analytes in a wide range of different matrices. The method proved to be accurate, precise, sensitive, selective, and robust for clinical samples in form of cataract cell pellets and biological samples in form of plant tissues.

CHAPTER 1. INTRODUCTION

1.1. Heavy Metals and Health

Heavy metals are often classified as metals having a density greater than 5 g/cm^3. Much of metal toxicity is based on its amount, therefore the assessment of heavy metal concentrations in different matrices is fundamental. In this thesis, a method was developed for the analysis of lead, cadmium, chromium, copper, and zinc in human cataract samples and environmental samples.

1.1.1. Lead

Lead makes up 0.0018% of the earth's crust[1] and has been used throughout history because it has a low melting point and is easily malleable. The first use of lead was documented in ancient Egypt 5,000 years ago.[1] The Romans exploited lead for cosmetics because of its colorful hues as well as a sweetener for wine. The recognition of lead's toxicity dates back as far as the second century B.C. when Greek physician Nikander noticed colic and paralysis following the ingestion of lead.[2] However, this did not deter people from lead usage in food and it was not until the 16th century that Europe banned its use in winemaking.[2] Lead has been greatly reduced from paints, ceramic products, caulking, pipe solder, and gasoline products. However, even with reducing lead in these products, lead poisoning can still occur today as humans are exposed to lead accidentally through drinking water, paint, or industrial uses. Children under the age of six

are at the highest risk for lead poisoning due to dust and chips from deteriorating lead paint on interior surfaces in buildings built before 1978.[3] When exposed, a person will show a large range of symptoms: joint and muscle pain, difficulties with memory or concentration, headache, abdominal pain, with more severe symptoms being high blood pressure, abnormal sperm, or reduced count, as well as miscarriage, stillbirth, or premature birth.[2]

Lead's toxicity can be explained because it is a divalent cation that can bind strongly to sulfhydryl groups in proteins, attributing to the distortion of enzymes, structure of proteins, and the development of endogenous opiate systems.[4] Lead can affect many organs but it interferes most with the central nervous system where it competes with calcium at picomolar concentrations.[5]

If heavy metal poisoning does occur, treatment typically involves administration of a chelator, which binds lead more strongly than the protein sulfhydryl groups bind and is thus excreted from the body. A common compound used to treat lead poisoning is British Anti-Lewisite (BAL), $C_3H_8OS_2$, which contains two sulfide groups that can capture the metal.[6]

Due to lead's toxic nature, different instrumentation has been utilized to detect lead within biological samples some being electrochemical,[7, 8, 9 10] ion chromatography (IC),[11, 12] inductively coupled plasma mass spectrometry (ICP-MS),[13, 14, 15, 16] colorimetric assays,[17, 18, 19] total reflection X-ray fluorescence (TXRF),[20 21 22] flame atomic absorption (FAA),[23, 24, 25] and graphite furnace atomic absorption (GFAA).[26, 27, 28 29]

1.1.2. Cadmium

Cadmium is a rare, naturally occurring element commonly found in ores along with zinc, lead, and copper.[30] It makes up about 5×10^{-5} % of the Earth's crust.[1] Cadmium is utilized in paints as an orange pigment and in batteries in form of NiCd, both of which are major

environmental sources.[6] Cadmium is typically introduced into the environment as a by-product of zinc smelting which puts people living in the vicinity at an elevated risk for cadmium exposure. Cadmium exposure can still happen accidentally, its main route is through ingestion. Cadmium typically bioaccumulates in certain foods such as leafy vegetables, potatoes, grains, seeds, liver, kidneys, crustaceans, and mollusks.[31, 32]

Unlike other metals, cadmium has a long biological half-life of 20-40 years in humans due to its low secretion rate.[33] Long-term cadmium exposure causes skeletal damage and was first documented in Japan during the 1950s. This became known as itai-itai (ouch-ouch) disease. This disease is a combination of osteomalacia and osteoporosis and was caused by cadmium-contaminated water from local rice fields.[30] Cadmium has been classified as a carcinogen for humans since 1993.[31]

The lethal dose for cadmium in human is 2,000 ng/mL,[31] and symptoms after acute ingestion of cadmium consist of abdominal pain, burning sensations, nausea, vomiting, salivation, muscle cramps, vertigo, shock, loss of consciousness and convulsions.[31] These symptoms usually appear within the first 15-30 minutes after ingestion.[31] Cadmium toxicity is determined via urine analysis.[31] Metallothionein protein is used to treat cadmium poisoning since it has many sulfhydryl groups that bind to cadmium. This is an example of chelation therapy as cysteinyl thiol groups have a high binding affinity towards cadmium, which allows cadmium to be excreted through urine.[34, 35]

Cadmium has been detected utilizing multiple different instrumentation such as electrochemical, [8, 10, 36] IC,[11, 12] ICP-MS,[13-16, 37, 38] colorimetric assays,[17, 19] TXRF,[20, 39] FAA,[40, 41] and GFAA.[27, 42, 43, 29]

1.1.3. Chromium

Chromium makes up 0.02% of the Earth's crust and is a more common element than lead and cadmium.[1] Chromium was discovered by French chemist Louis-Nicolas Vauquelin, who would grind up precious stones to explain their color and discover beryllium in the same manner.[44] Chromium is widely implemented in pigments and paints,[44] and for electroplating, corrosion protection, and leather tanning.[6] Due to this, it is a widespread water pollutant and a focus of this study.

Chromium occurs in two dominant oxidation states, Cr(III) and Cr(VI),[6] with Cr(III) being an essential nutrient whereas Cr(VI) being a toxic and carcinogen.[6] Chromate (VI) ion (CrO_4^{2-} or $Cr_2O_7^{2-}$) can enter cells due to its similar structure to the sulfate ion (SO_4^{2-}). Once inside the cell, Cr(VI) reacts with DNA and RNA.[6] It has been reported that cell exposure to Cr(VI) has resulted in the formation of various forms of DNA damages.[45]

Exposure for chromium pollution is through two major routes. The first being exposure in the workplace while the second is consuming contaminated food. Chromium can bioaccumulate in aquatic life, especially in bottom-feeders, and in plants, where it is found primarily within the root.[32] Chromium in form of Cr(VI) impacts the health through inhalation, absorption and ingestion.[32,46] Once in the body, Cr(VI) is reduced to Cr(III) and then excreted in urine within a week.[47] There are a few treatment options but these have not been proven with clinical trials.[48]

Chromium is a difficult metal to monitor as its toxicity is dependent upon its oxidation state. Regardless, chromium has been detected within biological samples from instrumentation such as electrochemical,[49] IC,[50] ICP-MS,[51,52,53] colorimetric,[54,55,56] TXRF,[20,57,21] FAA,[25,58,59] and GFAA.[59,60,61]

1.1.4. Copper

Copper makes up 0.007% of the Earth's crust and occurs naturally in minerals such as copper pyrites or copper glance.[1] Copper was first used about 10,000 years ago in which it was implemented in weapons, tools and medicines.[62] Today the use of copper is widespread on account of its excellent heating and conducting properties. Copper is commonly employed in brewing vats, vacuum pans, soldering irons, stills, heating, and cooling coils, sheets, wires, pipes, and much more.[1, 44] Copper is introduced into the environment mostly by copper pipes as well as additives administered to control algal growth.[63]

Copper is an essential metal and participates in many enzymatic reactions.[44] Copper deficiencies have been linked to diseases such as Wilson's Disease and Menkes Disease. In high doses, copper can cause abdominal pain, hematemesis, melena, jaundice, anorexia, severe thirst, diarrhea, and vomiting associated with erosive gastropathy.[64]

There are a few treatments for copper poisoning. Common treatments include zinc or with chelators such as D-Penicillamina or ethylenediaminetetraacetic acid (EDTA).[64] Copper is one of the elements being analyzed within this study. Instrumentation that have successfully detect copper are the following: electrochemical,[10 65] IC,[11, 66 67] ICP-MS,[13, 37, 52] colorimetric, [19, 68] TXRF,[22 69 21 57 20] FAA,[59 70 71] and GFAA.[27, 59 29 72]

1.1.5. Zinc

Zinc makes up about 0.012% of the earth's crust and is an essential metal. In humans, zinc has been reported in levels between 2-4 g.[1] The first use of zinc was for the production of brass by the Romans but it was not till the 1400s that it was produced in India. Today, the application of zinc is widespread, as zinc oxide is implemented in glass, ceramics, and dyes as

well as in the production of brass, bronze solders, and steel.[1] Zinc pollution is a result of mining, purifying zinc, lead, and cadmium ores, steel production, coal burning, and burning of wastes.[73]

In the past, zinc deficiency has been studied thoroughly as this metal is important for human growth and development. With the increased use of vitamin supplements, zinc toxicity through ingestion has started to become more common as a source for chronic ingestion[74] and can manifest "swayback" syndrome leading to slow progression of neuropathy and anemia with increasing fatigue, spasticity, gait abnormalities, and sensory ataxia.[75] Improper zinc monitoring in industry can put workers at risk. Metalworkers who inhaled zinc are subject to metal fume fever or "zinc shakes" and present with flu-like symptoms such as cough, fever, chills, headache, muscle ache, nausea, and malaise.[75]

Zinc levels in humans are measured from blood samples.[73] There are several treatment therapies designed for zinc toxicity which are dependent upon the route of exposure, however, copper sulfate treatment can be used almost universally. Another option is chelation therapy with calcium disodium edetate ($CaNa_2EDTA$) which has been shown to decrease zinc concentrations in patients.[75]

Zinc is a vitally important co-factor within the body. Therefore, zinc is a focus in this study. The instrumentation that has been successfully utilized for zinc quantification in biological samples are electrochemical,[10 76] IC,[66 67] ICP-MS,[13, 37, 52] colorimetric,[77 78] TXRF,[20 39 57 21 69 22] FAA,[79 80] and GFAA.[81 82]

Human exposure to any of these metals can have detrimental health outcomes thus having a robust chemical measurement process which can detect multiple analytes in different biological matrices is important and the purpose of this work. Table 1 summarizes all analytes of

interest for this study and places these in the context of regulations found within the United States and the World Health Organization (WHO).

Table 1. Summary of limits for metals in food, water, and air

Regulation Agency	Element				
	Cadmium	**Chromium**	**Copper**	**Lead**	**Zinc**
Environmental Protection Agency (EPA)	5 ppb in drinking water[32]	0.1 ppm in drinking water [83]	1.3 ppm in drinking water[84]	15 ppb in drinking water 0.1 ppm in candy 50 ppb in juice[32]	5 ppm in drinking water[73]
Food and Drug Administration (FDA)	5 ppb in bottled drinking water[32]	0.1 ppm in drinking water[32]	1 ppm in drinking water[85]	0.005 ppm in drinking water[85]	5 ppm in drinking water[85]
Occupational Safety and Health Administration (OSHA)	5 μg/m^3 of workplace air for an 8-hour workday, 40-hour workweek[32]	An average 0.0005 – 1 mg/m^3 of workplace air for an 8-hour workday, 40-hour workweek depending on compound[32]	0.1 mg/m^3	50 μg/m^3 for an 8 hour workday, 40 hour workweek[3]	1 mg/ m^3 for $ZnCl_2$ fumes & 5 mg/m^3 for ZnO, 8 hour workday, 40 hour workweek[73]
Recommended Daily Allowance (RDA)	No recommended	Men: 35 mg/day Women: 25 mg/day[86]	Adults: 900 μg/day Children dependent on age: 340 - 900 μg/day[84]	No recommended	Infants: 2-3 mg/day Child: 5-9 mg/day Women: 8 mg/day Men: 11 mg/day[73]
World Health Organization (WHO)	Food: 25 μg/kg of body weight a month Water: 3 ppb[87]	Food: 250 μg/day Water: 0.05 ppm[88]	Food: men: 12 mg/day Women: 10 mg/day Water: 2 ppm[89]	Food: Not Listed Water: 0.01 ppm[90]	Food: 20 mg/day Water: Not Listed[91]

1.2. Instrumentation utilized for the quantification of lead, cadmium, chromium, copper, and zinc

A number of analytical methods are available for the determination of the five heavy metals, including differential pulse voltammetry (DPV), flame atomic absorption (FAA), graphite furnace atomic absorption (GFAA), ion chromatography (IC), inductively coupled plasma mass spectrometer (ICP-MS), colorimetric and total reflection X-ray fluorescence (TXRF). The advantages and disadvantages of the most common methods are listed in Table 2. For this study, GFAA was utilized as it has high sensitivity for lead, cadmium, chromium, copper, and zinc and requires only a few microliters of sample for quantitative analysis.

Table 2. Advantages and disadvantages of instrumentation utilized for trace analysis of heavy metals

Instrumentation	Advantages	Disadvantages
Electrochemical	• Multi-elemental analysis • Low detection limits	• 10 mL sample size • Sample used during analysis
Flame Atomic Absorption	• Quick analysis • Low detection limits for group I metals • Low instrumental maintenance	• 10 mL sample size • Sample combusted during analysis • Limited sensitivity for certain elements • Single elemental analysis
Graphite Furnace Atomic Absorption	• Small sample size • Sensitive (low ng/mL) • Low instrumental maintenance	• Sample combustion during analysis • Sample combusted during analysis • Single elemental analysis
Inductively Coupled Plasma Mass Spectrometer	• Multi-elemental analysis • Small sample size • Sensitive (high pg/mL)	• Sample used during analysis • High instrument maintenance
Ion Chromatography	• Multi-elemental analysis • Small Sample Size	• Use sample in analysis • Sample used during analysis
Total Reflection X-Ray Fluorescence	• Multi-elemental analysis • Small sample size • Sample analysis does not use up sample • Low instrument maintenance	• Limited sensitivity for certain elements • Spectral overlap

1.3.1. Atomic Absorption Spectrometry

The origins of atomic spectrometry can be attributed to Robert Bunsen and Gustav Kirchoff who systematically characterized colors of heated elements with the use of a rudimentary spectroscope to record spectra. By the mid-19th-century, they were able to identify the characteristic spectrum of sodium, lithium, and potassium. This newly found method helped Bunsen discover cesium and rubidium because of their unique emission spectrums.[92] Kirchoff formulated the relationship between emission and absorption stating that any material can emit radiation at a specific wavelength and it can also absorb radiation at the same wavelength.[1] For a long time, the importance of these properties were overlooked and it was not till the late 1950s that these were applied for analytical quantification. Quantification using atomic absorption is only possible due to Beer Lambert's Law which will be discussed further in section 1.3.3.

The commercialization of atomic absorption spectrometers did not occur until the 1960s. The first atomic absorption spectrometer was proposed by Walsh who implied that a flame could be used to radiate atoms for their direct measurement. This was later supported by Alkemade & Milatz who demonstrated that the absorption was related to the concentration of elements introduced in the flame.[93] This was accomplished with a monochromatic light source, sodium discharge lamp, for the detection of sodium.[94] However, flame atomic absorption spectrometry (FAAS) had reported limit of detection in the low parts-per-million (ppm) and large spectral interferences. It was because of these shortcomings that the instrumentation was further developed. One of the biggest breakthroughs for instrumental development was accomplished by L'vov who proposed using a 'graphite crucible.' The implementation of the graphite furnace effectively increased the sensitivity and decreased interferences noticed when using FAAS.[95] In 1968, the first commercially available graphite furnace atomic absorption spectrometer was

available. Since then, much improvement has been made to this type of instrumentation and it has been used to successfully detect heavy metals in environmental,[96-98] food,[98, 99] biological,[96, 97, 98] and clinical samples.[98, 100]

1.3.2. Graphite Furnace Atomic Absorption Instrumentation

An atomic absorption spectrometer consists of two basic components, an optical system for signal measurement and an atomization cell that generates ionized atoms. The optical system is composed of an excitation source, slit, monochromator, and detector. The most common excitation source is a hollow cathode lamp (HCL). A HCL is a line source that emits only at discrete wavelengths. The main components of a HCL are depicted in Figure 1. Typically, a HCL is made of quartz because it is transparent over the wavelengths 200-2,500 nm.[101] The HCL consists of a glass envelope containing a cathode and anode. The glass envelope contains either a quartz or borosilicate end window, the material of the end window is based on the transmittance of the analyte spectral lines. Elements that emit at wavelengths of less than 300 nm, quartz is used while borosilicate is used for higher wavelengths.

The cathode is a metal cup composed of the same element being analyzed. The glass envelope contains an inert gas, typically neon, at low pressure. If the element being analyzed has absorption lines close to that of neon, argon will be used instead. The excitation process in the HCL to produce the emission line occurs over three steps. The first is sputtering, this happens when an electrical potential is applied between the cathode and the anode causing some of the gas atoms (neon or argon) to become ionized. The positively charged gas ions collide with the negatively charged cathode and dislodge individual metal atoms. The second step occurs when the dislodged metal atoms are then excited by the electrical potential. The final step is the

emission of the analytical wavelength.[1] Wavelengths will then continue through the atomization cell and then the analytical wavelength will be further isolated using slits and monochromator.

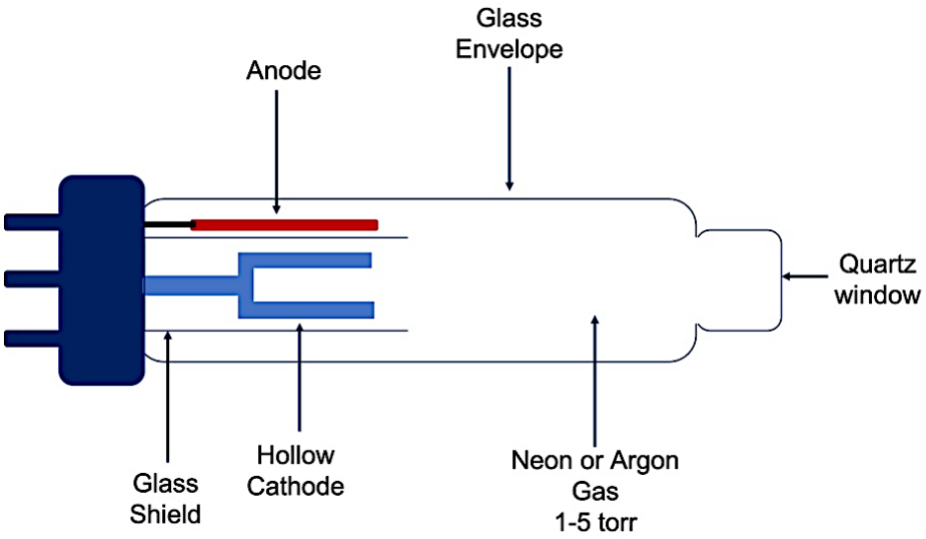

Figure 1. A hollow cathode lamp

The wavelengths will first pass through an entrance slit which is responsible for spectrum resolution and limits the amount of bandwidths for the monochromator.[93] A Czerney-Turner grating monochromator is utilized to isolate analytical wavelength. Light enters the monochromator through the slit and is reflected from a concave mirror, creating parallel rays onto a refraction grating surface. This separates light into multiple wavelengths which are then reflected onto a secondary concave mirror. The second concave mirror focusses a specified wavelength to the exit slit,[102] as shown in Figure 2.

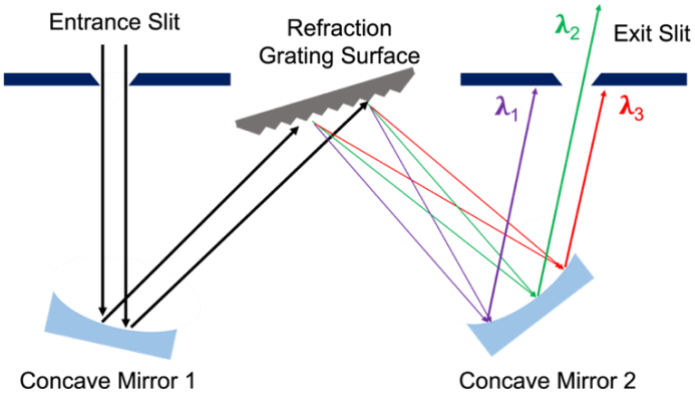

Figure 2. The Czerney-Turner grating monochromator

The isolated wavelength then enters the detector, which can produce an electrical current dependent on the light intensity. Typically, the detector consists of a photomultiplier tube. The photomultiplier tube is responsible for the amplification of the analytical signal. This occurs when the light passes through the input window of the photomultiplier tube. The light then excites electrons in the photocathode emitting photoelectrons. The photoelectrons are then accelerated and focused onto a series of dynodes, with electrons being amplified at each dynode and the signal is collected by an anode. This is now the amplified absorption signal used for analysis.[103] The process is depicted in Figure 3.

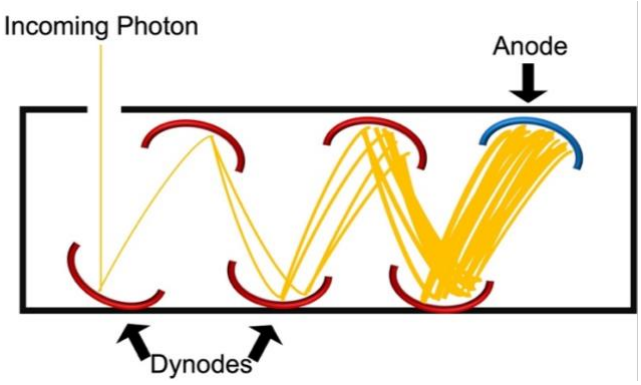

Figure 3. Photomultiplier tube

The heart of the atomic absorption spectrometer is the atomization cell. The first stage is the heating stage which heats the sample to 150°C to remove aqueous residues. This is followed

by the pyrolysis, or ashing, stage which heats the chamber to 800°C to remove organic material without losing the analyte. The third stage is the atomization phase, which is responsible for ionizing the analyte and the absorption measurements. The final stage is the cleaning stage in which the chamber is heated to temperatures higher than 2500°C, removing any residual sample and priming the atomization chamber for the analysis of the next sample.[93, 95] The process is depicted in Figure 4.

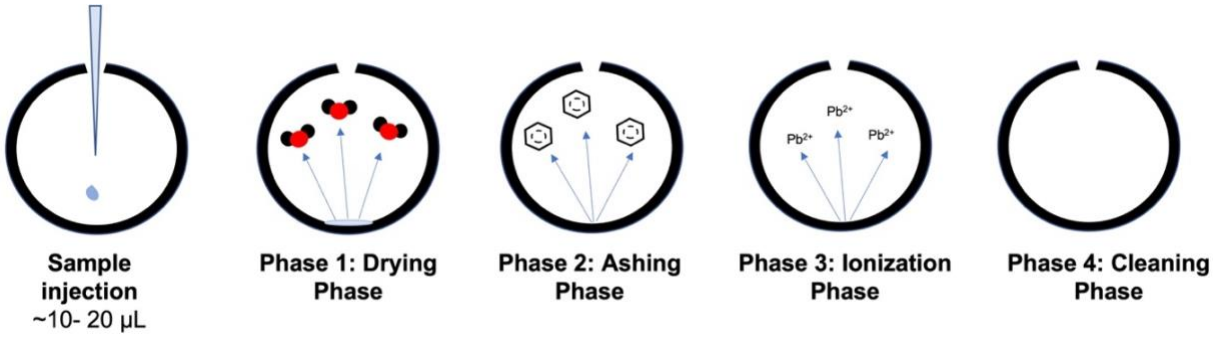

Figure 4. The temperature program applied within the atomization chamber

Background correction is necessary for graphite furnace atomic absorption spectrometry. Different background correction methods were developed, but in the instrumentation used for this study, background correction is done by continuum source radiation and depicted in Figure 5. This correction has two excitation sources, the HCL and a continuum source. The continuous source is a deuterium lamp (D_2) exciting the entire spectrum used for atomic absorption from 180 nm to 370 nm. Initially, a measurement will be taken with the HCL (Figure 5A, red line), then a rotating chopper mirror will allow for an absorption measurement to be taken with the D_2 lamp obtaining a second absorption reading (Figure 5B, blue line) as background signal. The difference between these two absorption signals is then used to produce a corrected absorption reading. The chopper mirror is continuously rotating throughout the analysis, so the background

is continuously monitored. Since the GFAA allows for accurate quantification and low detection limits, it is the main method that will be utilized throughout this study.

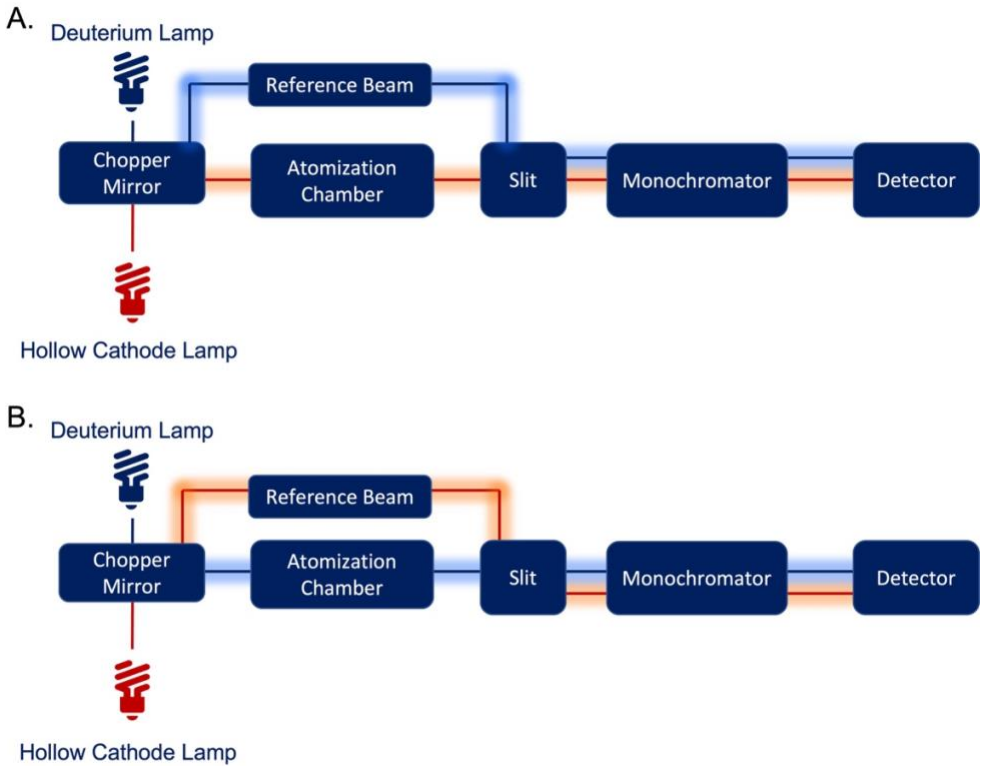

Figure 5. A) Schematic representation of atomic absorption to obtain sample signal B) Schematic representation of atomic absorption to obtain background signal

1.3.3. Beer Lambert's Law

Quantification of analytes by atomic absorption is possible due to Beer-Lambert's Law. Beer-Lambert's Law is an equation used to relate the absorbance of a homogenous sample to the concentration of an analyte as shown in Equation 1.[101]

$$A = \varepsilon bC \qquad \textit{Equation 1}$$

This equation states that absorption is proportional to the concentration of the absorbing species, or C. The molar absorptivity, ε, is a proportionality factor and a function of wavelength.[1] The path length, or b, is a constant since it is based upon the instrumentation configuration. Based on this relationship, concentration can be determined from absorption.

Certain requirements must be met to use Beer Lambert's Law such as the concentration of the absorbing analyte should be low; scattering should be negligible in comparison to the atomic absorption signal and the sample must be homogenous.

The relation of absorption to concentration can be expressed as calibration curve. A well-fit linear regression of the calibration curves provides slope of the line and the y-intercept. This provides a mathematical equation that can be used to determine an unknown concentration of an analyte. The linear regression can also be used to determine the limit of detection (LOD) and limit of quantification (LOQ).[93] In this study, the linear regression was used to determine the LOD and LOQ and is discussed further in section 3.1.2.

1.4. The Human Eye

The human eye consists of three distinct layers: tunica fibrosa, tunica vasculosa, and the tunica nervosa or outer, middle, and inner regions. Each of these regions has specific components. The outer region contains the cornea and sclera. The middle region comprises of iris, ciliary body, lens, and choroid and finally, the inner region holds the retina and optical nerve endings. The regions are surrounded by fluid; either the aqueous humor or the vitreous humor. All components work together to achieve vision as light enters through the cornea and is refracted towards the iris. The iris controls pupil dilation, thus adjusting the amount of light that will reach the lens. The lens reflects light towards the back of the eye onto the retina, which is composed of nerve endings, producing neurological signals from the captured light. These signals are then transmitted by the optical nerve to the occipital lobe allowing for sight to occur.[104] The eye components must work harmoniously as any dysfunction could result in hindrance or loss of sight. A common result of dysfunction within the eye is known as a cataract.

A cataract develops within the lens when the microarchitecture of the lens breaks down. This produces either a light scattering effect or entirely prevents light from reaching the retina.

The lens's primary function is to transmit and focus light onto the retina. The contents of the lens and its shape are important to its function. In the lens core, all cells have degraded their organelles, and this area is deemed an organelle-free zone (OFZ).[105] The loss of organelles in cells is a phenomenon originally noted by Meyer in 1851 and described further in 1899 by Rabl.[106, 107] Meyer and Rabl both noticed the disappearance of the nuclei from maturing fiber cells, and hypothesized that this was a necessary process for lens transparency. The growth of the lens is often compared to that of a tree, where the oldest rings are found in the center and the youngest rings in the peripheral. This is the same pattern noticed within the lens as the oldest fiber cells, which are developed in utero, are in the center.[105] While the lack of organelles within the fiber cells provides exceptional optical properties, it also means that once matured, there is little capacity to recycle or repair damaged proteins, and lack of capacity to express new ones.[105, 108] The low turnover rate and longevity of the lens, could potentially be a bioaccumulation cite for heavy metals.

Cataracts are the leading cause of blindness in the world and are classified as the slow process of the opacification of the lens in the eye.[109] The environment within the lens is maintained by metal ions, the concentrations of which are closely regulated.[110] Research within this field began in the 1960s characterizing alkali (H^+, Na^+, and K^+) and alkaline earth element (Mg^{2+} and Ca^{2+}) channels, carriers, and pumps.[111] Not only are metals relied upon to maintain the lens environment, but when mis-regulated or exposed to heavy metals, this can be a stressor for the lens and has been reported to induce protein aggregation.[112] The documentation of essential and non-essential metals within the human cataract lens began in the 1970s by

researchers Swanson & Truesdale,[113] Oerdogh & Racz,[114] and Lakomaa & Eklund.[115] The impact of their research promoted the observation of new trends and reports for the next three decades. At the start of the 2000s, interest in this research waned and little progress was made.

This study's goal is the quantify cadmium, chromium, copper, lead, and zinc in cataract patients collected between 2018 and 2019. The data was then compared to previously reported concentrations to identify any differences. Table 3 summarizes studies conducted for the quantification of heavy metals within the human eye lens, only including heavy metals which were also measured in this study.

Table 3. Overview of Previous Cataract Studies involving the quantification of Pb, Cd, Cr, Cu, and Zn

Metal	Concentration		Source of lens	Number of samples	Analysis	Source
	Cataract Concentration (ng/g)					
Pb	13± 18		During autopsy - healthy eyes only	16 subjects (30 eyes total)	ICP-MS	[116]
Cd	20 ± 18					
	Aqueous Humor (ug/L)	**Lens Fragment (ug/L)**				
Cr	243 ± 223	62.8 ±66.6	Lenses collected during cataract surgery	13, 13	TXRF	[117]
Cu	133 ±228	11.2 ± 7.3		9, 5		
Zn	132 ± 198	--		7, 0		
Zn	31.15 ± 8.28	23.43 ± 5.21	Rats	12 exposed to cigarette smoke, 12 not	FAA	
Cu	0.79 ±0.15	0.80 ± 0.03				
	Mean concentration (μg/g)					
Pb	0.0018 ± 0.0017		Human eyes without cataract formation, post-modem	32 human donors	ICP-MS	[109]
Cd	0.0058 ± 0.0082					
Cr	0.017 ± 0.027					
Cu	0.41 ± 0.16					
Zn	13.6 ± 2.2					
	Diabetic Senile Cataract (μg/g)	**Cataract (μg/g)**				
Cu	31.83 ± 7.94	22.32 ± 7.12	Human	10 diabetic patients and 10 non-diabetic patients	FAA	[118]
Zn	25.86 ± 14.45	21.64 ± 6.61				
	Control (μg/g)	**Cataract (μg/g)**				
Cr	1.974 ± 1.007	0.841 ± 0.476	Humans	Control: 9 Cataract: 37	GFAA	[119]

Continuation of Table 3. Overview of Previous Cataract Studies involving the quantification of Pb, Cd, Cr, Cu, and Zn

Metal	Concentration		Source of lens	Number of samples	Analysis	Source
	Diabetic Senile Cataract (μmol/g)	**Cataract (μmol/g)**				
Zn	0.56 ± 0.05	0.42 ± 0.03	Humans	29 diabetic patients and 35 non-diabetic patients	FAA	[120]
	Control (mg/kg)	**Cataract (mg/kg)**				[121]
Pb	3.0 ± 1.2	111.0 ± 67.9	Humans	10 controls 50 cataract lenses	FAA	
Cu	0.4 ± 1.2	0.5 ± 2.0				
Zn	280.0 ± 82.2	165.0 ± 133.4				
	Diabetic Cataract (μmol/g)	**Cataract (μmol/g)**				[122]
Cu	1.24 ± 0.60	0.34 ± 0.28	Humans	10 diabetic patients and 9 non-diabetic patients	FAA	
Zn	28.33 ± 6.79	23.82 ± 5.65				
	Control (μg/g)	**Smoker Cataract (μg/g)**				[123]
Pb	--	5.90 ± 1.04	Humans	9 controls and 12 cigarette smokers	GFAA	
Cd	0.045 ± 0.004	1.19 ± 0.09				
Cu	0.69 ± 0.15	2.11 ± 0.29				

1.5. Environmental Samples

Environmental samples are water, soil, air, wastes such as sludges, and biological materials.[6] Contaminants in the environment can bioaccumulate in the food chain in either plant or animal tissues and are classified as biological environmental samples. Sampling biological materials is a method to establish the extent of pollution. In this study, the focus of environmental samples was on selected biological samples, specifically vegetation *Daucus Carota* also known as Queen Anne's Lace, within the Calumet industrial corridor.

1.5.1. The Calumet Industrial Corridor

An industrial corridor is a designated area in Chicago zoned for strictly industrial manufacturing and generally aligned with railroad embankments, waterways, or highways. Some of these areas throughout Chicago have had this association for over 150 years, however these areas were not classified as industrial corridors until the 1990s, effectively banning the areas for residential or retail land use after that.

The Calumet industrial corridor lies on the southside of Chicago and runs alongside the Calumet River and around Calumet Lake cluster as shown in Figure 6.[124] This area can trace its industrial history back to the 1840s. By 1848, the Illinois Central Railroad, Michigan Southern and Northern Indiana railroads connected Chicago to Buffalo, NY. For industrial use, this was vitally important as there was now a working railroad connecting the entire region from east to west, attracting more settlers in search of opportunities. It is responsible for Chicago's first industrial boom.[125] The area has remained important for the transportation of goods and has been used heavily with little to no environmental safety regulations.[126] The industrial growth of the area continued due to steel production and related industries which reached its height in World War II and did not decline until the 1970s.[124]

Figure 6. Area view of the Calumet industrial corridor provided by the Department of Planning and Development of Chicago[124]

With a history of heavy industrial use and no government regulation until the 1970s when the Environmental Protection Agency (EPA) was established, the region has sparked much interest in terms of heavy metal pollution. In the early 1970s, it was believed that Calumet water ways could not meet the interim goals of the Clean Water Act of 1972.[127] The Clean water act was established to regulate the discharge of pollutants into waters within the United States and to monitor the amount of pollutants within the region for protection of aquatic life.[128] However, even today, the water within this area is still not safe to engage in activities such as boating and

wading and it is not recommended to eat fish caught in these waters.[129] The Calumet industrial corridor has been a source for pollution for decades which has led to many studies focused on the monitoring of different environmental samples within the area.

1.5.2. Previous Studies related to Heavy Metal Quantification in the Calumet Industrial Corridor

In the past, environmental monitoring of the Calumet industrial corridor has occurred utilizing water or soil samples as summarized in Table 4, but no environmental monitoring using *Daucus Carota* has been done. Therefore, the quantification of heavy metals in *Daucus Carota* within the Calumet industrial corridor will not only demonstrate the versatility of the developed method but also provide preliminary environmental monitoring within the Calumet industrial corridor. Please note that the table only includes the five analytes for which the chemical measurement process was developed and tested within this study.

Environmental sampling of vegetation has been used in the past in multiple different studies to monitor pollution and other environmental risks. This was done in locations such as Bengaluru, India,[130] Mount Lyell, Australia, Dexing, Jiangxi province, China,[131] Sierra de Famatina, La Rioja, Argentina.[132]

Heavy metals are typically absorbed at the root surface of the plant. This occurs through two pathways, the apoplastic pathway and the symplastic pathway. The apoplastic pathway is passive diffusion while symplastic pathway is an energy dependent process in which is an energy dependent process. The most common pathway into cells is through the symplastic pathway.[133] Eventually, at high heavy metal concentration exposure it can trigger the production of reactive oxygen species (ROS). This can result in oxidative stress and produce DNA damage, protein oxidation, and inhibit the cellular process.[134] Once heavy metals are within plants, it becomes

easier for transfer of heavy metals to either animals or humans through ingestion. The heavy metal bio-accumulation can be an indirect indicator of an environmental problem within an area. Specifically, certain metals can be linked to specific industries and pollution sources. Such as cadmium being a by-product of zinc smelting or chromium being a by-product of tanning industry. *Daucus Carota* was chosen due to common growth and can easily grow along roadsides, ditches, dry fields, and open areas.

In this study, the concentration of metals in vegetation might provide specific information about locations which have heavy metal pollution and where more intense sampling and monitoring could occur.

Table 4. Previous reports of heavy metals in Calumet industrial corridor

Element	Concentration			Environmental Sample Type	Source
Pb	**Land Use**	**1992**	**2001**	Surface Water from Different Land uses	135
	Residential	4	9		
	Commercial	9	14.5		
	Barren Land	1.52	1.7		
	Forest	1.5	2.2		
	Grassland	0.9	5		
	Agriculture	1.1	.93		
	Developed	1.6	2.37		
	Woody Vegetation	0.8	0.6		
	Emergent wetland	0	0		
Cd	**Land Use**	**1992**	**2001**		
	Residential	0.75	0.73		
	Commercial	1.25	1.23		
	Barren Land	0	0		
	Forest	0.3	0.18		
	Grassland	0.5	0.9		
	Agriculture	1	0.8		
	Developed	1.05	1.15		
	Woody Vegetation	0.3	0.21		
	Emergent wetland	0.8	0.62		
	Range Concentration (mg/kg)			Soil	136
Pb	4.7 – 647				
Cu	1.0 – 156				
Zn	5.5 – 798				
	Range Concentration (mg/kg)			Soil	137
Pb	1.2-160				
Cu	0.61 – 130				
Zn	2.8 – 320				
	Range Concentration (mg/kg)			Soil	138
Pb	24-14,428				
	Sampling Location	**Dry Weight (mg)**		Sediment from Grand Calumet River	139
Toxic Units of Metals: Cd, Co, Ni or Zn	IH-25	0.38			
	IH-26	0.47			
	IH-27	1.3			
	IH-28	0.53			
	IH-29	2.2			

Continuation of Table 4. Previous reports of heavy metals in Calumet industrial corridor

Element	Concentration	Environmental Sample Type	Source
Pb	IH-30	0.31	[140]
Cd	1.8		
Cr	76.7		
Cu	57.5		
Zn	341.0		
Cu	0.262		
	Concentration (mg/kg)	Sediment	[141]
Pb	46.82		
Cd	0.67		
Cr	17.41		
Cu	20.89		
Zn	33.67		
	Concentration (mg/kg)	Surface Water	[142]
Cu	0.262		

CHAPTER 2. MATERIALS AND METHODS

In this chapter, the materials and methods used within this study are presented. A major goal of this study was to develop a method for multi-elemental analysis utilizing graphite furnace atomic absorption spectrometry (GFAA) in complex biological matrices. This was done sequentially as shown in Figure 7. The first step was to develop a method for the analysis of lead in *E. coli* cell pellet (ECP) by exploring previously reported methodologies for lead detection in other biological materials. Initially tested methods were further optimized, and the method's validity was determined by analyzing percent recoveries, repeatability, and selectivity. The method that provided the most reliable results proved to be microwave-assisted acid digestion (MAAD). MAAD was then applied for the analysis of other heavy metals: cadmium, chromium, copper, and zinc in ECPs. The final validation step of the developed method was analysis of CRM before application to human cataract cell pellets and environmental samples.

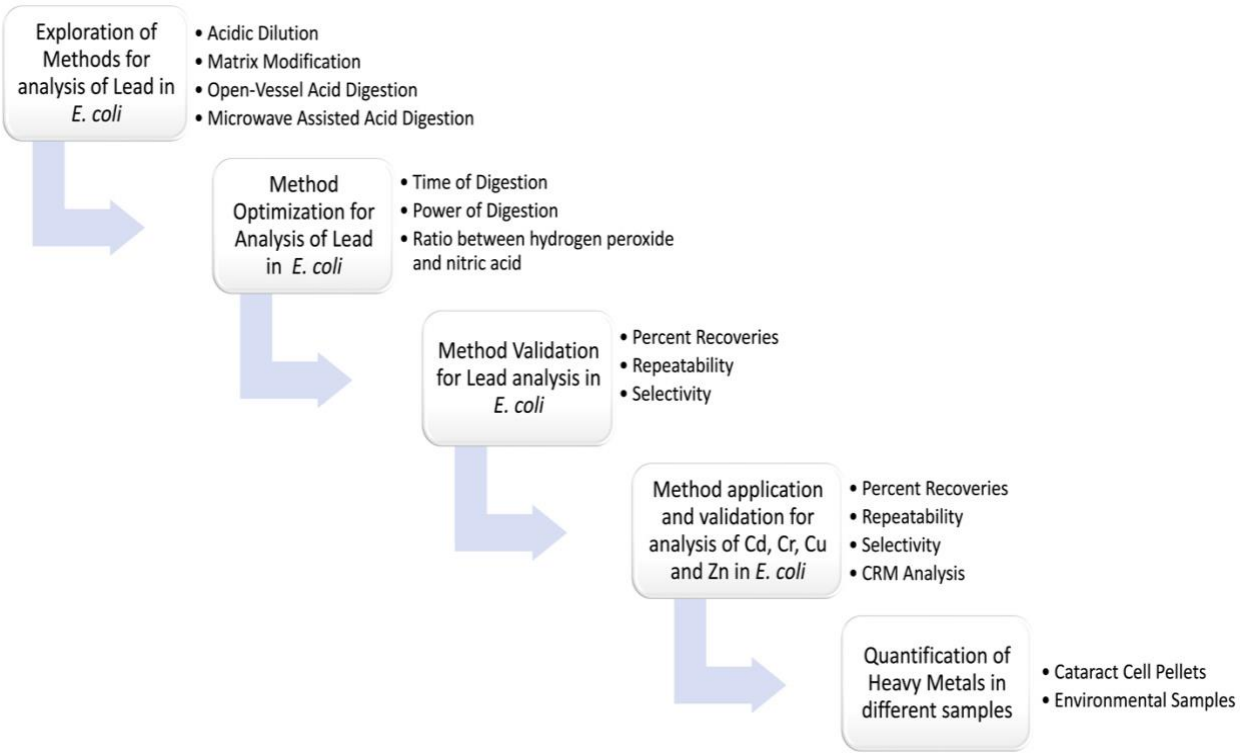

Figure 7. Outline of method development for the quantification of heavy metals in biological and environmental samples

2.1. Materials of Study

All materials used were reagent grade or better. Nitric acid 70%, hydrogen peroxide 30 wt. %, and atomic absorption standard solutions for cadmium, copper, chromium, and lead were acquired from Sigma-Aldrich (St. Louis, MO, USA). Zinc standard stock solutions were made from $ZnCl_2$. A variety of salts used to determine the selectivity of the method were purchased from Sigma-Aldrich (St. Louis, MO, USA), Thermo-Fisher (Waltham, MA, USA), and EMD (Chicago, IL, USA). The matrix modifiers tested were: $Mg(NO_3)_2$, $NH_4H_2PO_4$, and oxalic acid were all purchased from Sigma-Aldrich. The certified reference material BCR 679 – White Cabbage was acquired from Sigma-Aldrich (St. Louis, MO, USA) and stored at room temperature. Ultrapure water was obtained via a Purelab Flex purification system, >18 MΩ (ELGA® Labwater, High Wycombe, UK). The *E. coli* was grown in Luria broth purchased from

Fisher BioReagents (Waltham, MA, USA). The buffered saline solution (BSS) used for *E. coli* cell pellet preparation was obtained from Loyola University Medical Center (LUMC).

Digestions were carried out with polytetrafluoroethylene (PTFE) vessels (Anton Parr; Moline, IL, USA) and a standard household microwave oven (MW535OW; Samsung Corp, Suwon, Korea). The drying of the *E. coli* and human cataract cell pellets was done in a SpeedVac SC110 vacuum centrifuge (Savant, Hyannis, MA, USA).

All samples were analyzed by a graphite furnace atomic absorption spectrometer (AA-7000, Shimadzu, Kyoto, Japan) at 228.8 nm (Cd), 357.9 nm (Cr), 283.3 nm (Cu), 283.3 nm (Pb), and 213.9 nm (Zn) wavelengths. Hollow cathode lamps (HCL) of 1.5" standard were purchased from Varsal Incorporated (Warminster, PA, USA). Samples analyzed with GFAA were pipetted in 20 μL aliquots into the atomization chamber and measured in triplicate following the furnace program shown in Table 5 (Shimadzu, Kyoto, Japan). Graphite pyrolytic coated tubes were purchased from Shimadzu and were exchanged every 500 firings to ensure high sensitivity. The AA-7000 has reported sensitivities for chromium, copper, lead, and zinc of 0.01 ng/mL, while cadmium has a reported sensitivity of less than 0.01 ng/mL.[143] (Shimadzu)

All glassware was washed with a 1:3 H_2SO_4 to HNO_3 solution by filling the glassware to the brim, soaking it for an hour, and rinsing thoroughly with ultrapure water. The digestion vessels were cleaned twice between each digestion. The washing protocol was accomplished by addition of 1 mL of 15 M HNO_3 into the digestion vessels and was digested for one minute at 1200 Watts. The vessels were allowed to rest for one hour and then rinsed excessively with ultrapure water.

2.2. Sample Collection and Storage

2.2.1. Escherichia Coli Samples: Preparation and Storage

The *E. coli* cells used in this study were grown from a BL21 cell line in Luria broth (LB). The LB growth solution was prepared by diluting 2.5 grams of LB powder in 100 mL of ultrapure water and then autoclaved. The BL21 cell line was then added to the sterilized LB broth and grown for 12-18 hours at 37°C. The cells were collected as pellets after centrifugation at 5,000 rpm for 5 minutes removing the LB solution followed by two subsequent washes with 5 mL of 50 mM HEPES (4-(2-hydroxyethyl)-1-piperazineethanesulfonic acid, pH=7.5; Sigma-Aldrich). After the second wash with HEPES, the *E. coli* cells were re-suspended in 500 µL of BSS to mimic the conditions used in clinical settings. The resuspended *E. coli* cells were dispensed as 50 µL aliquots into 1.5 mL microcentrifuge tubes, dried overnight at 95°C, creating an *E. coli* cell pellet or ECP. The ECPs were stored at room temperature until further use.

2.2.2. Human Cataract Samples: Collection and Storage

Cataract samples were collected during phacoemulsification, a surgical procedure to remove cataracts. This surgical procedure took place at LUMC and was performed from March thru July 2018 and in January 2019. The product of surgery is a slurry containing the broken pieces of cataract and the BSS solution. The BSS by-product was centrifuged to separate the supernatant from the cataract pellet. The cataract pellet is the area of interest in this study and will be referred to as a cataract cell pellet or CCP. The samples were then transferred to Loyola Lakeshore Campus on ice and were stored at -80°C until ready for analysis.

2.2.3. Environmental Samples: Collection and Storage

Environmental samples were collected from within the Calumet industrial corridor. The plant species collected were *Daucus Carota (*Queen Ann's Lace) and was taken in multiple places throughout the industrial corridor. This plant was collected in its entirety and placed in plastic Ziplock bags for transport. The locations of which are shown in Figure 8, Location 1 was collected in November 2021 and Locations 2 and 3 were collected in June of 2022. Samples were then stored at 4°C until ready for the drying procedure. The drying procedure involved an excessive washing of the plant with deionized water and placing the leaves into pre-cleaned beakers. The sample were then dried in an oven at 100 °C for 24 hours. The dried samples were ground into a fine powder using a porcelain mortar and pestle and placed into a pre-cleaned glass vial and stored at room temperature until ready for analysis.

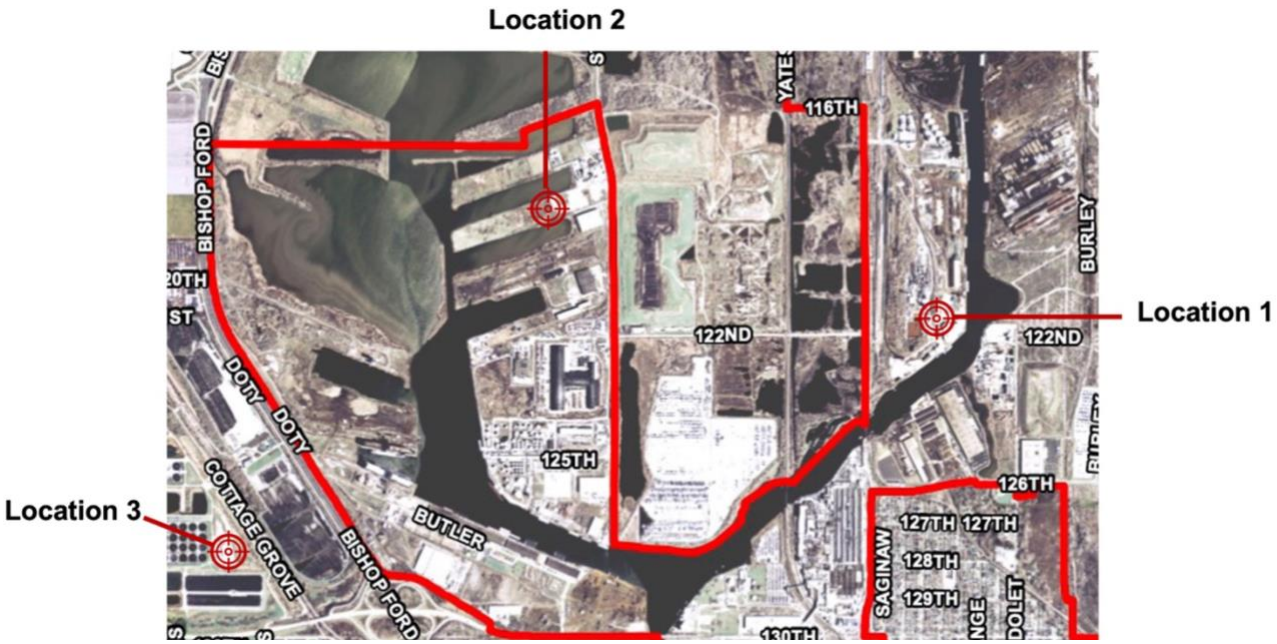

Figure 8. Locations of environmental samples collection

2.3. Optimization of Graphite Furnace Thermal Program

The thermal program used for the atomization of the sample is necessary to obtain accurate absorption. When properly done it can achieve the highest level of sensitivity, however, if this temperature program is not correctly optimized analytes could be lost during the pyrolysis stage or interferences could be present during the atomization stage. For all elements analyzed within this study, the thermal program was optimized individually. Initially, the pyrolysis stage was optimized by first measuring the absorption of a sample containing no analyte and then measuring the absorption of an analyte spiked sample to obtain percent recoveries under different thermal conditions. The spiked concentration differed depending upon which analyte was being optimized. For cadmium, chromium, and lead thermal optimization the spiked concentration was 3.0 ng/mL while for copper and zinc thermal optimization, the spiked concentration was 5.0 ng/mL. These concentrations were chosen based on the calibration curves, the limits of detection (LOD) and concentrations of the analytes commonly found within biological matrices.[144] The temperature of the pyrolysis stage was modified in 100°C increments over the range of 300°C to 800°C until the highest recovery rate was achieved and was reproducible. The atomization stage was optimized by changing temperatures from 1700°C to 2400°C in 100°C increments. The optimal thermal program is described for each analyte in Table 5.

Table 5. Optimal Furnace Temperature Program for the analysis of cadmium, chromium, copper, lead, and zinc on GFAA

Element:		**Cadmium**	**Chromium**	**Copper**	**Lead**	**Zinc**	
Wavelength (nm)		λ = 228.8	λ = 357.9	λ = 324.8	λ = 283.3	λ = 213.9	
Lamp Current (mA)		8	10	10	10	8	
Step	**Process**	**Temperature °C**					**Time (sec)**
1	Drying	60	60	60	60	60	3
2		150	150	150	150	150	20
3		250	250	250	250	250	10
4	Pyrolysis	300	300	800	400	700	10
5		300	300	800	400	700	10
6		300	300	800	400	700	3
7	Atomization	2200	2100	2400	2000	2000	3
8	Cleaning	2500	2500	2500	2500	2500	2

2.4. Method Development for Lead Analysis using Escherichia Coli as Model Substrate

Four different methods were investigated for the analysis of lead in ECPs. These methods were acid dilution, matrix modification, conventional heating acid digestion, and microwave-assisted acid digestion. Specific parameters were used to determine whether a method was suitable for the quantification of lead in complex matrices. These parameters were percent recovery, the limit of detection (LOD), the limit of quantification (LOQ), repeatability, and selectivity. The calculations for percent recovery, LOD, LOQ, and repeatability, which is represented by the relative standard deviation (RSD), will be discussed in Chapter 3.

2.4.1. Acid Dilution Method

Acid dilution was examined by varying the dilution factor which is represented by volume per volume (v/v), a dilution based on volume and represented by percentage. The percentage of 10:1 nitric acid to hydrogen peroxide was what was evaluated. For each v/v percentage, a set of four ECPs were spiked with concentrations of 0.0, 3.0, 5.0, and 7.0 ng/mL lead was prepared, and is referred to a sample set. The concentrations of nitric acid has been

reported to affect the sensitivity for lead detection, therefor this parameter was optimized. [145] Five volume per volume (v/v) percentages of 10:1 HNO_3 to H_2O_2 solution in water were analyzed for acid dilution. The v/v percentages examined were 0%, 10%, 25%, 50%, and 75% v/v 10:1 HNO_3 to H_2O_2 solution. Table 6 shows the different volumes of the digestion solution (10:1 HNO_3 H_2O_2) used to obtain the different v/v percentages.

Table 6. Preparation of volume per volume percentages of 10:1 HNO_3 to H_2O_2

Percentage Analyzed	**Volume of 10:1 HNO_3 H_2O_2 Solution (µL)**	**Volume of Water**	**Total Volume (µL)**
0%	0	1000	1000 µL
25%	250	750	
50%	500	500	
75%	750	250	

All samples underwent ultrasonication for 30 minutes, followed by centrifugation for five minutes at 5,000 rpm. The supernatant was collected for analysis as shown in Figure 9. Based on the results, 50% v/v of 10:1 HNO_3 H_2O_2 was determined as the optimal solution and was used throughout the rest of the study.

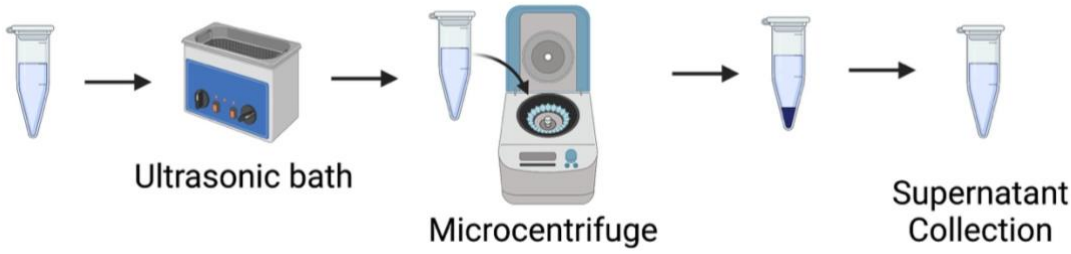

Figure 9. Schematic representation of the dilution methodology explored

2.4.2. Matrix Modification Method

Three different matrix modifiers were initially analyzed: $Mg(NO_3)_2$, $NH_4H_2PO_4$, and oxalic acid. These matrix modifiers were chosen as they have successfully aided to detect lead in water,[146, 147] biological,[148] and food samples.[149, 150] Matrix modification was accomplished by treating sample sets with 500 µL of 10:1 HNO_3 to H_2O_2 solution, 100 µL of 1000 ng/mL matrix

modifier and diluting to 1.0 mL with ultrapure water. Each matrix modifier was analyzed separately. The resulting sample sets were ultrasonicated for 30 minutes, followed by centrifugation for five minutes at 5,000 rpm. The supernatant was collected for analysis as depicted in Figure 10. The $NH_4H_2PO_4$ matrix modifier had more promising results and therefore was optimized further.

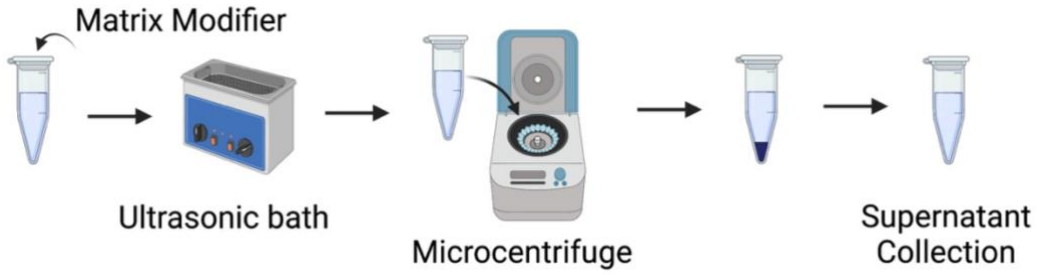

Figure 10. Schematic representation of the matrix modifier method

Different concentrations of $NH_4H_2PO_4$ were further explored besides the initial concentration of 100 ng/mL. For this, the method described above was repeated with concentrations of 50 ng/mL, 100 ng/mL and 200 ng/mL $NH_4H_2PO_4$. However, there was no improvement in the recovery of lead with the variation thus the concentration of $NH_4H_2PO_4$ was kept constant at 100 ng/mL. The ratio of HNO_3 to H_2O_2 was also examined. Four sample sets were used to test the following ratios: 2:1, 5:1, 10:1, and 15:1 of nitric acid to hydrogen peroxide. Table 7 describes how the stock solution of each ratio was made. From the stock solution, 500 μL was used to maintain the v/v 50% dilution. There was little to no improvement in the percent recoveries, so other methods were investigated.

Table 7. Different nitric acid to hydrogen peroxide ratios and the associated volumes of nitric acid and hydrogen peroxide

Ratio	**Volume of 15 M HNO_3**	**Volume of 30% H_2O_2**
2:1	2 mL	1 mL
5:1	5 mL	1 mL
10:1	10 mL	1 mL
15:1	15 mL	1 mL

2.4.3. Conventional Heating Acid Digestion Methods

Temperature controlled acid digestion and open-vessel acid digestion (OVAD) were explored. Temperature controlled acid digestion was performed in a water bath at 85°C. ECP sample sets spiked with 0.0, 3.0, 5.0, and 7.0 ng/mL of lead and 50% v/v of 10:1 HNO_3 to H_2O_2 were allowed to digest for 15 minutes, 30 minutes, 1.0, 2.0, 3.0, and 4.0 hours. Sample resuspension was not necessary as there was no noticeable loss of sample. After digestion, samples were sonicated for 30 minutes followed by centrifugation of five minutes at 5,000 rpm. (Figure 11A) The supernatant was collected and analyzed. The two-hour digestion time provided the highest percent recoveries and was kept constant while the ratios of HNO_3 to H_2O_2 were varied between 2:1, 5:1, 10:1, and 15:1. This was made in the same manner as shown in Table 7. Only the ratio between HNO_3 and H_2O_2 was varied, the v/v percentage was kept constant at 50%. However, this variation did not improve the observed large standard deviation, therefore this method was not scrutinized further.

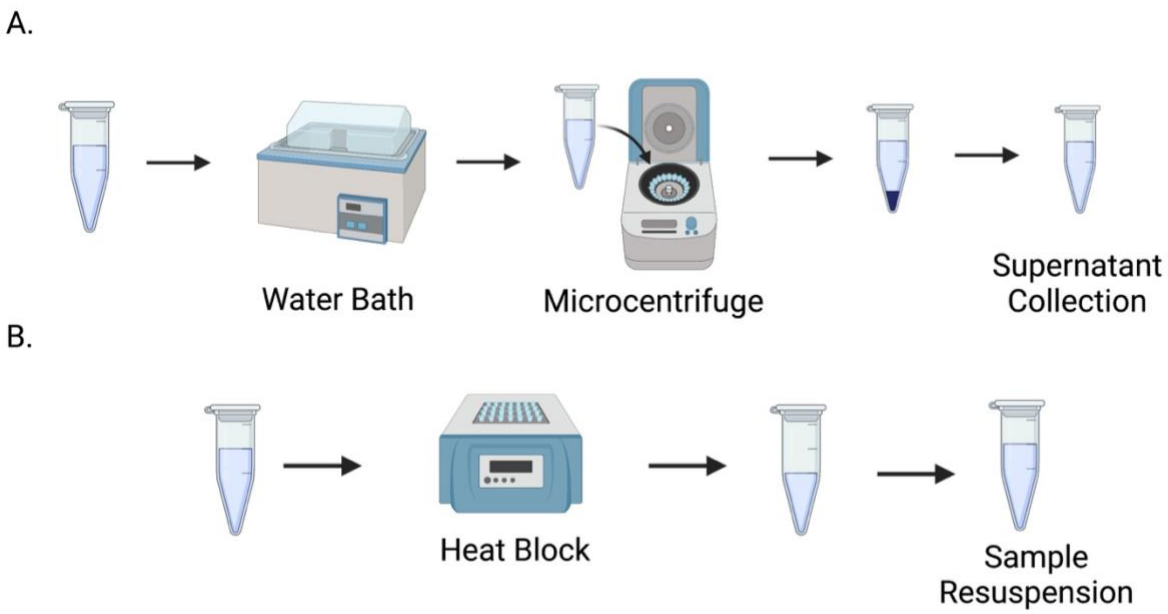

Figure 11. Schematic representations of acid digestion, a) temperature controlled acid digestion and b) open-vessel acid digestion

Open vessel acid digestion (OVAD) was performed using a digestion block. Five sample sets were treated with 500 μL of 10:1 HNO_3 to H_2O_2 solution and diluted to 1 mL with ultrapure water. Each sample set was allowed to digest for either 30 minutes, 1.0, 2.0, 3.0, and 4.0 hours at 100°C. Sample loss due to evaporation had to be recompensated to 1.0 mL total volume with 50% v/v solution of 10:1 HNO_3 to H_2O_2 solution as shown in Figure 11B. Similarly, to temperature controlled acid digestion, a two-hour digestion time provided the highest percent recovery. The two-hour digestion time was kept constant and the ratios of 2:1, 5:1, 10:1, and 15:1 of HNO_3 to H_2O_2 were examined (Table 7). There was little to no improvement in the percent recoveries and the standard deviation remained large. Therefore, this method was not continued further.

2.4.4. Microwave-Assisted Acid Digestion Method

The final method tested was microwave-assisted acid digestion (MAAD). A sample set containing spiked amounts of 0.0, 3.0, 5.0, and 7.0 ng/mL of ECPs was treated with 500 μL of 10:1 HNO_3 to H_2O_2 solution and diluted to 1.0 mL with ultrapure water, followed by a sample transfer to 23 mL PTFE sample cups. The samples were then digested in a microwave at 600W power for 40 seconds. This method is depicted in Figure 12. Like the previous methods, the microwave-assisted acid digestion method was further improved to obtain optimal results.

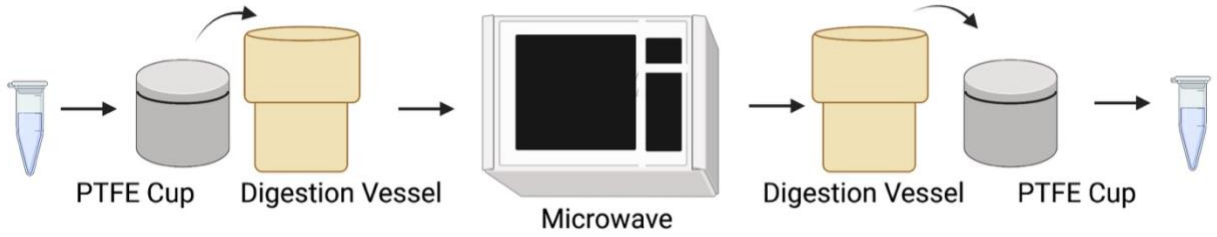

Figure 12. Schematic representation of microwave-assisted acid *digestion*

Further optimization of MAAD involved an assessment of digestion time, power setting, and nitric acid to hydrogen peroxide ratio, respectively. This was executed consecutively starting with the digestion time.

To optimize digestion time, all samples were treated with 500 μL of 10:1 HNO_3 to H_2O_2 solution and diluted to 1.0 mL with ultrapure water. A total of seven sample sets were tested at varying microwave times of 30, 40, 50, 60, 70, 80, and 90 seconds while keeping the power at 600 W. This was done to accurately determine the optimal digestion time for the MAAD, which was found to be 60 seconds.

The microwave power setting was then optimized. A total of five sample sets were tested with varying power, starting with the lowest setting of 600W, and slowly increasing the power in 120W increments until the maximum power of 1200W was reached. The power settings are

shown in Table 8. The digestion time was constant at 60 seconds and the optimal power setting was found to be 1200 W, the maximum power of the equipment.

Table 8. Power settings employed for the microwave acid digestion procedure

Power Setting Tested (W)
600
720
840
960
1080
1200

In the last step, the ratio between nitric acid to hydrogen peroxide in the digestion solution was optimized. Six sample sets were treated with one of the following ratios: 2:1, 4:1, 5:1, 6:1, 10:1, and 15:1 HNO_3 to H_2O_2 solution, similar as what was shown in Table 7. This analysis was performed using the optimal parameters of 60-second digestion time and microwave power of 1200 W. The percent recoveries were calculated, and the optimal ratio was found to be the 4:1 HNO_3 to H_2O_2 solution.

2.5. Optimal Method for Detection of Lead in Escherichia Cell Pellets

The microwave-assisted acid digestion was determined to be the optimal method for the detection of lead in biological samples. The optimized method is as follows: samples are treated with 500 μL of 4:1 HNO_3 to H_2O_2 and diluted to 1.0 mL with ultrapure water. The samples are transferred into 23 mL PTFE sample cups and digested for one minute at 1200 Watts as shown in Figure 13. The samples are left to cool for one hour before collection and are then analyzed. Before the next sample digestion, the PTFE sample cups are washed twice using 1.0 mL of 15 M nitric acid and digested for one minute at 1200 Watts. This method was then further evaluated by confirming its sensitivity, reproducibility, and selectivity.

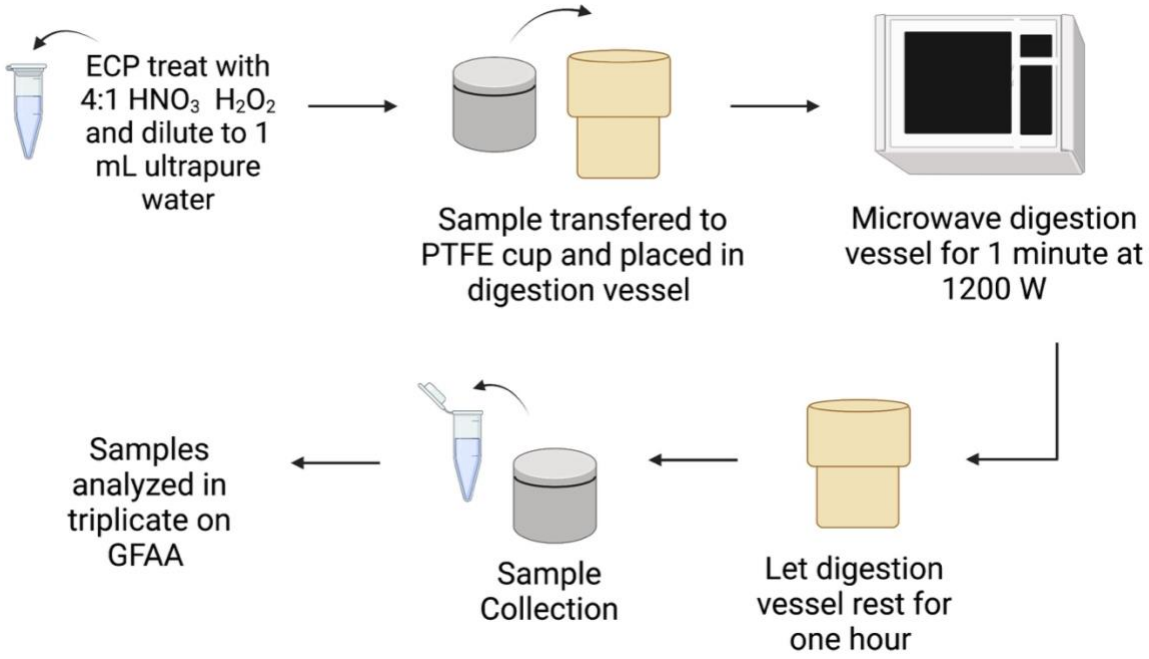

Figure 13. Schematic representation of the optimized method for the determination of lead in Escherichia coli cell pellets

2.5.1 Method Validation for Lead Detection in Escherichia coli Cell Pellets

The repeatability was assessed for the $NH_4H_2PO_4$ matrix modifier and MAAD method as these had high initial percent recoveries and low standard deviations indicating that these methods could potentially work as a method for lead detection in biological materials. The assessment of a method's repeatability involved 12 ECPs spiked with 4.0 ng/mL of lead and 3 controls containing only BSS. All samples were treated as described in section 2.4.2 and 2.5. The recoveries were calculated after subtracting the blanks (controls) from the spiked ECPs. The average, absolute standard deviation, and relative standard deviation (RSD) for the sample set were determined. RSD served as a measure for repeatability and its calculation will be described in Chapter 3.

A method is selective when it is not impacted by chemical or spectral interferences.[102] To determine the selectivity of each method, sample sets of ECPs containing 0.0, 3.0, 5.0, and 7.0

ng/mL of lead were additionally spiked with potential elemental interferences. The interfering element concentrations were kept constant within a sample set. Each sample set was specific for one interference. A total of thirteen elemental interferences were examined as shown in Table 9. The concentrations of the potential interferences were selected based on a previous study.[117] The average concentrations reported within that study were then doubled to account for the large variation typically present in clinical and environmental samples.

Table 9. Concentrations of metals used for the selectivity study

Element	**Amount Spiked (ng/mL)**
Na	380
Mg	380
K	380
Ca	380
Cr	120
Mn	60
Fe	120
Co	50
Ni	75
Cu	120
Zn	60
Ga	100
Cd	60
Mixture	380 of Na, Mg, K, & Ca, 120 Fe & Cu, 75 Ni, and 60 Zn

The sample sets were digested according to the procedures described in sections 2.4.2 and 2.5. To prove the method is selective for lead analysis in ECP, the percent recoveries needed to remain within the range of 100 ± 15% while in the presence of a high concentration of interference.

2.6. Quantification of Heavy Metals in Escherichia coli Cell Pellets Utilizing Developed Method

The other heavy metals of interest in this study were cadmium, chromium, copper, and zinc. Multiple parameters were used to determine if the MAAD method established for lead detection could be also applied for the detection of these elements zinc in the same complex matrices using GFAA analysis. These parameters evaluated determined were percent recoveries, repeatability, selectivity, and the analysis of certified reference materials (CRM).

Percent recoveries were determined for each analyte individually. This was done by spiking the ECPs with concentrations of 0.0, 3.0, 5.0, and 7.0 ng/mL of either cadmium, chromium, copper, and zinc. All samples were then treated as described in section 2.5. The percent recoveries should remain within 100 ± 15%, as this indicates little to no loss of analyte is occurring during sample treatment.[151]

The repeatability of the method was considered for each analyte separately. A total of 12 ECPs were treated with the optimized method and spiked with the specific analyte being studied. As stated previously, concentrations of analytes should cover the reported range of concentration within the sample and should be at least five times higher than the LOD.[144] Therefor the spiked concentration used for cadmium and chromium was 4 ng/ml, while for copper and zinc, the concentration used as spike was 6 ng/mL. All repeatability studies included 3 controls containing only BSS. The recoveries were calculated by subtracting the concentration of the blanks (controls) from the spiked samples. The RSD was then computed as a measure of the method repeatability for the detection of cadmium, chromium, copper, and zinc in *E. coli*.

A selectivity study of the method was repeated for each analyte using the same procedure performed for lead as described in section 2.5.8. Briefly, sample sets of cadmium, chromium, copper, and zinc were prepared with 0.0, 3.0, 5.0, and 7.0 ng/mL of analyte and were then spiked

with the interferences summarized in Table 9, excluding the analyte being analyzed, but including lead. The concentration of lead was 60 ng/mL which was based on previous reports of lead in cataracts. It was then doubled to account for any variation observed in clinical samples.[116, 121] The sample sets were then digested as described in section 2.5. Like for lead, the percent recoveries should remain high when purposely exposing the sample to interferences to indicate that the method developed is selective for analysis of either cadmium, chromium, copper, and zinc.[151]

2.7. Methodology Validation with Certified Reference Material

The final step in validating the developed method was analysis of a certified reference material CRM. The CRM and analysis of the same sample by a secondary comparable analytical method. The CRM chosen was a white cabbage powder and was selected based on its complex matrix and similarity to the biological and environmental samples being analyzed besides having reported data for cadmium, chromium, copper, and zinc.

The secondary method used was total reflection X-ray fluorescence (TXRF). The analytical requirements for TXRF are similar to that of GFAAS with the exception of using an internal standard for quantification instead of calibration curves. The internal standard was added in the beginning of the sample preparation process to account for losses.

A small amount of certified reference material BCR 679 was first placed on a watch glass and allowed to dry to completion overnight in an oven at 100 °C. After that an approximate amount of 0.100-gram subsample of the dried sample was accurately weighted and treated following the same experimental procedure as described in section 2.5. Briefly, the dried subsample of 0.100 g was treated with 1.0 mL 4:1 nitric acid to hydrogen peroxide solution, 100 μL/mL of 100 ng/mL Ga as internal standard for TXRF and 900 μL of ultrapure water were

added to the subsample and the samples digested for one minute at 1200 Watts. The total volume of 2.0 mL ensured that the sample were fully resuspended and digested and kept the acidic dilution percentage at a 50% v/v. The number of subsamples analyzed for each element differed and is shown in the table below. The reasoning for the different number of subsamples was to match what was measured for the certified reference material.

Table 10. Comparison of number of subsamples analyzed of BCR 679

Element Analyzed	**Certified number of accepted sets of data**	**Experimental subsamples analyzed**
Lead	Not analyzed	10
Cadmium	15	15
Chromium	5	5
Copper	15	15
Zinc	22	22

The reported concentrations for cadmium, chromium, copper, and zinc were compared to the ones reported in the certificate to determine the accuracy of the method. In addition, copper concentrations were compared between GFAAS and TXRF. Lead was also analyzed for the certified reference material even though it was not included in the reported values.

2.8. Real Life Applications of Developed Method

The developed method for the analysis of lead, cadmium, chromium, copper, and zinc was then applied to different sample types to demonstrate its versatility.

2.8.1. Quantification of Heavy Metals in Human Cataract Samples

In preparation for analysis, the cataract samples were removed from the -80°C freezer and allowed to thaw to room temperature. The samples were then spun in a vacuum centrifuge, removing any remaining aqueous residue. The cataract mass was obtained by weighing the centrifuge tubes before analysis when the CCP was a dried pellet within the tube and after when

the tube was empty. The difference between these masses gave the weight of the cataract, this was done in triplicate of with a sensitivity of ± 0.0001 grams.

The cataract samples were prepared in the following manner: dried CCP were spiked with 100 ng/mL of Ga and treated with 500 μL of 4:1 HNO_3 to H_2O_2 solution and diluted to 1 mL with ultrapure water. Samples were digested in the microwave for one minute at 1200 W power and allowed to rest at room temperature for one hour. Spiking with gallium permitted the analysis of the same sample also by TXRF. All CCPs samples were then analyzed in triplicate for cadmium, chromium, copper, lead, and zinc utilizing GFAA and TXRF.

2.8.2. Quantification of Heavy Metals in Environmental Samples

The preparation of environmental samples was similar to what was described in section 2.7 for the CRM material. A small amount of the environmental sample collected from the Calumet industrial corridor was first placed on a watch glass and allowed to dry to completion overnight in an oven at 100 °C. After that a subsample weighing ~ 0.100 gram of dried sample was allocated for analysis. The dried mass of ~0.100 gram was treated with 1.0 mL of 4:1 HNO_3 to H_2O_2 solution, 500 ng/mL of internal standard gallium and then diluted to 2.0 mL. The total volume had to be adjusted to ensure the powdered sample could be fully digested. The samples were then transferred to the PTFE sample cups and digested for one minute at 1200 Watts. A total of ten subsamples were analyzed for each of the collected samples. The digested samples were then analyzed in triplicate by GFAA and TXRF for lead, cadmium, chromium, copper, and zinc.

CHAPTER 3. METHOD DEVELOPMENT FOR ANALYSIS OF HEAVY METALS IN BIOLOGICAL, CLINICAL AND ENVIRONMENTAL SAMPLES

The following chapter is a compilation of the results and discussion pertaining to method development for elemental analysis in *Escherichia coli* cells. The chapter is divided into four parts. Part I describes the figures of merit calculations; Part II provides an in-depth analysis of several methodologies examined for the detection of lead in *Escherichia coli* cells and demonstrates how an accurate, precise, sensitive, repeatable, and selective methodology was obtained. Part III discusses how the developed method was successfully applied for the analysis of cadmium, chromium, copper, and zinc in *Escherichia coli* cells; Part IV validates the developed procedure through analysis of certified reference material (CRM) by graphite furnace atomic absorption (GFAA) and total reflection X-ray fluorescence (TXRF).

3.1. Part I. Figures of Merit Calculations

The analytical properties known as figures of merit, measure accuracy, precision, and repeatability to determine a method's validity. Additional figures of merit are the limit of detection (LOD), and the limit of quantification (LOQ), both are an assessment of a method's sensitivity and are necessary when performing trace analysis.

3.1.1. Accuracy, Precision and Repeatability

When designing a method, accuracy and precision are two important factors to consider. Percent recovery measures an analytical method's accuracy and is determined using Equation 3-2. Equation 3-2 accounts for the change of concentration of analyte in a spiked and non-spiked sample.[101] C_s is the concentration of the spiked sample, C_{NS} is the concentration of the non-spiked sample, and C is the spike concentration.

$$Percent\ Recovery = \left(\frac{C_s - C_{NS}}{[C]}\right) * 100 \qquad \textit{Equation 3-2}$$

Standard deviation is a measurement of precision and is calculated using Equation 3-3, where x_i is the concentration of the individual data point, $\bar{x}$ is the average concentration of the data set, and n is the number of data points being analyzed.

$$SD = \sqrt{\frac{\sum(x_i - \bar{x})^2}{n-1}} \qquad \textit{Equation 3-3}$$

For a method to be considered both accurate and precise the percent recovery should maintain an average of 100 ± 10%.[152, 153] However, this is less stringent for biological and environmental samples, where natural variability adjust recovery rate to 100 ± 15%.[152,153]

Relative standard deviation (RSD) is a measurement of the method's repeatability, and is otherwise known as the 'coefficient of variation,' or 'CV,' as shown in Equation 3-4. [101] For biological samples these values should remain less than 15%.[152, 153]

$$RSD = \left(\frac{SD}{\bar{x}}\right) * 100 \qquad \textit{Equation 3-4}$$

3.1.2. Limit of Detection and Limit of Quantification

The limit of detection (LOD) and limit of quantification (LOQ) both measure the sensitivity of a method. The LOD is defined as the lowest amount of analyte that can be reliably detected, whereas the LOQ quantifies the smallest amount of analyte that can be quantified

within a given range of accuracy and precision. [101] This distinction is essential as certain methods can detect the analyte but are unable to quantify the analyte.

There are three ways to determine the LOD and LOQ. The first is based on the standard deviation of the blank, the second bases its determination on the signal-to-noise ratio, and the third utilizes the linear regression of the calibration curve.[154] [155] In this study, LOD and LOQ were determined based on the third method, linear regression of the calibration curve. (Equations 3-5 and 3-6) For atomic absorption spectrometry, the instrument response is linearly related to the standard concentrations over a specific range which is monitored by using the r^2 value.[156] This procedure accounts for the standard deviation of the y-intercept, representing the "noise" within the measurements and is denoted 'S_y' and the slope of the regression line 'm'.[101, 154]

$$LOD = \frac{3 * S_y}{m} \qquad \textit{Equation 3-5}$$

$$LOQ = \frac{10 * S_y}{m} \qquad \textit{Equation 3-6}$$

3.2. Part II: Method Development for Lead Analysis in Escherichia coli

A major goal of this study was to develop a method for the quantitative analysis of lead within biological samples, and then transfer this method to other elements. To achieve this, *E. coli cell pellets* (ECPs) were chosen as a model matrix, and the process was divided into the following subsections: instrumental thermal program optimization, sample preparation procedure exploration, and method comparison with respect to repeatability, sensitivity, and selectivity. The sample preparation procedures explored were acid dilution, matrix modification, conventional heating acid digestion procedures, and finally microwave-assisted acid digestion. The accuracy and precision were evaluated by percent recovery and standard deviation, the repeatability was assessed with the RSD, sensitivity was monitored by the LOD and LOQ, and

the selectivity was monitored using recovery rates in the presence of high concentrations of potential interferences.

3.2.1. Graphite Furnace Atomic Absorption Thermal Program Optimization for Lead Analysis

The thermal program optimization for the analysis of lead in biological samples was meticulously implemented to avoid significant loss of analyte during the heating process. The experimental procedure of this study is described in more detail in section 2.3. Optimization was accomplished first for the pyrolysis stage (Figure 14A) and then again for the atomization stage (Figure 14B). Lead absorbance was monitored while changing the thermal conditions to identify the optimal conditions. The highest absorbance was achieved at 400°C with the smallest standard deviation. Therefore, 400°C was used for all experimentation going forward. The optimal temperature for the atomization stage was found to be 2000°C as is clearly shown in Figure 14B. This atomization temperature produced the highest absorbance and the smallest standard deviation.

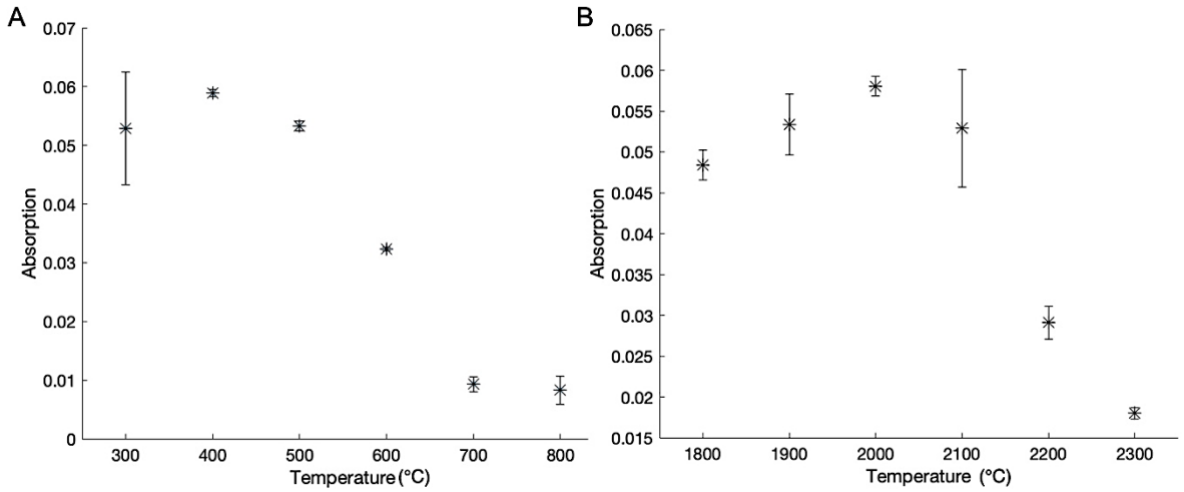

Figure 14. Thermal program optimization for lead analysis in ECPs A) pyrolysis stage and B) atomization stage

From the optimization experiments, the lead graphite thermal program was determined as reported in Table 11.

Table 11. Optimized Graphite Thermal Program for Lead Detection

Step	Process	Temperature °C	Time (sec)
1	Drying	60	3
2		150	20
3		250	10
4	Pyrolysis	400	10
5		400	10
6		400	3
7	Atomization	2000	3
8	Cleaning	2500	2

3.2.2. Methods Explored for Lead Quantification in Escherichia Coli

Four distinct sample preparation methods were explored for the detection of lead in ECPs. These methods were acid dilution, matrix modification, conventional heating acid digestion, and microwave-assisted acid digestion. Acid dilution, matrix modification, and conventional heating acid digestion procedures are simple, time efficient, and inexpensive. However, these methods can exhibit poor recoveries, large standard deviations, and have difficulties with selectivity. Microwave-assisted acid digestion (MAAD) method permits for high reaction temperatures, and a more complete digestion of the sample, requiring lower amounts of reagents, and minimizing the loss of analytes and the risk of contamination. The obstacles of utilizing the MAAD method include the necessity for specialized, costly pressure-resistant vessels, which do not allow the addition of reagents during the digestion process due to the procedural sealing within the digestion vessels.[157]

3.2.2.1. Acid Dilution

Dilution is an efficient and inexpensive method. The most common diluent for organic and inorganic matrices is nitric acid. Nitric acid acts as an oxidizing and digestion agent, and in some studies has also been considered as a matrix modifier.[158, 159, 147] However, when samples have a high organic content, like biological samples, a combination of nitric acid and hydrogen peroxide is often more suitable. When nitric acid is used without the aid of hydrogen peroxide, a build-up of carbonaceous residue can occur within the graphite furnace due to the incomplete matrix decomposition, ultimately changing the surface of the graphite furnace. This can alter the heating rate and atomization conditions as the buildup of residue may obstruct the optical path resulting in a higher background interference.[159] Acid dilution was evaluated for the detection of lead in ECPs with a combination of 10:1 nitric acid to hydrogen peroxide solution.

The concentrations of nitric acid has been reported to affect the sensitivity for lead detection, therefore this parameter was optimized. [145] Five volume per volume (v/v) percentages of 10:1 HNO_3 to H_2O_2 solution in water were analyzed for acid dilution. The v/v percentages examined were 0%, 10%, 25%, 50%, and 75% v/v 10:1 HNO_3 to H_2O_2 solution.

The LOD and LOQ were monitored while this percentage was changed and are summarized in Table 12. The 50% v/v 10:1 nitric acid to hydrogen peroxide solution had the lowest LOD and LOQ while the 75% v/v dilution had the highest.

Percent recovery of lead was also monitored for different nitric acid dilution v/v percentages. (Figure 15) By changing the v/v percentage of the 10:1 HNO_3 to H_2O_2 solution from 0% to 10%, a 10-fold increase in the percent recovery of lead was found and a further increase of the percentage from 10% to 50% resulted in an almost 6-fold increase in percent recovery of lead. However, when the v/v percentage was increased from 50% to 75%, a decrease

in the percent recovery of lead was observed. Therefore, the dilution percentage used throughout the study was 50%v/v nitric to acid to hydrogen peroxide digestion solution.

Table 12. Summary of the LOD and LOQ calculated while varying the percentage of v/v 10:1 HNO_3 to H_2O_2 solution

	Percentage of 10:1 Nitric Acid to Hydrogen Peroxide v/v				
	0%	**10%**	**25%**	**50%**	**75%**
LOD (ng/mL)	8.279 ± 1.496	3.609 ± 0.1916	1.645 ± 0.3244	0.9704 ± 0.6046	4.617 ± 0.4289
LOQ (ng/mL)	27.60 ± 4.988	12.03 ± 0.6387	5.483 ± 1.082	3.235 ± 2.015	15.39 ± 1.430

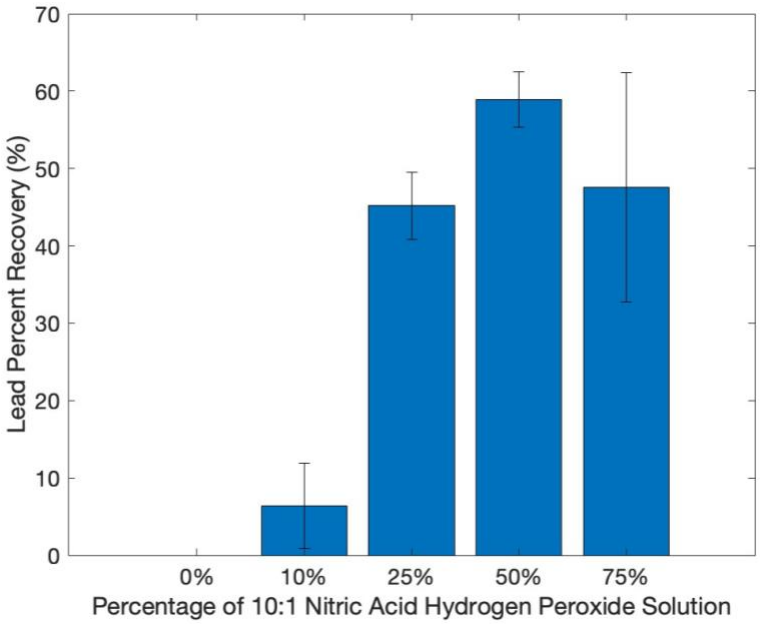

Figure 15. Lead recovery rates found while optimizing the acid dilution percentage of the 10:1 HNO_3 to H_2O_2 ratio used for detection of lead in ECPs

3.2.2.2. Matrix Modification

A matrix modifier is classified as a chemical additive to aid in the detection of analytes within a sample. These modifiers are often needed when a complex matrix is being analyzed, as is the case for ECPs. The ECPs matrix can cause instability of the analytes or lead to adsorption within the graphite furnace. Either of these interactions will decrease the amount of analyte

present in the ionization phase. By adding a matrix modifier, the analytes are isolated and stabilized for analysis.[160, 161] In this study, three different matrix modifiers were explored for the analysis of lead in biological samples: magnesium nitrate, ammonium dihydrogen phosphate, and oxalic acid.

Magnesium nitrate was proposed as a matrix modifier by Slavin *et. al.* in 1985.[162] Initially this matrix modifier was applied for the determination of the elements, aluminum, beryllium, chromium, and manganese.[1] Nonetheless, it was later also successfully applied for the detection of lead and cadmium in food samples.[150]

Ammonium dihydrogen phosphate has been studied extensively for the detection of lead and cadmium.[1] Ammonium helps reduce the concentrations of chloride salts commonly found in biological samples by forming ammonium chloride which decomposes at temperatures around 320°C, effectively removing this part of the matrix before analysis.[161] It has also been classified as a thermal stabilizer for lead and cadmium.[163] Ammonium dihydrogen phosphate has been successfully implemented for the determination of lead in food samples.[149, 150, 61]

Oxalic acid was the last modifier tested as it had been successful in the detection of lead in seawater.[146] When oxalic acid is used, chloride is removed during the drying phase effectively reducing the background signal. [147, 146]

Typically, the atomization of lead is delayed and a high background signal is found when salts or organic matrices are present. Nitric acid, ammonium, and oxalic acid have all been documented to modify the chloride within the matrix thus decreasing its interference. Based on previous successful applications, each of these modifiers was initially tested at a concentration of 100 ng/mL. The original testing of these matrix modifiers determined that ammonium dihydrogen phosphate was the most promising with an initial percent recovery of 102.5 ±

22.42% (Figure 16). However, the magnesium nitrate matrix modifier was more sensitive by a factor of two as shown in Table 13. Oxalic acid matrix modifier was neither sensitive nor accurate and was therefore excluded from further studies. According to the recovery rates of the analyte (Figure 16), magnesium nitrate was clearly less suitable than ammonium dihydrogen phosphate. Therefore, only ammonium dihydrogen phosphate was further explored.

Table 13. Summary of the LOD and LOQ for initial selection of a matrix modifiers

	Matrix Modifier		
	Magnesium Nitrate	**Ammonium Dihydrogen Phosphate**	**Oxalic Acid**
LOD (ng/mL)	0.7335 ± 0.2448	1.967 ± 1.047	3.889 ± 1.223
LOQ (ng/mL)	2.445 ± 0.8161	6.555 ± 3.489	12.96 ± 4.11

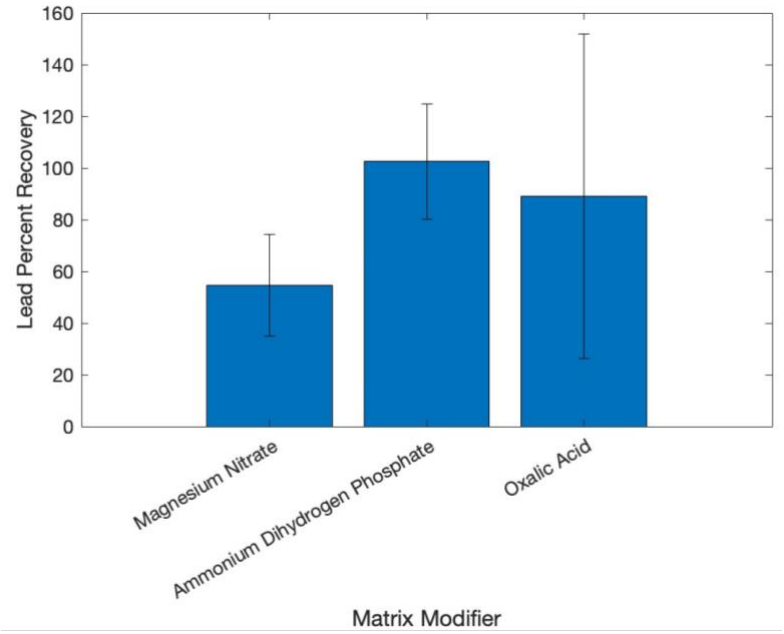

Figure 16. Lead recovery rates found for the three different matrix modifiers

The sensitivity of the ammonium dihydrogen phosphate modifier required improvement for the purpose of this study, resulting in the application of an optimization process. The first parameter optimized was the concentration of ammonium dihydrogen phosphate followed by the variation of the ratio between nitric acid and hydrogen peroxide.

The concentrations of ammonium dihydrogen phosphate analyzed were 50 ng/mL, 100 ng/mL, and 200 ng/mL. Figure 17 and Table 14 show clearly that the initial concentration of 100 ng/mL ammonium dihydrogen peroxide matrix modifier was the optimal choice, as it remained the most sensitive. The percent recovery did not improve with the variation of matrix modifier concentration: at 50 ng/mL concentration there was little to no recovery of lead and at 200 ng/mL concentration of matrix modifier a decrease in lead recovery rates was observed. As a result, it was decided that the 100 ng/mL concentration should be kept constant while the ratio of nitric acid to hydrogen peroxide was varied.

Table 14. Summary of LOD and LOQ for different concentrations of ammonium dihydrogen phosphate matrix modifier

	Concentration of Ammonium Dihydrogen Phosphate		
	50 ng/mL	**100 ng/mL**	**200 ng/mL**
LOD (ng/mL)	3.587 ± 0.1189	1.287 ± 0.8262	2.088 ± 0.6328
LOQ (ng/mL)	11.96 ± 0.3962	4.290 ± 2.754	6.959 ± 2.109

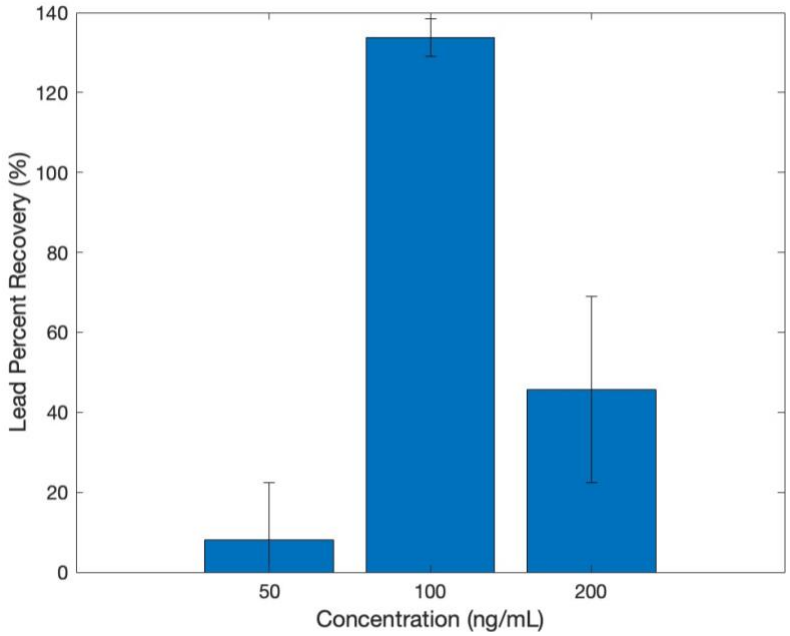

Figure 17. Lead recovery rates during optimization of ammonium dihydrogen phosphate modifier concentration for the detection of lead in ECPs

The ratio of nitric acid to hydrogen peroxide was evaluated in the attempt to maintain the high percent recovery for lead in ECP's and decrease the standard deviation, LOD, and LOQ values. However, as seen in Figure 18 and Table 15 there was no improvement for these parameters. It was therefore decided that for the repeatability study the method used was the addition of 100 ng/mL of ammonium dihydrogen phosphate as the matrix modifier and treatment with 50% v/v 10:1 HNO_3 to H_2O_2 solution.

Table 15. Summary of LOD and LOQ for different ratios of 50% v/v HNO_3 to H_2O_2 solution for the detection of lead using 100 ng/mL ammonium dihydrogen peroxide as a matrix modifier in ECP

	The Ratio of Nitric Acid to Hydrogen Peroxide			
	2:1	**5:1**	**10:1**	**15:1**
LOD (ng/mL)	2.480 ± 0.03012	2.374 ± 0.4434	1.786 ± 0.8458	4.154 ± 0.2756
LOQ (ng/mL)	7.001 ± 0.1004	7.913 ± 1.478	5.953 ± 2.819	13.85 ± 0.9186

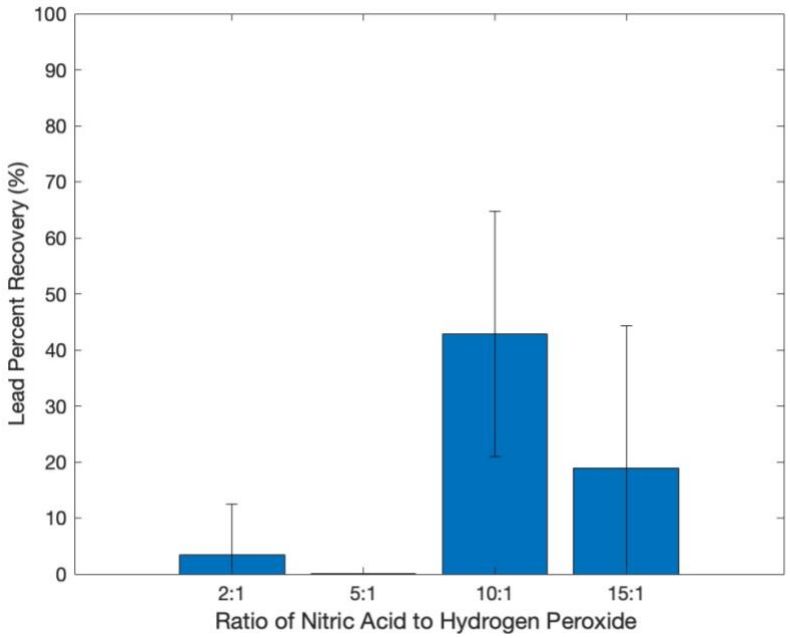

Figure 18. Lead recovery rates during optimization of the ratio of 50% v/v HNO_3 to H_2O_2 for the detection of lead in ECPs within the matrix modifier method

3.2.2.4. Conventional Heating Digestion Methods

Acid digestion is accomplished by adding an oxidizing agent such as nitric acid, and subsequently applying heat. Heating the solution accelerates the decomposition process.[164] Two conventional heating methods were evaluated in this study: temperature controlled acid digestion and open-vessel acid digestion (OVAD). These acid digestion methods were explored based on reports of successful lead detection in wine,[165] crude oil,[166] foodstuff,[167, 168,163] and human hair.[169, 170, 171]

3.2.2.4.1. Temperature Controlled Acid Digestion

Temperature control acid digestion uses a heat block in which the samples are place. Six digestion times, 0.25, 0.5, 1.0, 2.0, 3.0, and 4.0 hours were evaluated. Figure 19 displays the lead recovery rate in response to digestion time. Figure 19 indicates that digestion times of less than one hour had the highest standard deviations, but at the two-hour digestion time, the standard deviations dropped drastically. Applying a two-hour digestion time also provided the highest percent recovery for lead whereas a longer digestion time yielded lower recovery rates. The LOD and LOQ for the two-hour digestions time were found to be 1.030 ± 0.5385 ng/mL and 3.433 ± 1.795 ng/mL respectively, and a two-hour digestion time was utilized throughout the optimization process for lead detection in ECPs.

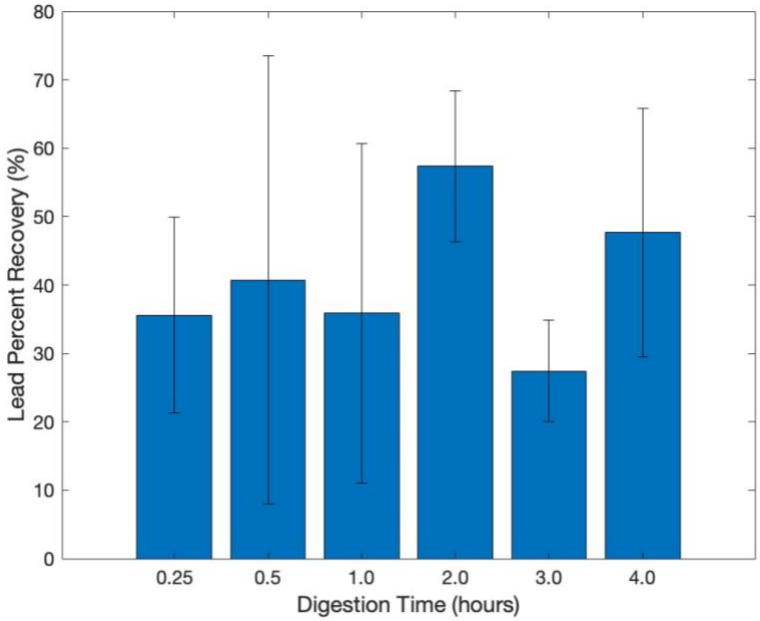

Figure 19. Lead recovery rates during optimization of digestion time utilizing the heat-assisted acid digestion method in 50% v/v HNO_3 to H_2O_2 solution

The other variable that was optimized for temperature controlled acid digestion was the ratio of nitric acid to hydrogen peroxide. The ratios tested were of 2:1, 5:1, 10:1 and 15:1. The 10:1 nitric acid to hydrogen peroxide solution maintained the highest percent recovery but only achieved a percent recovery of 60.0 ± 14.3% as shown in Figure 20. This ratio additionally had the lowest LOD and LOQ as seen in Table 16. As a result, the two-hour digestion time and the 50% v/v 10:1 ratio of HNO_3 to H_2O_2 were considered the optimal conditions. However, these conditions were unable to reach the required recovery rate of 100 ± 15% and this method was not explored further.

Table 16. Summary of lead LOD and LOQ for different HNO_3 to H_2O_2 ratios with 50% v/v HNO3 using heat-assisted acid digestion

	Ratio of Nitric Acid to Hydrogen Peroxide			
	2:1	**5:1**	**10:1**	**15:1**
LOD (ng/mL)	2.396 ± 1.923	4.231 ± 3.487	1.037 ± 0.4399	7.377 ± 0.1519
LOQ (ng/mL)	7.988 ± 6.411	14.10 ± 11.62	3.458 ± 1.466	24.59 ± 0.05064

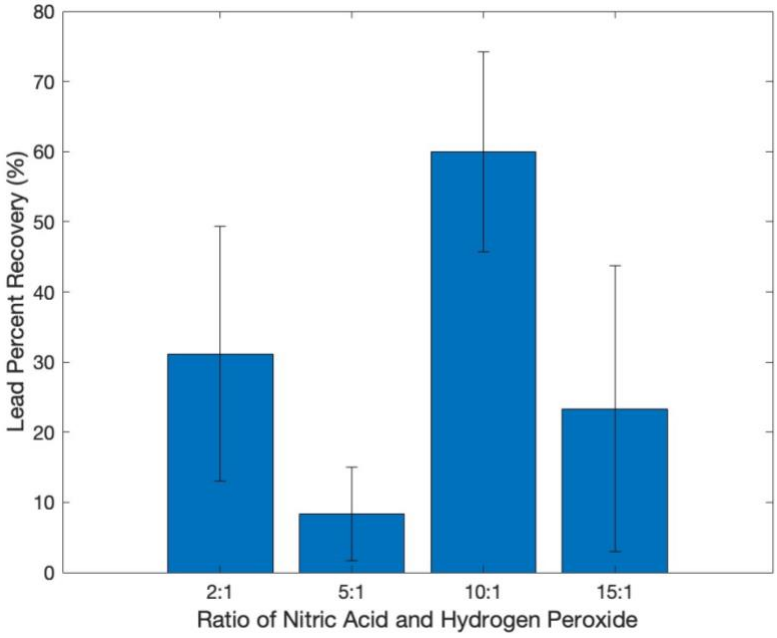

Figure 20. Lead recovery rates for different HNO_3 to H_2O_2 ratios using 50% v/v nitric acid applied to heat assisted acid digestion

3.2.2.4.2. Open-Vessel Acid Digestion Method

Open vessel acid digestion (OVAD) was explored as an alternative conventional heating digestion method. Initially, digestion times inspected were 0.5, 1.0, 2.0, 3.0, and 4.0 hours. Figure 21 reports the lead recovery rate for the different digestion times. All sample sets showed high standard deviation, with the exception of four hours digestion time. Unfortunately, the four-hour digestion time had the lowest lead recovery rate, indicating loss of analyte. The LOD and LOQ were found to be 0.2413 ± 0.1016 ng/mL and 0.8043 ± 0.3385 ng/mL, respectively. Despite the two-hour digestion time having a large standard deviation, it was still used for further optimization.

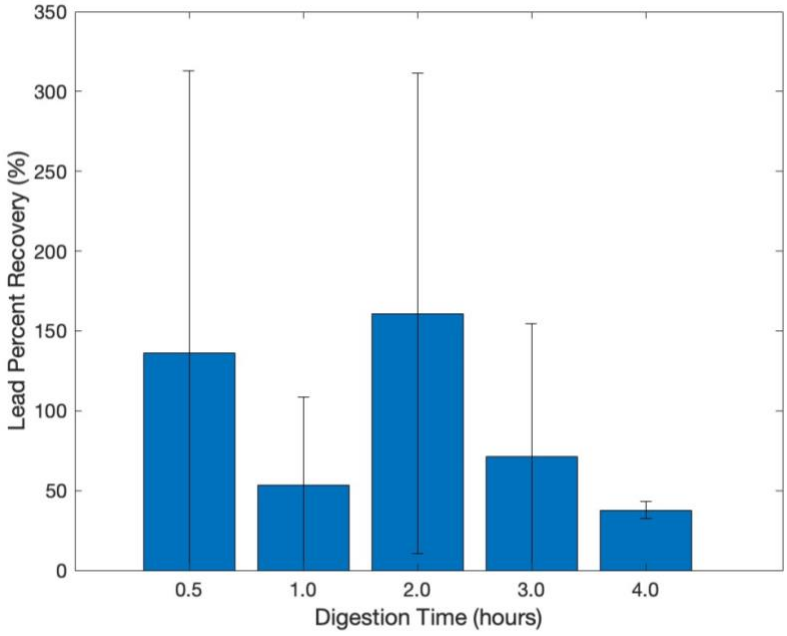

Figure 21. Lead recovery rates at different digestion times utilizing the open-vessel acid digestion method in 50% v/v 10:1 HNO_3 to H_2O_2 solution

The ratios of nitric acid to hydrogen peroxide solution tested were 2:1, 5:1, 10:1 and 15:1 nitric acid to hydrogen peroxide, similar to the temperature controlled acid digestion. The original 10:1 ratio provided the lowest LOD and LOQ and the highest percent recovery of lead (Figure 22, Table 17**)**. Similar to the previous conventional heating methods, this approach was unable to reach the necessary recovery rates and was not explored further.

Table 17. Summary of lead LOD and LOQ for different HNO_3 to H_2O_2 ratios with 50% v/v nitric acid using open-vessel acid digestion

	Ratio of Nitric Acid to Hydrogen Peroxide			
	2:1	**5:1**	**10:1**	**15:1**
LOD (ng/mL)	2.396 ± 1.923	2.391 ± 0.1335	0.2413 ± 0.1016	0.5128 ± 0.1966
LOQ (ng/mL)	7.988 ± 6.411	7.969 ± 0.4450	0.8043 ± 0.3385	1.709 ± 0.6552

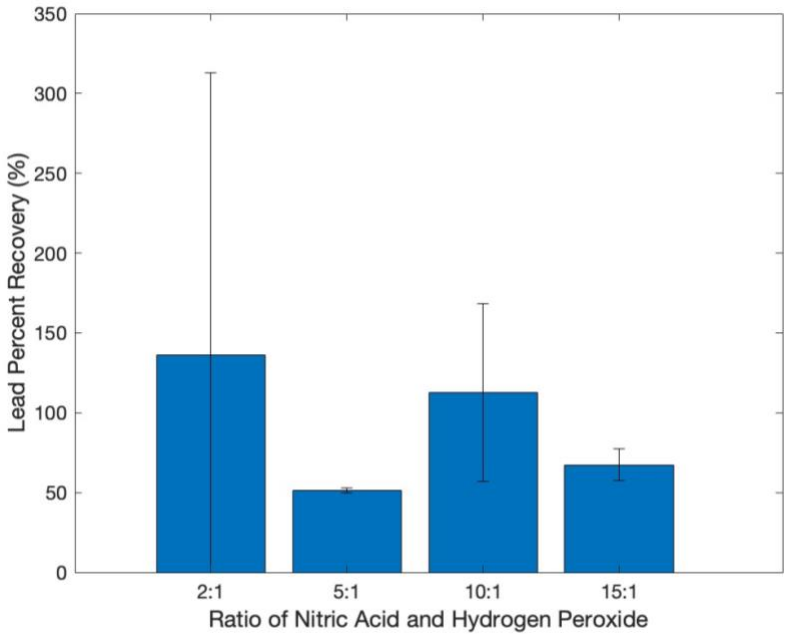

Figure 22. ECP lead recovery rates for different HNO_3 to H_2O_2 ratio with 50%v/v and utilizing the open-vessel acid digestion method

3.2.2.5. Microwave-Assisted Acid Digestion

Microwaves heat solvents by dielectric heating processes, dipolar polarization or ionic conduction. Dipoles generate heat when irradiated with microwaves on account of the oscillating microwave field causing the dipoles to rotate, producing friction, and consequently heat. In ionic conduction, dissolved charged particles oscillate back and forth when irradiated with microwaves causing a collision between the charged particles thus creating heat.[172] These processes are essential, as they allow samples to be heated from within, while in conventional methods as demonstrated in the previous sections, the samples are heated from externally. (Figure 23)

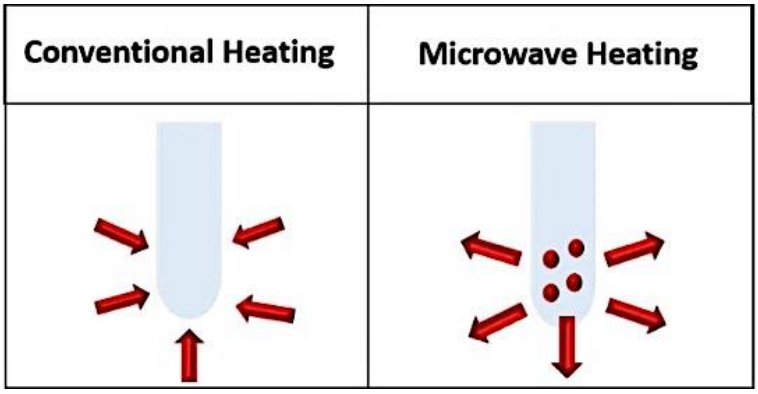

Figure 23. Depiction of conventional heating compared to heating with microwaves

Microwave irradiation interacts differently depending on the type of material. These interactions are either through reflection, absorption, or transmission as shown in Figure 24. For metals, the microwaves are reflected while materials made of Teflon, glass, or quartz allow for transmission and solvents will absorb the microwave radiation.[172]

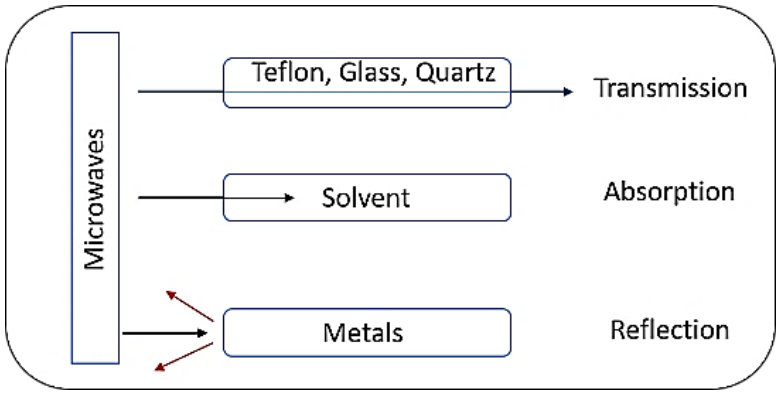

Figure 24. Different interactions that microwaves have with different materials

Besides the heating process, an additional important property of microwave digestion is that the digestion vessels are closed and sealed allowing for heating of the solution beyond its boiling point.[173] This property can greatly diminish digestion times and potential contamination. Using microwave-assisted acid digestion (MAAD) was already successfully implemented for the detection of lead in a multitude of sample matrices such as pitch or crude oil, [174] scalp hair,[169, 170] foodstuffs, [16, 61,99, 163, 168, 175-177] lipstick,[178] cigarette filters,[179] and fish.[180, 181] This suggests that

MAAD would be a promising approach for the quantification of lead in *E. coli* and other biological and environmental samples.

As described in section 2.4.4 a sample set was initially digested for 40 seconds at 600 watts using a 50% v/v 10:1 HNO_3 to H_2O_2 solution. The percent recovery for lead was 74.80 ± 19.85%, which was not sufficient to meet the requirements. To improve the percent recovery of lead, the time, power applied, and the ratio of nitric acid to hydrogen peroxide solution were varied systematically.

For the microwave digestion time optimization, seven digestion times were assessed, ranging from 30 to 90 seconds at 10-second intervals. The percent recovery of lead found at each microwave digestion time is shown in Figure 25. The highest percent recovery of lead was found at 60 seconds, which was then applied for all subsequent experiments. The LOD was 0.6037 ± 0.3500 ng/mL and LOQ was 2.012 ± 1.167 ng/mL.

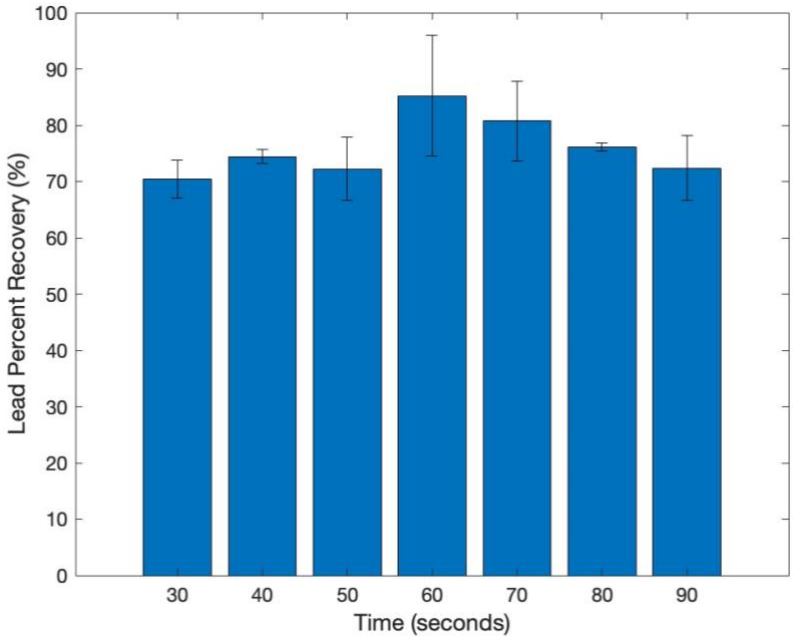

Figure 25. Lead recovery rates at different microwave digestion time for ECP's in 10:1 HNO_3 to H_2O_2 solution.

The next parameter optimized was the power applied for the digestion of ECPs. Similar to previous procedures, the percent recovery of lead was determined, but with changed power settings, and maintaining a constant time of digestion at 60 seconds. As depicted in Figure 26 there was no change in lead percent recovery for the different power settings applied, therefore in all studies going forward, the maximum power of 1200 watts was used. The LOD and LOQ remained sensitive at 0.4849 ± 0.1478 ng/mL and 1.616 ± 0.4925 ng/mL, respectively.

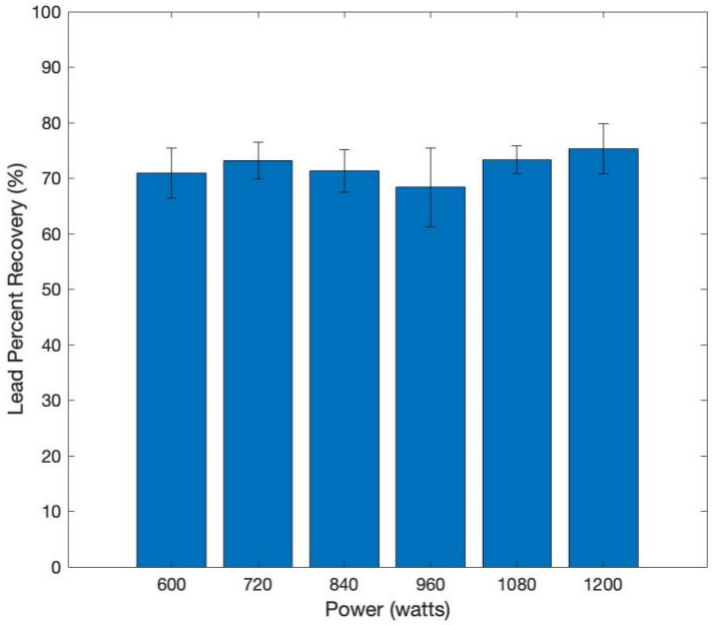

Figure 26. ECP lead recovery rates for different microwave power settings and 60 seconds digestion time and 50% v/v 10:1 HNO_3 to H_2O_2 solution

The final parameter optimized was the ratio between nitric acid and hydrogen peroxide. Initially, the ratios examined were the same as before 50% v/v; 2:1, 5:1, 10:1, and 15:1. However, the 5:1 showed the highest percent recovery for lead with 80.1 ± 2.23%. This was not sufficiently close to 100% and the ratios of 4:1 and 6:1 were also investigated. It was found that a ratio of 4:1 gave the highest recovery of 90.7 ± 10.04%. (Figure 27) The LOD and LOQ for each ratio were also determined and are summarized in Table 18, finding all values to be less than 1 ng/mL and 3 ng/mL respectively. The 4:1 acidic ratio had the second lowest LOD and

LOQ of 0.5647 ± 0.4016 ng/mL and 1.882 ± 1.339 ng/mL. The low LOD and LOQ values indicated that the sensitivity of the method was improved after varying the ratio of nitric acid to hydrogen peroxide, which had been previously reported as well.[145]

The optimal parameters for the MAAD procedure is summarized as treatment of samples with 500 μL of 4:1 HNO_3 to H_2O_2 solution, diluting it to 1.0 mL with ultrapure water and digesting the sample for one minute at 1200 watts. This procedure will be further studied in the repeatability and selectivity studies.

Table 18. Summary of LOD and LOQ for lead in ECP for different nitric acid to hydrogen peroxide ratios using 50% v/v ratios of HNO_3 to H_2O_2 and microwave assisted acid digestion

Ratio of Nitric Acid to Hydrogen Peroxide	**LOD (ng/mL)**	**LOQ (ng/mL)**
2:1	0.9742 ± 0.2033	3.247 ± 0.6779
4:1	0.5647 ± 0.4016	1.882 ± 1.339
5:1	0.7158 ± 0.3616	2.386 ± 1.205
6:1	0.4332 ± 0.1193	1.444 ± 0.3975
10:1	1.426 ± 1.091	4.755 ± 3.635
15:1	2.274 ± 0.2432	7.580 ± 0.8106

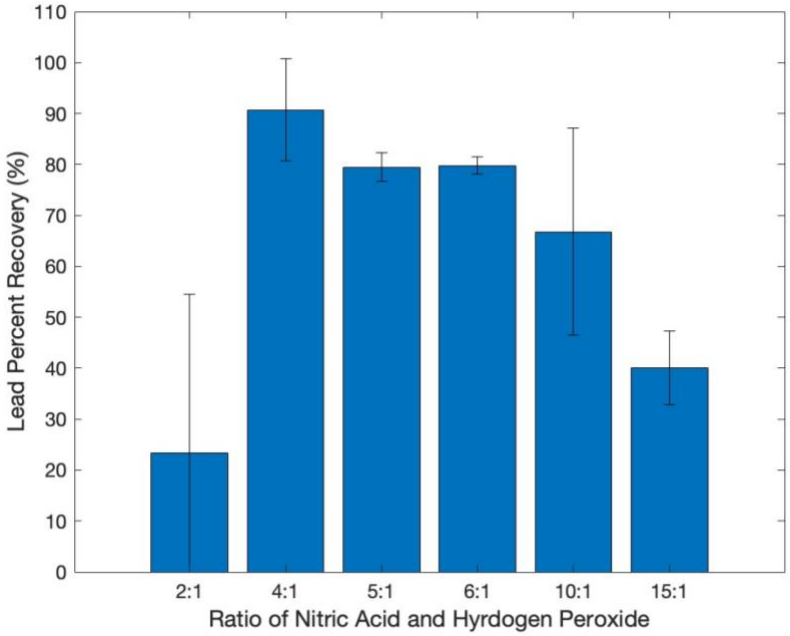

Figure 27. ECP lead recovery rates for different HNO_3 to H_2O_2 and 50% v/v nitric acid utilizing microwave-assisted acid digestion

3.2.3. Figures of Merit for the Best Performing Sample Preparation Methods

In the subsequent steps, the repeatability, sensitivity, and selectivity were all assessed for the methods explored which met the recovery rate requirements of 100 ± 15%. The comparison was made between the matrix modifier and MAAD methods at optimal conditions: matrix modification using 100 ng/mL $NH_4H_2PO_4$ and 50% v/v 10:1 HNO_3 to H_2O_2 solution and microwave-assisted acid digestion using 60 second digestion time at 1200 watts and 4:1 HNO_3 to H_2O_2 solution.

3.2.3.1. Repeatability for the Best Performing Sample Preparation Methods

The repeatability study was determined as described in section 2.5.1 by assessing average percent recovery and RSD value. Both are summarized in Table 19.

Table 19. Lead Average percent of recovery and RSD values for matrix modifier and MAAD.

Method	Average Lead Percent Recovery (%)	RSD
Matrix Modifier: $NH_4H_2PO_4$	41.79 ± 36.81	88.08%
Microwave-Assisted Acid Digestion	99.01 ± 9.46	9.55%

The results listed in Table 19 clearly show that the MAAD method is superior to matrix modification for the analysis of lead in ECPs. It was the only method that met the criteria of a percent recovery of 100 ± 15% and a low RSD of 15%. The higher recovery rates were most likely due to the more complete digestion of the samples that occur with MAAD methods. The boiling point for nitric acid is 83°C and temperatures during decomposition within the digestion vessels can reach up to 170°C allowing for the sample to be heated well beyond its boiling point, thus resulting in a more complete digestion of the sample.[164] The MAAD method had an average recovery of 99.01 ± 9.46% for lead. This value illustrates that this method was both accurate and precise. MAAD also had a reported RSD value of 15.75% indicating that it was repeatable. This was the smallest RSD value of all explored analytical procedures.

3.2.3.2. Sensitivity for the Best Performing Sample Preparation Methods

The LOD and LOQ were used as a measurement of sensitivity and are summarized in Table 20 for ease of comparison.

Table 20. Lead LOD and LOQ values for matrix modification and MAAD.

Method	LOD (ng/mL)	LOQ (ng/mL)
Matrix Modification	1.680 ± 0.9060	5.599 ± 3.021
Microwave-Assisted Acid Digestion	0.5647 ± 0.4016	1.882 ± 1.339

Matrix modification had a substantially higher LOD and more importantly a higher LOQ than MAAD. This aligns with previous studies reporting that matrix modification methods have

difficulties with sensitivity[160] and clearly shows that MAAD is more sensitive than the matrix modification method.

3.2.3.3. Selectivity for Best Performing Sample Preparation Method: MAAD

Selectivity describes a method's ability to determine the analyte in the presence of other chemicals within the sample without interferences.[101] Determination of analytes can be negatively impacted by the presence of large amounts of contaminants within a sample, as these can cause interference during sample preparation and/or during spectrochemical analysis. Generally, interferences are classified as either spectral or non-spectral. Main causes of spectral interference are direct overlapping of the analytical line with the absorption line of another element, absorption at the analytical line by other molecules, absorption by concomitants from the radiation source that are not properly separated by the monochromator, and scattering.[1] To eliminate spectral interferences, the most common approach is to change to an alternate analytical line.[1] A non-spectral interference is present when forms of the analyte are no longer completely dissociated at the atomization temperature causing inaccurate absorption readings. This occurs when the interference forms stable compounds with the analyte.[182] Non-spectral interferences is minimized by dilution and properly accounting for the matrix within the calibration curve or by the use of a matrix modifier.[1] Since MAAD was the only sample preparation method which met the performance criteria, the selectivity was determined only for this method. It was found that MAAD method maintained the recovery rates of 100 ± 15% while in presence of interferences (Figure 28) thus the method was selective for analysis of lead in ECPs.

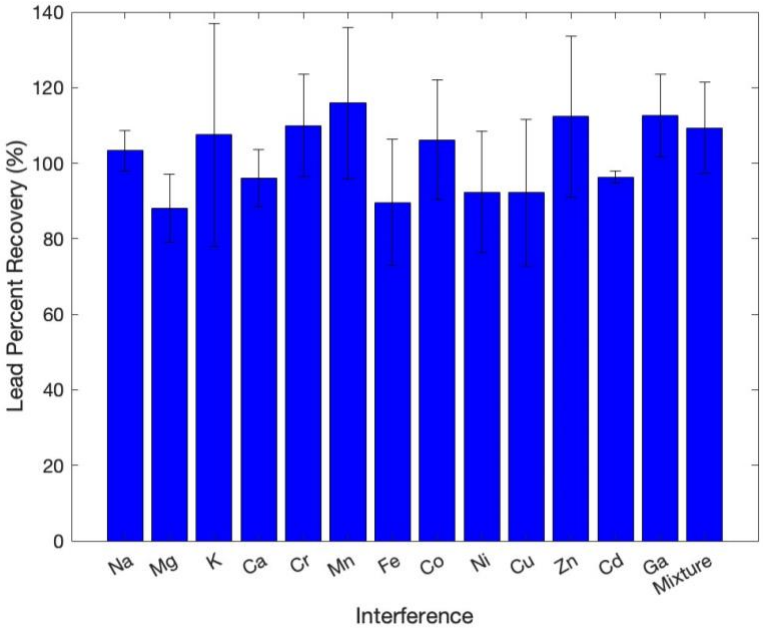

Figure 28. Lead Recovery rate in dependency of interfering element utilizing Microwave Assisted Acid Digestion

3.2.4. Summary of Part II

Five different analytical procedures were examined and evaluated for the detection of lead in ECPs. Table 21 summarizes the data showing that neither acid dilution, matrix modification, temperature control, nor OVAD met any parameters required for accurate and precise analysis. The only method that met all the parameters was MAAD. Therefore, this method was then also applied for the determination of cadmium, chromium, copper, and zinc in ECPs.

Table 21. Summary of method figures of merit requirements

Method	Accurate	Precise	Repeatable	Sensitive	Selective
Acid Dilution	⊘	⊘	⊘	✓	⊘
Matrix Modifier	⊘	⊘	⊘	⊘	⊘
Temperature Controlled Acid Digestion	⊘	⊘	⊘	✓	⊘
Open-Vessel Acid Digestion	⊘	⊘	⊘	✓	⊘
Microwave-Assisted Acid Digestion	✓	✓	✓	✓	✓

3.3. Part III: Quantification of Cadmium, Chromium, Copper, and Zinc in Escherichia coli cell pellets

The MAAD sample preparation method was applied for the determination of the additional analytes; cadmium, chromium, copper, and zinc in ECPs using the same validation process as was used for lead. A similar MAAD approach was successfully applied for the analysis of cadmium,[99, 174, 177, 183] chromium,[99, 183, 184] copper[99, 177, 183] and zinc[170, 174, 177, 184] in a variety of different matrices, therefore using *E. coli* will be an extension of these studies.

As for lead the parameters investigated were optimization of the analytes furnace program, assessing the validity of MAAD based on figures of merits, and finally assessing the method's selectivity analysis for the different analytes.

3.3.1. Optimization of the Graphite Furnace Thermal Program for Cadmium, Chromium, Copper, and Zinc

As described in section 2.3, the thermal program of the instrument was optimized for each analyte.

3.3.1.1. Cadmium

The optimization of cadmium for the pyrolysis and atomization stage is shown in Figure 29. For the pyrolysis stage optimization cadmium absorption were monitored for temperatures ranging from 300 to 800°C. It was found that the absorption for cadmium was higher at lower temperatures with the highest absorption and smallest standard deviation at 300°C (Figure 29A). Therefore, this temperature was used for the analysis of cadmium in biological samples. The atomization program optimization was accomplished by varying temperatures from 1750-2400°C, as well as by monitoring cadmium absorption. It was determined that a range of temperatures from 2200°C was suitable for atomization temperature (Figure 29B), as it had the highest absorption.

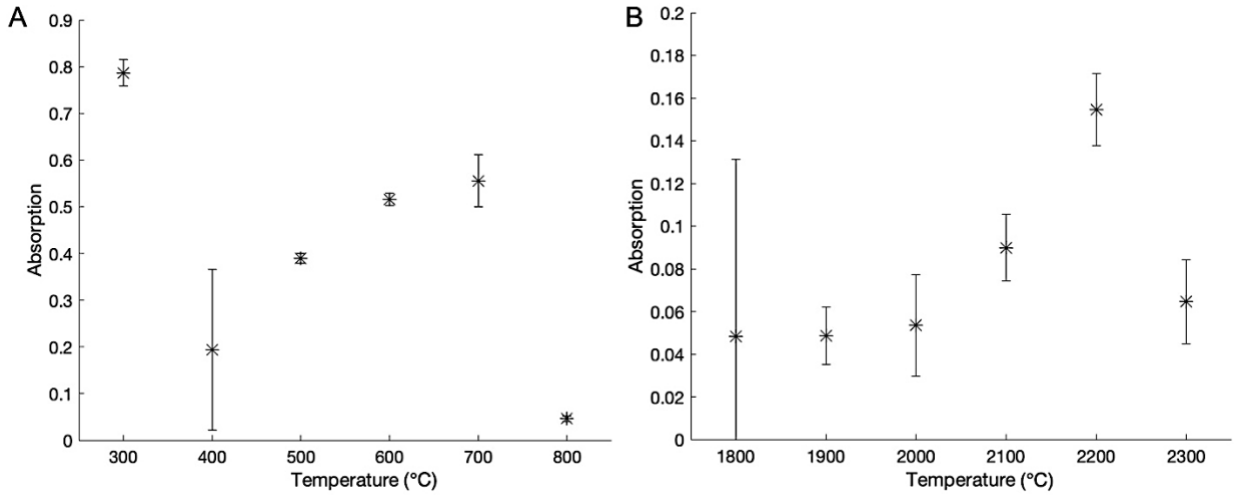

Figure 29. Thermal program optimization for cadmium analysis in biological samples A) pyrolysis stage optimization and B) atomization stage optimization

The optimized graphite furnace program that was used for cadmium analysis throughout this study is shown in Table 22.

Table 22. Optimized Graphite Furnace Thermal Program for Cadmium Quantification

Step	Process	Temperature °C	Time (sec)
1	Drying	60	3
2		150	20
3		250	10
4	Pyrolysis	300	10
5		300	10
6		300	3
7	Atomization	2200	3
8	Cleaning	2500	2

3.3.1.2. Chromium

Optimization of the chromium graphite furnace thermal program was accomplished as shown in Figure 30. Figure 30A displays the optimization of the pyrolysis stage, demonstrating that temperatures between 300-700°C are suitable as pyrolysis temperature. A pyrolysis temperature of 300 °C was then selected throughout the study since it had the highest absorption and the smallest standard deviation. Atomization optimization is shown in Figure 30B. The highest absorption was found at an atomization temperature of 2100 °C, and this temperature was used for the analysis of chromium. Table 23 lists optimized graphite thermal program for chromium analysis used throughout this study.

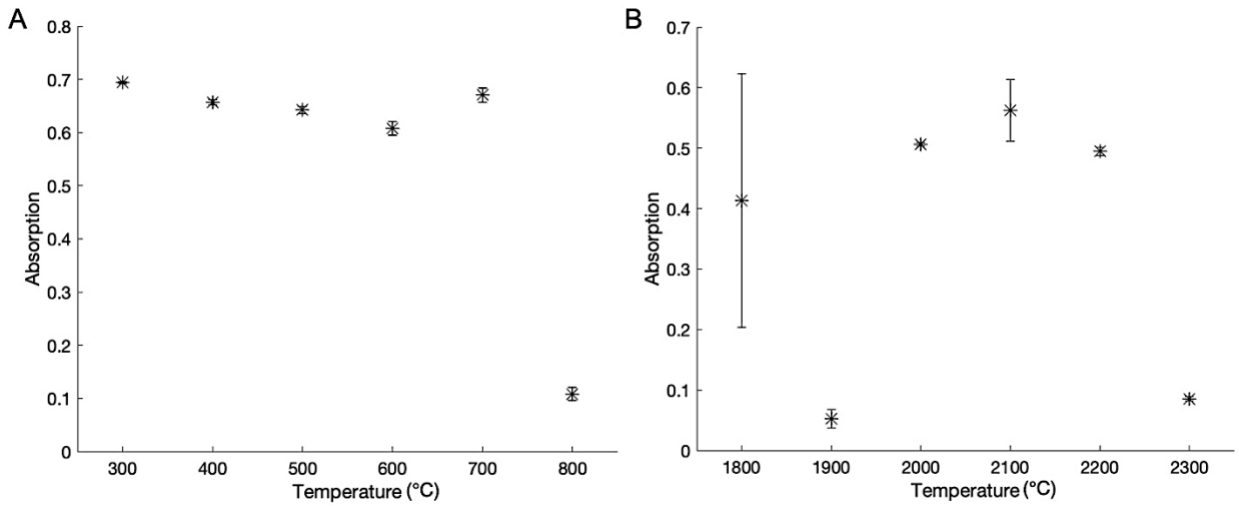

Figure 30. Thermal program optimization for chromium analysis in biological samples A) pyrolysis stage optimization and B) atomization stage optimization

Table 23. Optimized Graphite Furnace Thermal Program for Chromium Quantification

Step	Process	Temperature °C	Time (sec)
1	Drying	60	3
2		150	20
3		250	10
4	Pyrolysis	300	10
5		300	10
6		300	3
7	Atomization	2100	3
8	Cleaning	2500	2

3.3.1.3. Copper

The graphite furnace thermal program for copper was optimized in the same manner as the previous analytes. The optimal temperature for the copper pyrolysis stage was found to be 800°C as it had the highest absorption and the smallest standard deviation (Figure 31A). For the optimization of the atomization stage, the highest copper recovery rate was obtained when using 2400°C (Figure 31B). As a result, 800°C and 2400°C were used as the pyrolysis and atomization temperatures for the graphite furnace thermal program for copper analysis throughout the study. Table 24 summarizes these results.

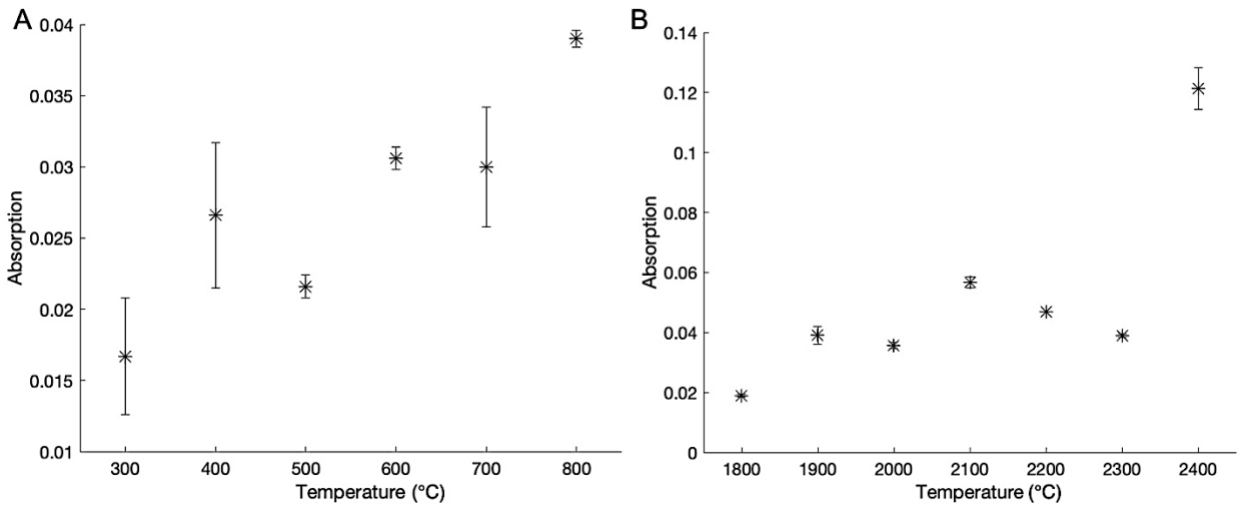

Figure 31. Graphite furnace thermal program optimization for copper analysis in biological samples A) pyrolysis stage optimization and B) atomization stage optimization

Table 24. Optimized Graphite Furnace Thermal Program for Copper Quantification

Step	Process	Temperature °C	Time (sec)
1	Drying	60	3
2		150	20
3		250	10
4	Pyrolysis	800	10
5		800	10
6		800	3
7	Atomization	2400	3
8	Cleaning	2500	2

3.3.1.4. Zinc

The final element that needed graphite furnace thermal program optimization was zinc and the results are shown in Figure 32. The optimized pyrolysis temperature was found to be 700 °C, which provided the highest absorption and the smallest standard deviation. Even though 800°C had a higher recovery rate, it had a large standard deviation, which was not acceptable. The optimized atomization temperature was determined to be 2000°C as it gave the highest

absorption (Figure 32B). The optimized thermal program used for zinc analysis is reported in Table 25.

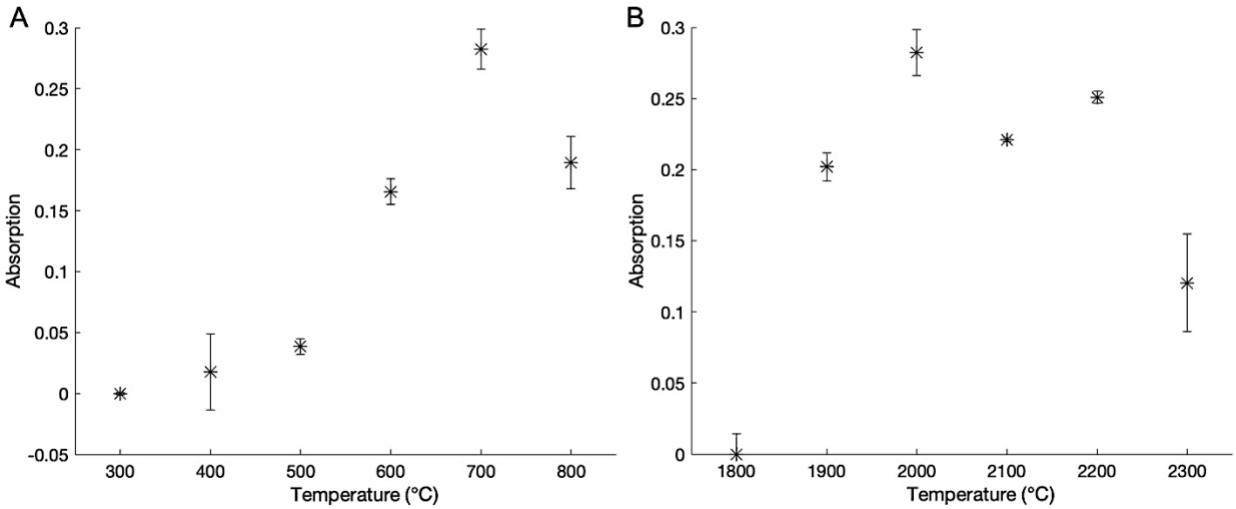

Figure 32. Graphite furnace thermal program optimization for zinc analysis in biological samples A) pyrolysis stage optimization and B) atomization stage optimization

Table 25. Optimized Graphite Furnace Thermal Program for Zinc Quantification

Step	Process	Temperature °C	Time (sec)
1	Drying	60	3
2		150	20
3		250	10
4	Pyrolysis	700	10
5		700	10
6		700	3
7	Atomization	2000	3
8	Cleaning	2500	2

3.3.2. Figures of Merit for Quantification of Cadmium, Chromium, Copper, and Zinc

Accuracy, precision, LOQ, and repeatability were determined for Cd, Cr, Cu, and Zn. It was found that the MAAD method performed equally well for all the above analytes except for zinc. Zinc had a LOQ value of 50.42 ± 13.86, ng/mL which is nearly ten times higher than the other elements determined in this study. The reason for a higher zinc LOQ value is likely related

to the method of LOQ determination. The linear range in the regression curve for zinc was 1.0 - 70 ng/mL, whereas the linear range for copper and chromium was between 0.25 and 20 ng/mL, and cadmium had a linear range of 0.1 and 5.0 ng/mL. The LOD and LOQ in this study were determined utilizing the linear range. Table 26 summarizes the data.

Table 26. Performance of the developed and optimized sample preparation method for cadmium, chromium, copper, and zinc

Element	**Percent Recovery (%)**	**LOD (ng/mL)**	**LOQ (ng/mL)**	**RSD (%)**
Cadmium	109.8 ± 11.6	0.1364 ± 0.04605	0.4547 ± 0.1534	10.6 %
Chromium	98.66 ± 9.48	0.4974 ± 0.3248	2.366 ± 0.7999	9.61 %
Copper	99.23 ± 4.79	1.19 ± 0.162	3.953 ± 0.5390	4.83 %
Zinc	100.3 ± 11.9	15.12 ± 4.162	50.42 ± 13.86	11.8 %

Based on these results, it was concluded that the developed MAAD method can be used to accurately and precisely determine the analytes cadmium, chromium, copper, and zinc.

3.3.3. Selectivity of the method for Quantification of Cadmium, Chromium, Copper, and Zinc

The selectivity of the method was assessed similarly to that of lead for cadmium, chromium, copper, and zinc. The results for each element are summarized in Figure 33. Cadmium and copper both maintained percent recoveries of 100 ± 15% and the detection for these analytes was considered selective (Figure 33A & 33B).

The detection of chromium had a recovery rate of 100 ± 15% except when spiked with 380 ng/mL of zinc (Figure 33B) producing an artificially high value of 120.8 ± 21.79%. This deviation could not be attributed to spectral overlap as the analytical line of chromium at 357.9 nm is too far from the main emission lines for zinc at 213.9 nm. The interference is likely caused by a non-spectral interference[182] and related to chemical interferences caused by a change in the fraction of analyte dissociated, ionized, and excited in the vapor phase. Inside the graphite furnace such interference is typically caused by anions, like chlorides which are difficult to

dissociate. The change in dissociation ratio can shift the absorption peak results in an absorption peak enhancement.[185, 186] The mechanisms of chemical interference are not well understood at this time, and no reports of this specific interaction were found.

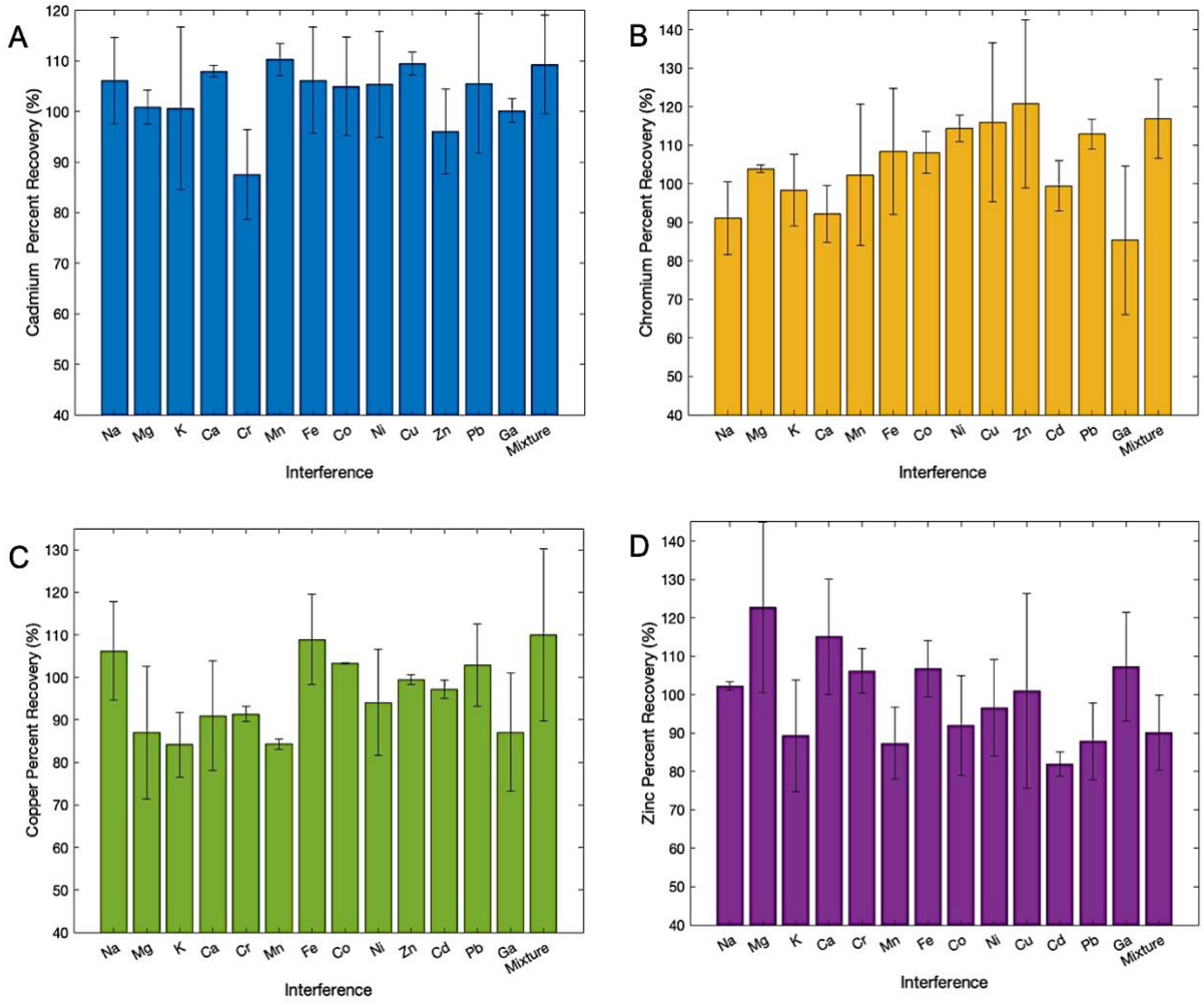

Figure 33. Selectivity of the Method A) Cadmium B) Chromium C) Copper and D) Zinc

The determination of zinc also fell outside of the recovery range when exposed to high concentrations of magnesium and cadmium. In the presence of high concentrations of magnesium, zinc had an artificially high recovery rate of 122.8 ± 22.22% (Figure 33D). Zinc's analytical line was measured at 213.9 nm, and spectral overlap also unlikely, as the nearest magnesium absorption line is located at 202.6 nm. As before, it is likely that the artificially high

value was the result of a vapor phase interference from the thermal decomposition of $MgCl_2$. This has been previously reported in regards to magnesium by Huang & Shih when detecting zinc in sea water.[187]

In the presence of high concentrations of cadmium, the zinc recovery rate decreased below 85%. This decrease is most likely related to the graphite furnace thermal program for zinc, which may not sufficiently remove cadmium from the sample at high concentrations. The spiked concentration for cadmium was 60 ng/mL. Even though this concentration was much lower than the reported lethal dose for cadmium in human of 2,000 ng/mL,[31] for clinical samples, the concentration selected for the cadmium spike is unlikely as reported by Davis *et. al.* and da Silva *et. al.*[188] [189] Therefore, the graphite furnace thermal program remained unchanged. Overall, the MAAD method proved to selectively quantify cadmium, chromium, copper, and zinc in ECPs.

3.4. Part IV. Analysis of Certified Reference Material

The developed method was validated using a certified reference material (CRM). The CRM is a material that has certified values for its elemental concentration chemical, and allows for the assessment of the accuracy of a developed method and the calculation of relative error.[101] Since no clinical or biological CRM exist, BCR-679-white cabbage powder was chosen because of its similar matrix composition compared to biological and environmental samples besides having reported values for four out of the five analytes being studied. The CRM material was treated as described in section 2.7. The number of subsamples differed for each analyte as instructed by the certificate. Lead did not have a reported value and 10 subsamples were evaluated as it is common practice in such cases.[190] The mass fractions (mg/kg) determined using the developed MAAD method are summarized in Table 27. The last two columns show the

deviation from the certified value in percent and the number of subsamples analyzed for each element, respectively.

Table 27. Comparison of the measured and certified mass fractions for Pb, Cd, Cr, Cu, and Zn determined in BCR 679 and using the developed sample preparation method.

Element	Experimental Mass Fraction (mg/kg)	Reference Mass Fraction (mg/kg)	Percent Deviation (%)	Number of Subsamples
Lead	0.2078 ± 0.03926	Not reported	NA	10
Cadmium	1.586 ± 0.1608	1.66 ± 0.07	4.457	15
Chromium	0.5836 ± 0.05665	0.6 ± 0.1	2.717	5
Copper	2.743 ± 0.3045	2.89 ± 0.12	5.087	15
Zinc	78.29 ± 2.861	79.7 ± 2.7	1.769	20

To confirm that the calculated concentrations were accurate, the percent deviation was calculated as shown in Equation 3-7, where x is the experimental concentration and μ is the certified reference value shown in the third column of Table 27.

$$Percent\ Deviation\ from\ certified\ value\ (\%) = \frac{|x-\mu|}{\mu} * 100 \qquad \textit{Equation 3-7}$$

The percent deviation from the certified value for cadmium, chromium, copper, and zinc was 5% or less, confirming that the MAAD procedure was accurate.

An alternative approach of validating the accuracy of a method is by analyzing the same sample with a different analytical method and comparing the results. In this case, a secondary analysis was performed with total reflection X-ray fluorescence spectrometry (TXRF). TXRF has comparable analytical requirements to GFAAS and is a multi-elemental method capable of analyzing several analytes simultaneously. The TXRF is less sensitive for lead, chromium, and cadmium than GFAAS. The zinc concentration of the CRM is very high and lies outside the linear range, therefore, only copper was included in the quantitative comparison and the results are listed in Table 28. The table shows that the results obtained for TXRF analysis were close to

the GFAAS and had a percent deviation from the certified value of 1.73%. This confirms that the MAAD procedure could also be applied for copper analysis by TXRF.

The relative percent difference between the GFAA and TXRF measurements was calculated using Equation 3-8. Where V_1 is the mass fraction determined by GFAA and V_2 is the mass fraction determined by TXRF.

$$Relative\ Percent\ Difference = \frac{|V_1 - V_2|}{\left(\frac{(V_1+V_2)}{2}\right)} * 100 \qquad \textit{Equation 3-8}$$

Table 28. Concentration of copper determined by GFAA and TXRF in CRM

Element	**Instrumentation**		**Relative Percent Difference**
	GFAA (mg/kg)	**TXRF (mg/kg)**	
Copper	2.743 ± 0.3045	2.84 ± 0.0500	3.58%

The low percentage of 3.58% indicated that the measurements were in agreement and both methods were suitable for quantification of copper in BCR-679.

CHAPTER FOUR. APPLICATIONS OF THE DEVELOPED METHOD

To demonstrate the versatility of the developed method, one set of clinical samples and one set of environmental samples were analyzed. The results of those examinations are presented in this chapter.

4.1. Determination of Heavy Metals in Human Cataract Cell Pellets

4.1.1. Quantification of Heavy Metals in Human Cataract Cell Pellets by GFAAS

Human cataract cell pellets were prepared following the validated sample preparation method outlined in the previous chapter. Briefly, sample were collected during surgical removal of cataracts at Loyola University Medical Center (LUMC). At LUMC, the clinical samples were then centrifuged, the supernatant was removed, leaving a cataract cell pellet. At this point, the cataract cell pellets were transferred to Loyola University Chicago, Northshore campus and stored at -80°C. The samples were then analyzed, and selected elements were quantified by GFAAS and TXRF. A total of 57 CCP samples were analyzed, and Table 29 summarized the quantitative data obtained for lead, cadmium, chromium, copper, and zinc. Finally, the results obtained for this study were compared to previously reported data from studies of heavy metal concentrations found in human lens materials. In previous reports, patient data such as age, gender, smoking habits, and diabetic diagnosis were often reported to correlate heavy metal bioaccumulation within these risk groups. As it has been reported that people who are older, female, smoke and have diabetes have a greater risk of developing cataracts. [191]

However, in this study, no patient data was available therefor, no comparison between cataract risk groups was able to be performed.

Table 29. Dry mass (μg/g) and concentration range for heavy metals in CCP quantified by GFAA

Element	Average (μg/g)	Range (μg/g)
Cadmium	0.0899 ± 0.0820	0.0167 – 0.281
Chromium	3.32 ± 6.04	0.0220 – 33.6
Copper	3.16 ± 1.83	0.679 – 6.99
Lead	6.57 ± 10.4	0.0101 – 45.1
Zinc	35.1 ± 22.6	0.869 – 89.3

4.1.2. Quantification of Copper in Human Cataract Cell Pellets by TXRF

As previously done for CRM in section 3.4, the CCPs were also analyzed by TXRF for the quantification of copper. The average copper concentration obtained by both GFAAS and TXRF for the same samples are listed in Table 30. The last column of the table shows the difference of the averages between the two measurement methods in percent. The low value of 1.26% indicates that both analysis methods agree. The determined copper concentration are considered accurate.

Table 30: Dry mass (μg/g) of copper in CCP determined by GFAA and TXRF

Element	Instrument		Relative Percent Difference
	GFAA (μg/g)	TXRF(μg/g)	
Copper	3.15 ± 1.83	3.19 ± 2.32	1.26%

4.1.3. Comparison of Previous Reported Concentrations to Quantified Concentrations within Human Cataract Lenses

Table 3 compiled previously quantified concentrations of heavy metals in cataract samples. This allowed for direct comparison of the metal concentrations obtained for a similar sample type, using the developed MAAD method.

In this study, the concentration range for lead was 0.0480 – 45.1 μg/g. A total of four examined studies reported concentrations of lead in lenses. For ease of comparison, studies reporting concentrations of lead in eye lenses are listed in Table 31.

Table 31. Previous studies of quantification of lead in human lens

Study	**Lead Concentration (μg/g)**	
Developed Method	Cataract Lens: 6.57 ± 10.4	
Erie *et. al.*[116]	Normal Lens: 0.013 ± 0.018	
Langford-Smith *et. al*[109]	Normal Lens: 0.0018 ± 0.0017	
Shukla *et. al.*[121]	Normal Lens: 3.0 ± 1.2	Cataract Lens: 111.0 ± 67.9
Cekic[123]	Non-smoker: Not detectable	Smoker: 5.90 ± 1.04

In the studies performed by Erie *et. al.* and Langford-Smith *et. al.* the average concentration of lead in human lenses was determined, specifically normal lenses were collected post-mortem and had no cataract development. Erie *et. al.* and Langford-Smith *et. al.* reported average concentrations of lead in normal lenses of 0.013 ± 0.018 μg/g and 0.0018 ± 0.0017 μg/g, respectively.[116, 109] The lowest concentration of lead determined in our samples was 0.101 ± 0.0038 μg/g, about seven times higher than the concentrations reported by Erie *et. al.* and fifty-six times higher than what was reported by Langford-Smith *et. al.*

In a study by Shukla *et. al.* the comparison between eyes of normal and cataract developed lenses was conducted. This reported average concentrations of lead in normal lenses of 3.0 ± 1.2 μg/g and 111.0 ± 67.9 μg/g in cataract lenses.[121] The concentrations reported by Shukla *et. al.* were much higher than the concentrations of lead determined in cataract cell pellets in this study and much higher than what was reported for normal lenses by Erie *et. al.* and Langford-Smith *et. al.* This disparity could be for a variety of reasons but is most likely related to the location of where the study took place and possibly the type of instrumentation used for quantification analysis. Shukla *et. al.*'s study took place in 1996 in New Delhi, India. At the

time, the daily exposure rate of lead for adults was estimated to be between 55-112 μg/day in New Delhi.[121] The study conducted by Erie *et. al.* took place at the Mayo Clinic in 2005 and Langford-Smith *et. al.* study took place in the University of Manchester in 2016. Only 548 adults living in Minnesota in 2005 reported lead levels of 10 μg/dL.[192] Thus, the exposure rate for lead in Minnesota, USA in 2005 was much lower than the lead exposure rate in Delhi, India in 1996. This lower exposure rate could account for the lower lead concentrations reported by Erie *et. al.*

The instrumentation that was used by Shukla *et. al.* to quantify lead was FAA. The LOD for lead for FAA is typically in the parts per million (ppm) whereas in this study, the GFAA was utilized. GFAA typically has LODs reported in parts per billion (ppb). Erie *et. al.* and Langford-Smith *et. al.* quantified elements in normal lenses using ICP-MS, which also has superior LOD capabilities when compared to FAA.

Only one other study was conducted for the determination of lead within cataract cell pellets. This was done by Cekic who compared lead concentrations in patients who smoked to those that had no history of smoking. The control, or patients with cataracts and no smoking history, had no detectable amounts of lead. Cekic reported that patients with developed cataract with history of smoking had an average concentration of 5.90 ± 1.04 μg/g.[123] The average concentration reported in this study was 6.57 ± 10.4 μg/g, which is comparable to the findings reported by Cekic. The range in this study is larger, however there was no sorting of patient data in this study which could account for the larger range. Another possibility for the slight difference in values could be due to the amount of cataract lenses analyzed. Cekic analyzed only 22 cataract lenses of smokers and 15 cataract lenses for non-smokers. In this study, a total of 57 cataract samples were analyzed. Regardless of these differences, the concentrations of lead in

cataract lenses determined within this study closely match the values previously reported by Cekic.

The concentration range determined for cadmium was 0.0751– 0.281μg/g. In Table 32, a summary of previous studies for the quantification of cadmium in human lenses has been compiled.

Table 32. Previous studies of quantification of cadmium in human lens

Study	**Concentration (μg/g)**	
Developed Method	Cataract Lens: 0.0899 ± 0.0820	
Erie *et. al.*[116]	Normal Lens: 0.02 ± 0.018	
Langford-Smith *et. al.*[109]	Normal Lens: 0.0058 ± 0.0.0082	
Cekic[123]	Non-smoking Cataract Lens: 0.045 ± 0.004	Smoking Cataract Lens: 1.19 ± 0.09

Cadmium was reported in two previous studies conducted by Erie *et. al.* and Langford-Smith *et. al.* in which normal lenses were analyzed post-mortem, reporting concentrations of 0.02 ± 0.018 μg/g. and 0.0058 ± 0.0.0082 μg/g, respectively.[116, 109] The lowest concentration determined for cadmium in this study was 0.0167 ± 0.00239 μg/g, which is comparable to the concentration determined by Erie *et. al.* However, this concentration is about three times higher than reported by Langford-Smith *et. al.* in normal lenses. The one other study that determined cadmium in human cataract samples was conducted by Cekic, who compared the concentration of cadmium in patients who smoked versus those who did not. The concentration of cadmium in patients who did not smoke had a concentration value of 0.045 ± 0.004 μg/g while smoking patients had concentrations of 1.19 ± 0.09 μg/g.[123] The reported average concentration determined within this study was 0.0751 ± 0.0810 μg/g and between the two values reported by Cekic. While Cekic considered patient smoking history for the reported values, patient data was not accessible in this study. Therefore, all smoker and non-smoker concentrations were averaged

together, making the reported value in this study perfectly reasonable to be between Cekic's two values.

Chromium was the third element analyzed in this study having a range of 0.0220 – 33.6 μg/g. Table 33 contains the summary of previously reported chromium concentrations in the human lens.

Table 33. Previous studies of quantification of chromium in human lens

Study	**Concentration (μg/g)**	
Developed Method	Cataract Lens: 3.32 ± 6.04	
Langford-Smith *et. al.*[109]	Normal Lens: 0.017 ± 0.027	
Cekic *et. al.*[193]	Normal Lens: 1.974 ± 1.007	Cataract Lens: 0.841 ± 0.476

A total of three studies have been completed to quantify chromium in human lenses. Of the three, one was conducted to determine chromium content in normal lenses, while the other two studies involved cataract analysis. Langford-Smith *et. al.* reported concentrations of chromium in normal lenses at 0.017 ± 0.027 μg/g.[109] The lowest concentration quantified within our study was 0.0220 ± 0.0223 μg/g, which is comparable to the concentrations found within normal lenses by Langford-Smith *et. al.* However, the two other studies completed to determine chromium concentrations within cataract lenses, reported values in μg/L, not allowing for comparison as the total amount of sample is not specified.[117] A study conducted by Cekic *et. al.*, compared chromium concentrations in normal and cataract lenses and concentrations of 1.974 ± 1.007 μg/g and 0.841 ± 0.476 μg/g, respectively.[119] From these findings, Cekic *et. al.* determined that there was a decrease in chromium concentration from normal to cataract lenses. The concentration determined by Cekic *et. al.* also fell within the reported range determined in this study.

Copper had a concentration range of 0.679 – 6.99μg/g in our study. Table 34 has been compiled to aid the comparison of copper quantification in the human lens from previous studies.

Table 34. Previous studies of quantification of copper in human lens

Study	**Concentration (μg/g)**	
Developed Method	Cataract Lens: 3.16 ± 1.83	
Langford-Smith *et. al.*[109]	Normal Lens: 0.41 ± 0.16	
Shukla *et. al.*[121]	Normal Lens: 0.4 ± 1.2	Cataract Lens: 0.5 ± 2.0
Yildirim *et. al.*[118]	Diabetic Cataract Lens: 31.83 ± 7.94	Non-Diabetic Cataract Lens: 22.32 ± 7.12
Aydin *et. al.*[122]	Diabetic Cataract Lens: 78.8 ± 38.1	Cataract Lens: 21.6 ± 17.8
Cekic[123]	Non-smoking Cataract Lens: 0.69 ± 0.15	Smoking Cataract Lens: 2.11 ± 0.29

Copper concentrations in normal lenses were reported by Langford-Smith *et. al.* of 0.41 ± 0.16 μg/g,[109] which was comparable to the lowest concentration quantified here with 0.670 ± 0.00928 μg/g. Previous studies have been conducted to quantify copper in cataract lenses. However, some of these studies reported concentrations in μg/L making the comparison of the concentration determined within this study impossible.[117] Four studies had concentrations reported for copper within cataract lenses in μg/g making a comparison between previous studies and the findings here possible. In a study conducted by Shukla *et. al.*, a direct comparison between normal lenses and cataract lenses was accomplished, reporting 0.4 ± 1.2 μg/g and 0.5 ± 2.0 μg/g respectively.[121] From these findings, Shukla *et. al.* reported no significant change in copper concentration within the lens due to cataract development. The average copper concentration quantified within our study is roughly six times larger than the cataract concentration in Shukla *et. al.*'s study.

A study conducted by Yildirim *et. al.*, compared diabetic cataract lenses and non-diabetic cataract lenses reporting 31.83 ± 7.94 μg/g and 22.32 ± 7.12 μg/g respectively.[118] Yildirim *et. al.* concluded that diabetic cataract samples cell had an increased concentration of copper.[118] The values determined by Yildirim *et. al.* were between seven to ten times higher than what was determined within our study. The larger values could be due to the instrumentation used for quantification as Yildirim *et. al.* used FAA, which has a much higher LOD than GFAA. Aydin *et. al.* also performed an analysis of copper in diabetic and non-diabetic cataract lenses, reporting concentrations of 78.8 ± 38.1 μg/g and 21.6 ± 17.8 μg/g, respectively.[122] The values reported by Aydin *et. al.* were even higher than what was reported by Yildirim *et. al.* The values reported by Aydin *et. al.* was 25 times higher when comparing the diabetic cataract lenses and roughly 7 times higher when comparing the non-diabetic cataract lenses to the values within this study. A reason for this higher amount could be due to the OVAD method that was performed on these samples. Copper is a common contaminant[194] and OVAD method is easily contaminated as previous reports and experience have proven. Therefor their samples could have easily been contaminated.

The final study was done by Cekic where copper concentrations within cataracts were compared between smokers and non-smokers. This study found an increase of copper concentration of smokers from 0.69 ± 0.15 μg/g to 2.11 ± 0.29 μg/g, respectively.[123] The copper range determined within this study was slightly higher than what was reported by Cekic, however, this could be due to difference in the number of cataract samples analyzed. In this study, 57 cataract samples were analyzed, Cekic analyzed 15 cataract lenses for non-smokers and 22 cataract lenses of smokers. Another potential explanation for the slightly higher value could

be due to the lack of information regarding patient data. In this study, patient data was not accessible and therefore no categorizing was possible.

Zinc was the last element analyzed within this study, finding a concentration range of 0.869 – 89.3 μg/g. Table 35 is a summary of previous studies where zinc was quantified in the human lens.

Table 35. Previous studies of quantification of zinc in human lens

Study	**Concentration (μg/g)**	
Developed Method	Cataract Lens: 35.8 ± 22.2	
Langford-Smith *et. al.*[109]	Normal Lens: 13.6 ± 2.2	
Shukla *et. al.*[121]	Normal Lens: 280.0 ± 82.2	Cataract Lens: 165.0 ± 133.4
Yildirim *et. al.*[118]	Diabetic Cataract Lens: 25.86 ± 14.45	Non-Diabetic Cataract Lens: 21.64 ± 6.61
Aydin *et. al.*[122]	Diabetic Cataract Lens: 1,852 ± 444	Non-diabetic Cataract Lens: 1557 ± 369
Gündüz,, *et. al.*[120]	Diabetic Cataract Lens: 36.6 ± 3.3	Non-diabetic Cataract Lens: 27.46 ± 1.96

Langford-Smith *et. al.* determined the concentration of zinc within normal lenses to be 13.6 ± 2.2 μg/g.[109] The lowest zinc concentration determined within this study was 3.10 ± 0.300 μg/g which was similar to the value reported by Langford-Smith *et. al.*

Previous studies have been accomplished to quantify zinc in cataract lenses, however some of which had reported concentrations in μg/L making the comparison of the concentration determined within this study impossible.[117] There were four studies reporting concentrations in μg/g. In the study conducted by Shukla *et. al.*, the comparison of zinc concentration in normal to cataract lenses was performed finding a decrease of zinc concentration in cataract lenses from 280.0 ± 82.2 μg/g to 165.0 ± 133.4 μg/g.[121] The zinc quantified in our study was four times lower than what was reported by Shukla *et. al.* For normal lens concentrations Shukla *et. al.* was

much higher than what was determined by Langford-Smith *et. al*. A potential reason for this difference is that Shukla *et. al.* utilized FAA which has higher LOD than what has been reported for GFAA and ICP-MS, the instrumentation used in this present study and by Langford-Smith *et. al.*, respectively. Another possible explanation could be due to where the studies took place, and how people in the Shukla *et. al.* study were potentially exposed to higher amount of pollutants than in Langford-Smith *et. al.* study or in this study.

Three similar studies were conducted by Yildirim *et. al.*, Aydin *et. al.*, and Gündüz *et. al.* to compare zinc concentrations of cataract cell pellets of diabetic and non-diabetic patients. The average zinc concentration determined by Yildirim *et. al.* was 25.86 ± 14.45 μg/g and 21.64 ± 6.61 μg/g, reporting no significant difference between zinc concentrations in cataracts between diabetic and non-diabetic patients.[118] The concentrations determined by Yildirim *et. al.* was comparable to the concentrations determined within this study. Gündüz *et. al* had similar averages of zinc concentrations as reported by Yildirim *et. al.* reporting 36.6 ± 3.3 in diabetic cataract lenses and 27.46 ± 1.96 in non-diabetic cataract lenses.[120] The concentrations reported by Gündüz *et. al* was comparable to the concentrations determined within this study. The average zinc concentrations reported by Aydin *et. al.* were not comparable to the concentrations determined here. The average zinc concentrations determined by Aydin *et. al.* was 1,852 ± 444 μg/g diabetic lenses and 1557 ± 369 μg/g in non-diabetic cataract lenses.[122] This was 2-52 times higher than what was reported here. This is consistent to what was noted in the copper discussion. The large amount of zinc reported by Aydin *et. al.* could be contributed to the use of OAVD which is prone to contamination. Zinc is a common source of contamination and could have easily been accidently introduced into the sample.[195]

When comparing the values quantified within this study to previous reports, most values fell well within the reported range, suggesting that the method performs well, and quantification was accurate, and this method can be used for larger studies conducted in the future.

4.2. Determination of Heavy Metals in Daucus Carota (Queen Anne's Lace) within the Calumet industrial corridor

4.2.1. Quantification of Heavy Metals in Environmental Samples by GFAA

A set of environmental samples was analyzed using the developed procedure, and the results were compared between GFAA, TXRF, other studies conducted for heavy metals quantified in the Calumet Industrial Corridor, and studies quantifying metal uptake in *Daucus Carota*. The samples collected were plant material of the species *Daucus Carota* also known as "Queen Anne's Lace" and were treated as described in section 2.8.2. A total of ten subsamples were analyzed with the average mass fraction of each analyte in mg/g shown in Table 36.

Table 36. Mass fraction in mg/kg for Cd, Cr, Cu, Pb and Zn in Daucus Carota samples collected at different locations within Calumet industrial corridor and quantified by GFAA

Element	**Mass Fraction of Calumet Locations (mg/kg)**		
	Location 1	**Location 2**	**Location 3**
Cadmium	0.532 ± 0.0576	0.192 ± 0.0164	0.210 ± 0.0255
Chromium	1.86 ± 0.0932	3.85 ± 0.392	5.84 ± 0.816
Copper	20.0 ± 3.54	6.30 ± 0.720	7.75 ± 1.18
Lead	10.2 ± 1.68	0.970 ± 0.217	1.07 ± 0.190
Zinc	508 ± 16.3	256 ± 19.3	94.2 ± 13.6

The environmental samples investigated in this study were obtained within the Calumet industrial corridor at three different locations. Specific locations were chosen for samples collection based upon history and heavy metal pollution associated with industrial use. Many of these locations were fenced off, making it difficult to collect samples. As a result, the samples

were collected as close as possible to the pollution site. Location 1 was close to a series of railways (<1 kilometer) which is utilized by number of companies, namely Chicago Rail & Port LLC, Ozinga, and COFCO International. The railway also borders the Calumet river, allowing barges to offload their cargo to either train or truck making this a high traffic area for transportation of goods.[196]

Location 2 was in proximity to the old Acme Steel Furnace Plant. This plant originally opened in 1908, changed owners over the years, and closed in 2001. Acme Steel Furnace Plant had an 89-acre furnace plant and a 102-acre coke plant. This bordered Big Marsh Park which was used as a dump site for industrial waste since the late 1800s.[125]

Location 3 was in proximity to the Calumet Water Reclamation Plant (<1.5 kilometers) which has been operational since 1922.[197] Water treatment occurs in three stages. The first stage separates large debris from water, the second adds microorganisms and oxygen into the water to break down organic matter, and the final stage treats the water with chlorination to remove bacteria.[197] During the first and second stage, solid waste is removed and is known as "sewage sludge." Today, sewage sludge is contained into management areas, but in the past this waste was dumped directly into Lake Calumet and its surrounding area.[125]

The mass fractions of the elements differed depending upon the location of collection. For lead, cadmium, copper and zinc, Location 1 had the highest concentrations. For lead, the mass fraction was ten times higher at Location 1 than at other locations. Cadmium and copper's mass fraction were about 2.5 times higher at Location 1 than at the other locations while zinc mass fractions were about 1.8 times higher. Chromium was the only element that did not have the highest mass fraction at Location 1, instead it had it's highest mass value determined at

Location 3, followed by Location 2 and Location 1 had the lowest mass fraction reported for chromium. The reasoning for these trends will be discussed in section 4.2.3.

4.2.2. Quantification of Copper in Environmental Samples by TXRF

Lead, copper, and zinc concentrations were also determined by TXRF as these values were above the LOQ and did not experience spectral overlap. The mass fraction determined by both TXRF and GFAAS for the same samples are shown in Table 37. As the table indicates, the data for zinc obtained by GFAA were at least 2-5.7 times higher than the ones obtained by TXRF. This difference in results most likely can be attributed to the limitations of the linear range for GFAAS. The linear range for zinc was 0.5 – 50 ng/mL, which was much lower than the concentrations detected and even dilution did not help improve the results as it was still above the linear range. The problem with the calibration curve did not come to light until after the analysis of the environmental samples by TXRF. This is an example as why quantification should be determined utilizing different instrumentation as potential problems in reporting values can be caught. Since the zinc concentrations quantified by GFAAS were questionable, these values were not included in the calculation of the percent differences between GFAAS and TXRF. Table 38 lists only those measurements for lead and copper were included.

Table 37. Concentration(mg/kg) of lead, copper, and zinc quantified by GFAA and TXRF in Daucus Carota at difference locations within Calumet industrial corridor

Element	**Concentration Calumet Locations (mg/kg)**					
	Location 1		**Location 2**		**Location 3**	
	GFAA	TXRF	GFAA	TXRF	GFAA	TXRF
Copper	20.0 ± 3.54	23.7 ± 2.82	6.30 ± 0.720	8.54 ± 0.190	7.75 ± 1.18	9.71 ± 1.03
Lead	10.2 ± 1.68	14.1 ± 4.02	0.970 ± 0.217	1.60 ± 0.170	1.07 ± 0.190	1.66 ± 0.170
Zinc	508 ± 16.3	253 ± 29.2	256 ± 19.3	44.6 ± 2.98	94.2 ± 13.6	41.7 ± 3.56

Table 38. Relative Percent Difference of concentrations of lead and copper quantified by GFAA and TXRF

Element	Relative Percent Difference		
	Location 1	Location 2	Location 3
Copper	16.9%	30.2%	22.4%
Lead	32.1%	49.0%	43.2%

The relative percent differences determined within this study were all higher than 15%. A reason for this could be that the method was specifically designed for clinical and biological materials, not for plants. Plants contain cellulose, which is difficult to digest, manifested in the residues which were present for some of the subsamples.[198] Potentially, the digestion method is not the most suitable for plant material, as there was still some residue in the samples post digestion.

4.2.3. Comparison to Previous Results for heavy metals monitored within Calumet Industrial Corridor and at other locations

There are few previous studies monitoring lead, cadmium, chromium, copper, and zinc within the Calumet industrial corridor. Those studies did not measure the bioaccumulation of these analytes in *Daucus Carota*, but rather monitored the elements in either soil or water. However, uptake studies conducted in laboratories were performed for *Daucus Carota* and will also be used for comparison.

Lead was found to be in the range of 0.970 – 10.2 mg/kg in this study, depending on the location where the *Daucus Carota* samples were collected. Table 39 lists previous data obtained from quantifying lead in either soil samples within the Calumet industrial corridor or in the plant *Daucus Carota* at other locations. Since there are no previous studies quantifying lead in *Daucus*

Carota within the Calumet industrial corridor both of these studies can be used to provide a baseline of the amount of lead present within the Calumet industrial corridor.

Table 39. Previous studies quantifying lead in either Calumet industrial corridor or in Daucus Carota

Study	**Sample Type and Location**	**Dry Mass (mg/kg)**
Developed Method	*Daucus Carota* in Calumet Industrial Corridor	0.970 – 10.2
Illinois Environmental Protection Agency[136]	Soil samples in Calumet Industrial Corridor	4.7 – 647
Gonzalez, L *et.al.*[137]	Soil samples in Calumet Industrial Corridor	1.2 – 160
Haque, E. *et. al.*[138]	Soil samples in Calumet Industrial Corridor	24 – 14,428
Shafer *et. al.*[140]	Soil samples in Calumet Industrial Corridor	187.0
Perkey and Wadman[141]	Sediment samples in Calumet Industrial Corridor	46.82
Roy and McDonald[199]	*Daucus Carota* in laboratory setting and West Virginia	0.72 0.03
Jolly *et. al.*[200]	*Daucus Carota* in laboratory setting and Bangladesh	24
Al-Qahtani[201]	*Daucus Carota* in laboratory setting and Saudi Arabia	1.42 ± 0.06

The mass range reported for lead in soil was 1.2-14,428 mg/kg.[136, 137, 138, 140] and the concentration of lead in sediment was 46.82 mg/kg. [141] The data determined in this study fall within the lower part of the reported range for soil samples. Uptake values for *Daucus Carota* were reported by Roy and McDonald,[199] Jolly *et. al.*,[200] Ali and Al-Qahtani,[201] finding values between 0.72 - 24 mg/kg. The mass fractions determined within this study are within the range of the previous reported uptake lead values for *Daucus Carota*. The design of the studies by Roy and McDonald,[199] Jolly *et. al.*,[200] Ali and Al-Qahtani,[201] were similar by also evaluating heavy metals in soil and different plant species with the goal of identifying which plant species had the highest metal uptake ability. The difference of these studies were the geographical locations in

which they took place, West Virginia, Bangladesh, and Saudi Arabia, respectively. [199, 200, 201] The previous studies clearly demonstrate that the varying uptake values within *Daucus Carota* are dependent upon location in which it was collected. This was clearly demonstrated in this study as Location 1 had the highest lead values.

The monitoring of heavy metal pollution has been accomplished regarding railways, coking plants and sewage sludge. Table 40 summarizes those studies; however none had taken place in Calumet industrial corridor. These studies will be used to find and understand trends.

Table 40. Lead quantification in environmental samples dependent upon location

Study	**Mass Fraction (mg/kg)**	**Sample Type**	**Location**
Developed Method	10.2 ± 1.68	*Daucus Carota*	Location 1 (Railways)
	0.970 ± 0.217		Location 2 (Coking Plant)
	1.07 ± 0.190		Location 3: (Sewage Treatment Plant)
Stojic *et. al.*[202]	10.69 – 95.71	Soil	Railways in Serbia
Levengood *et. al.*[203]	60.0	Soil	Railways in suburban Chicago
Rachwal *et. al.*[204]	14.8 – 390	Soil	Coking Plants in Poland
Hu *et. al.*[205]	20.4 ± 15.6	Soil	Coking Plants in Northern China
Bastian[206]	170	Sewage Sludge	Across United States
Walter *et. al.*[207]	140.2 – 168.2	Sewage Sludge	Spain

Location 1 was close to a series of railways. There have been no previous studies relating heavy metal concentration in *Daucus Carota* in proximity to railways. However, this has been accomplished in for soils by Stojic *et. al.* in Serbia and Levengood *et. al.* in the suburban Chicago. Both evaluated concentrations of lead in soil with proximity to railways. Stojic *et. al* reported lead in a range of lead 10.69 – 95.71 mg/kg whereas Levengood *et. al.* reported a maximum concentration of lead of 60.0 mg/kg.

Locations 2 and 3 had similar values for lead reported in this study. Location 2 was in proximity to a coke plant, and there have been no previous studies relating heavy metals in *Daucus Carota* in relation to coke plants, this has been accomplished for soils by Rachwal *et. al.* in Poland[204] and by Hu *et. al.* In the study conducted by Rachwal *et. al.*, soil samples were collected that surrounded different coking plants in Poland, while Hu *et. al.* analyzed soil either directly on a coking plant facility or in the areas bordering it. Lead was reported in ranges of 14.8 – 390 mg/kg[204] by Rachwal *et. al.* and an average of 20.4 ± 15.6 mg/kg[205] lead was reported by Hu *et. al.*

The third location in this study was near a sewage treatment facility. There have been multiple studies analyzing heavy metals in sewage sludge throughout the United States, but no studies quantifying heavy metals in *Daucus Carota* which was collected near or in areas of sewage sludge. A study conducted by Bastian across the United States reported a lead concentration of 170 mg/kg lead,[206] whereas a secondary study conducted by Walter *et. al.* in Spain reported lead in a range of 140.2 – 168.2 mg/kg.[207]

Based upon the previous reports of lead in soil in proximity to railways, coking plants, and sewage facilities, the trend one would expect is that Location 3 should have the highest lead bioaccumulation in *Daucus Carota*, followed by either Location 1 or Location 2. This was not observed. The trend observed was Location 1 had the highest lead bioaccumulation in *Daucus Carota* followed by Location 3 and then Location 2. This could be for several reasons, the first is that sewage sludge is now held in large management areas and no longer directly dumped into the surrounding area, decreasing the lead pollution. Another reason could be due to the previous studies quantifying heavy metals in proximity to railways were not nearly as heavily trafficked as

the railway used in the Calumet industrial corridor, therefor those railways could be less polluted. However, without further analysis, this cannot be known for certain.

In this study, cadmium was found to be in the range of 0.192 – 0.532 mg/kg depending upon the location of collection. The analysis of cadmium bioaccumulation in *Daucus Carota* within the Calumet industrial corridor has never been accomplished, two types of previous studies had to be evaluated. This includes previous studies in the quantification of cadmium within the Calumet industrial corridor and cadmium bioaccumulation in *Daucus Carota* which are summarized in Table 41.

Table 41. Previous studies quantifying cadmium in either Calumet industrial corridor or in Daucus Carota

Study	**Sample Type and Location**	**Dry Mass (mg/kg)**
Developed Method	*Daucus Carota* in Calumet Industrial Corridor	0.192 – 0.532
Agency for Toxic Substances and Disease Registry	Surface water & soil samples in Calumet Industrial Corridor	Surface Water: 0.0522
		Soil: 28.9
Shafer *et. al.*[140]	Soil samples in Calumet Industrial Corridor	1.8
Perkey and Wadman[141]	Sediment samples in Calumet Industrial Corridor	0.67
Roy and McDonald,[199]	*Daucus Carota* in laboratory setting and West Virginia	40

In 2009, the Agency for Toxic Substances and Disease Registry studied cadmium in Lake Calumet and reported a cadmium concentration in surface water of 0.0522 mg/kg, and in soil around Lake Calumet of 1.8- 28.9 mg/kg.[140, 142] Sediment samples taken from Lake Calumet had a reported average cadmium dry mass of 0.67 mg/kg.[141] Other studies were also investigating cadmium in soil within the area, but reporting those in μg/L, making a comparison difficult without knowledge of sample mass.[135] Cadmium uptake values were reported to be up to 40 mg/kg in *Daucus Carota* by Roy and McDonald.[199], which was determined in the area

surrounding a zinc smelter in West Virginia. Zinc smelters are known to produce cadmium as one of its pollutants.[31] The cadmium range found within the Calumet industrial corridor was much lower than the maximum uptake value reported by Roy and McDonald. However, previous studies indicate that there was enough cadmium in the Calumet industrial corridor for bioaccumulation to occur. By analyzing the previous uptake study accomplished by Roy and McDonald, it was determined that cadmium bioaccumulation in *Daucus Carota* is dependent upon the location and its proximity to pollutants.

Table 42 is a summary of previous reports quantifying cadmium in the environment dependent upon its proximity to an industrial use. This will be used to understand the observed trends in this study.

Table 42. Cadmium quantification in environmental samples dependent upon location

Study	**Mass Fraction (mg/kg)**	**Sample Type**	**Location**
Developed Method	0.532 ± 0.0576	*Daucus Carota*	Location 1 (Railways)
	0.192 ± 0.0164		Location 2 (Coking Plant)
	0.210 ± 0.0255		Location 3: (Sewage Treatment Plant)
Stojic *et. al.*[202]	0.05 – 0.88	Soil	Railways in Serbia
Levengood *et. al.*[203]	1.20	Soil	Railways in suburban Chicago
Rachwal *et. al.*[204]	0.02 – 12.56	Soil	Coking Plants in Poland
Hu *et. al.*[205]	0.48 ± 0.33	Soil	Coking Plants in Northern China
Bastian[206]	25	Sewage Sludge	Across United States
Walter *et. al.*[207]	2.40-3.43	Sewage Sludge	Spain

Location 1 had the highest cadmium values, indicating that Location 1 suffers the highest cadmium pollution of the three locations sampled. There have been previous studies regarding heavy metals in soils in proximity to railways, coking plants and in sewage sludge for the quantification of cadmium. Based upon these studies, a trend that would be expected was to have

the highest cadmium pollution at Location 3, reported to have a maximum 212 mg/kg of cadmium by Gardiner *et. al.,*[208] who analyzed cadmium in sewage sludge, followed by Location 2 with a maximum cadmium concentration was reported at 20.6 mg/kg in soil surrounding coking plants by Rachwal *et. al.*[204] The Location with the expected lowest cadmium pollution would be Location 1 with the highest cadmium concentration in soil in proximity to railways reported to be 1.20 mg/kg which was reported by Levengood *et. al.*[203] However, the trend noticed in this study reported cadmium in the highest concentrations at Location 1, followed by Location 3 and had the lowest value reported at Location 2. A reason for this deviation in observed trend could be because Location 2 has been a site for major environmental clean-up by the EPA[209] while Location 3 stopped dumping sewage sludge into the surrounding area and now contains the sewage sludge in management areas.[125] This could be a reason as to why Location 1 has the highest cadmium bioaccumulation in *Daucus Carota*. The study conducted by Levengood *et. al.* evaluated soil and sediments along railways in suburban Chicago.[203] This could indicate that Location 1 has higher traffic for transporting goods and could be a higher source of pollution that what has been reported. However, this would need further investigation before any conclusions can be made.

There has been no information about chromium bioaccumulation within *Daucus Carota* growing naturally within the Calumet industrial corridor available until this study, which determined a chromium mass fraction between 1.86 - 5.85 mg/kg for the three locations in the Calumet industrial corridor. Table 43 contains an overview of previous studies either quantifying chromium within water samples in the Calumet industrial corridor and chromium bioaccumulation in *Daucus Carota* in other regions.

Table 43. Previous studies quantifying chromium in either Calumet industrial corridor or in Daucus Carota

Study	Sample Type and Location	Dry Mass (mg/kg)
Developed Method	*Daucus Carota* in Calumet Industrial Corridor	1.86 - 5.85
Agency for Toxic Substances and Disease Registry[142]	Surface water samples in Calumet Industrial Corridor	0.204
Shafer *et. al.*[140]	Soil samples in Calumet Industrial Corridor	76.7
Perkey and Wadman[141]	Sediment samples in Calumet Industrial Corridor	17.41
Bhatti, H.N. *et. al.*[210]	*Daucus Carota* in laboratory setting and	88.27
Lilli, M.A. *et. al.*[211]	*Daucus Carota* in laboratory setting and	15

There have been multiple reports monitoring chromium in the Calumet water system, however, these values were in mg/L or $\mu g/m^3$, making the comparison difficult without knowledge of total mass.[212, 213] A study accomplished by the Agency for Toxic Substances and Disease Registry reported 0.204 mg/kg chromium in surface water in the Calumet industrial corridor[142] and soil sediment samples were reported to have chromium values of 76.7 mg/kg by Shafer *et. al.*[22] and 17.41 mg/kg[140, 141] by Perkey and Wadman.[23] The values determined within this study are about 9 – 28 times larger than what has been determined in surface water. However, chromium was found to be 3-15 times lower than the values reported in soil and sediment. Chromium in *Daucus Carota* was determined in two separate studies with reported uptake values of 88.27 mg/kg,[210] and of 15 mg/kg.[211] In both studies, *Daucus Carota* was grown under different laboratory conditions, followed by an assessment of chromium bioaccumulation in a specific geographical location. The concentrations determined within the Calumet industrial corridor are well below the maximum uptake range of previous reported values determined

within *Daucus Carota*. This indicates that the locations in which samples were collected had low chromium pollution.

Certain location within this study had higher or content than others. Table 44 is a compilation of previous studies quantifying chromium regarding to proximity to common pollution sources.

Table 44. Chromium quantification in environmental samples dependent upon location

Study	**Mass Fraction (mg/kg)**	**Sample Type**	**Location**
Developed Method	1.86 ± 0.0932	*Daucus Carota*	Location 1 (Railways)
	3.85 ± 0.392		Location 2 (Coking Plant)
	5.84 ± 0.816		Location 3: (Sewage Treatment Plant)
Stojic *et. al.*[202]	9.19 – 80.76	Soil	Railways in Serbia
Levengood *et. al.*[203]	52.0	Soil	Railways in suburban Chicago
Rachwal *et. al.*[204]	1.2 – 20.6	Soil	Coking Plants in Poland
Hu *et. al.*[205]	35.9 ± 11.2	Soil	Coking Plants in Northern China
Bastian[206]	178	Sewage Sludge	Across United States
Walter *et. al.*[207]	25.5 – 119	Sewage Sludge	Spain

Chromium was the only element that did not have the highest mass fraction at Location 1. Chromium had the highest mass fraction at Location 3, where it was three times higher than what was determined in Location 1. According to previous studies, sewage sludge had the highest reported chromium values (up to 119 mg/kg)[207] when compared to soil samples surrounding railways (up to 80.76 mg/kg)[202] and coking plants (up to 20.6 mg/kg).[204] Therefore, the higher chromium value could be due to the historical background of Location 3, and the maintained presence of chromium in the area. However, without further investigation, this cannot be known for certain.

The mass fraction of copper was found to be between 6.30 – 20.0 mg/kg in the Calumet industrial corridor, which aligns with previous reports determining a mass fraction of copper in soil within the Calumet industrial corridor of 0.61 – 156 mg/kg.[136, 137, 140, 141] Sediment samples taken from Calumet Lake had an average of 20.89 mg/kg reported.[141] In addition, the Agency for Toxic Substances and Disease Registry reported 0.262 mg/kg of copper in surface water.[142] The copper dry mass determined in this study fell in the low end of what has been reported in soil samples throughout the area, and the high end of the determined range was close to what has been reported in sediment samples. This trend was also shown during the cadmium and chromium analysis. This indicates that the analyte soil value is a better representation of bioaccumulation potential. These values are summarized in Table 45 along with other previous studies quantifying copper in *Daucus Carota.*

Table 45. Previous studies quantifying copper in either Calumet industrial corridor or in Daucus Carota

Study	**Sample Type and Location**	**Dry Mass (mg/kg)**
Developed Method	*Daucus Carota* in Calumet Industrial Corridor	6.30 – 20.0
Illinois Environmental Protection Agency[136]	Soil samples in Calumet Industrial Corridor	1.0 – 156
Gonzalez, L *et.al.*[137]	Soil samples in Calumet Industrial Corridor	0.61 – 130
Shafer *et. al.*[140]	Soil samples in Calumet Industrial Corridor	57.5
Perkey and Wadman[141]	Sediment samples in Calumet Industrial Corridor	20.89
Agency for Toxic Substances and Disease Registry[142]	Surface water samples in Calumet Industrial Corridor	0.262
Roy and McDonald[199]	*Daucus Carota* in laboratory setting and in West Virginia	25
Ali and Al-Qahtani[201]	*Daucus Carota* in laboratory setting and in Saudi Arabia	3.6 ± 0.22

Uptake studies for *Daucus Carota* found mass fractions of copper to be 3.6 ± 0.22 mg/kg and 25 mg/kg, respectively.[201, 199] These values were determined by Roy and McDonald[199] as well as Ali and Al-Qahtani,[201] who evaluated soil and plant species in the regions of West Virginia and Saudi Arabia to assess which plant was more likely to bioaccumulate certain heavy metals. The values determined within this study fell between the values reported by Roy and McDonald,[199] and by Ali and Al-Qahtani.[201] Previous soil and sediment analysis already indicated that copper was present in high concentrations within the Calumet industrial corridor. Based on these previous studies, the bioaccumulation of copper in *Daucus Carota* is directly dependent on the location it is collected. This has been demonstrated in previous reports summarized in Table 46.

Table 46. Copper quantification in environmental samples dependent upon location

Study	Mass Fraction (mg/kg)	Sample Type	Location
Developed Method	20.0 ± 3.54	*Daucus Carota*	Location 1 (Railways)
	6.30 ± 0.720		Location 2 (Coking Plant)
	7.75 ± 1.18		Location 3: (Sewage Treatment Plant)
Stojic *et. al.*[202]	9.19 – 80.76	Soil	Railways in Serbia
Levengood *et. al.*[203]	34.0	Soil	Railways in suburban Chicago
Rachwal *et. al.*[204]	2.8 – 40.0	Soil	Coking Plants in Poland
Hu *et. al.*[205]	15.2 ± 10.8	Soil	Coking Plants in Northern China
Bastian[206]	616	Sewage Sludge	Across United States
Walter *et. al.*[207]	179.4 – 214.2	Sewage Sludge	Spain
Gardiner *et. al.*[208]	1,370	Sewage Sludge	Lithuania

Based on previous studies, the trend one would expect to see is that Location 3, followed by Location 1 and then Location 2. Based on previous studies, sewage sludge had the highest copper content with a maximum value reported of 1,370 mg/kg.[208] Railways in the suburbs of Chicago had the next highest value reported of 80.76 mg/kg[202] while coking plants had the

lowest maximum copper mass fraction reported at 40.0 mg/kg.[204] The higher mass fractions copper at Location 1 are most likely related to the on-going pollution generated from railways.[214] While Location 2 and Location 3 had a history of pollution, this has greatly reduced in recent times. Up to the 1980s, waste was illegally dumped into the waterways, which border Locations 2 and 3. Since then, major cleanup was accomplished in the area by the EPA, and is still on-going.[209] Location 1 has not had the same attention, which could contribute to its higher heavy metal content.

Zinc, in *Daucus Carota,* had a mass fraction range of 41.7 - 253 mg/kg within the Calumet industrial corridor, as determined by TXRF. Table 47 shows a comparison of this study to previous studies in environmental samples within the Calumet industrial corridor, as well as *Daucus Carota* zinc uptake ability.

Table 47. Previous studies quantifying zinc in either Calumet industrial corridor or in Daucus Carota

Study	**Sample Type and Location**	**Dry Mass (mg/kg)**
Developed Method	*Daucus Carota* in Calumet Industrial Corridor	41.7 - 253
Illinois Environmental Protection Agency[136]	Soil samples in Calumet Industrial Corridor	2.8
Gonzalez, L *et.al.*[137]	Soil samples in Calumet Industrial Corridor	798
Shafer *et. al.*[140]	Soil samples in Calumet Industrial Corridor	341.0
Perkey and Wadman[141]	Sediment samples in Calumet Industrial Corridor	33.67
Roy and McDonald[199]	*Daucus Carota* in laboratory setting and in West Virginia	950
Ali and Al-Qahtani[201]	*Daucus Carota* in laboratory setting and in Saudi Arabia	10.28 ± 0.67

Previous studies reported zinc concentrations in soil between 2.8 - 798 mg/kg within the Calumet industrial corridor.[136, 137, 140] The values determined in this study are well within this

range. Sediment samples taken by Perkey and Wadman reported zinc dry mass of 33.67 mg/kg within Lake Calumet.[141] In previous uptake studies conducted by Roy and McDonald, and by Ali and Al-Qahtani also evaluated zinc in *Daucus Carota*, reporting concentrations of 10.28 ± 0.67 mg/kg,[201] with a maximum value of 950 mg/kg,[199] respectively. The values determined here are well within the reported ranges. Overall, these results indicate that zinc pollution is directly related to the location of its collection.

Table 48 has been compiled for ease of comparison to determine trends of zinc contamination regarding its location of specific industrial use.

Table 48. Zinc quantification in environmental samples dependent upon location

Study	**Mass Fraction (mg/kg)**	**Sample Type**	**Location**
Developed Method	253 ± 29.2	*Daucus Carota*	Location 1 (Railways)
	44.6 ± 2.98		Location 2 (Coking Plant)
	41.7 ± 3.56		Location 3: (Sewage Treatment Plant)
Stojic *et. al.*[202]	5.85 – 191.4	Soil	Railways in Serbia
Levengood *et. al.*[203]	180	Soil	Railways in suburban Chicago
Rachwal *et. al.*[204]	5.4 – 1,850	Soil	Coking Plants in Poland
Hu *et. al.*[37]	65.6 ± 18.1	Soil	Coking Plants in Northern China
Bastian[206]	1,285	Sewage Sludge	Across United States
Walter *et. al.*[207]	4,070	Sewage Sludge	Spain

Similar trends arise for the quantification of zinc, in which the highest expected values would be found in Location 3, as it is in proximity to a sewage treatment facility. The maximum previously reported value for this was 4,070 mg/kg by Walter *et. al.*[207] Followed by Location 1 and then Location 2. As previous reports has maximum zinc mass fractions in close proximity to railways in soil to be 180 mg/kg,[203] and maximum values for zinc values in soil close to coking plants to be 1,850.[205] In this study, Location 1 had the highest zinc quantified followed by

Location 2 and then Location 3. The difference in mass ratios between Location 2 and Location 3 was very small. However, zinc concentration in Location one was roughly six times larger than Locations 2 and 3. As with the analytes, lead, cadmium, and copper, the most probable reason for the increase in pollution is that the railway in which the samples were in proximity to is still heavily used for industrial use, while the sewage treatment plant has been containing the sewage sludge in waste management facility and the coking plant has not been operational for many years. However, this further investigation is needed.

Overall, the concentrations of lead, cadmium, chromium, copper, and zinc determined throughout the Calumet industrial corridor in *Daucus Carota* were well within the range of previous reports for soil within the Calumet industrial corridor and for uptake studies conducted for *Daucus Carota.* As indicated for each analyte analyzed, the bioaccumulation of heavy metals within *Daucus Carota* varied depending upon the location of its collection. In this study, the proximity to railways had the highest heavy metal content for all analytes quantified within this study except for chromium. Therefore, the *Daucus Carota* plant could be used as an environmental monitor for heavy metal pollution in the Calumet Industrial Corridor.

REFERENCE LIST

(1) Welz, B.; Sperling, M. *Atomic Absorption Spectrometry*; Wiley-VCH, 1999.

(2) Needleman, H. Lead Poisoning. *Annul. Rev. Med.* **2004**, *55*, 209-222.

(3) Public Health Statement: Lead. Services, D. o. H. a. H., Registry, P. H. S. A. f. T. S. a. D., Eds.; 2007.

(4) Bailey, C.; Kichen, I. Ontogenesis of proenkephalin products in rat striatum and the inhibitory effects of low-level lead exposure. *Dev. Brain Res.* **1985**, *22*, 75-79.

(5) Brown, R. K.; Hingerty, B. E.; Dewan, J. C. Pb(II)-catalysed cleavage of the sugar-phosphate backbone of yeast tRNA(Phe)-implications for lead toxicity and self-splicing RNA. *Nature* **1983**, *303*, 543-546.

(6) Baird, C.; Cann, M. *Environmental Chemistry*; Clancy Marshall, 2008.

(7) Yantasee, W.; Hongsirikarn, K.; Warner, C. L.; Choi, D.; Sangvanich, T.; Toloczko, M. B.; Warner, M. G.; Fryxell, G. E.; Addleman, R. S.; Timchalk, C. Direct detection of Pb in urine and Cd, Pb, Cu, and Ag in natural waters using electrochemical sensors immobilized with DMSA functionalized magnetic nanoparticles. *Analyst* **2008**, *133*, 348-355.

(8) Rocha, D. P.; Squissato, A. L.; da Silva, S. M.; Richter, E. M.; Munoz, R. A. A. Improved electrochemical detection of metals in biological samples using 3D-printed electrode: Chemical/electrochemical treatment exposes carbon-black conductive sites. *Electrochimica Acta* **2020**, *335*. DOI: https://doi.org/10.1016/j.electacta.2020.135688.

(9) Raril, C.; Manjunatha, J. G. Fabrication of novel polymer-modified graphene-based electrochemical sensor for the determination of mercury and lead ions in water and biological samples. *Journal of Analytical Science and Technology* **2020**, *11* (3). DOI: https://doi.org/10.1186/s40543-019-0194-0.

(10) Kudr, J.; Nguyen, H. V.; Gumulec, J.; Nejdi, L.; Blazkova, I.; Ruttkey-Nedecky, B.; Hynek, D.; Kynicky, J.; Adam, V.; Kizek, R. Simultaneous automatric electrochemical detection of Zinc, Cadmium, Copper and Lead Ions in Environmental Samples using a Thin-Film Mercury Electrode and an Artificial Neural Network. *Sensors* **2015**, *15* (1), 592-610.

(11) Lu, H.; Yin, X.; Mou, S.; Riviello, J. M. Simultaneous determination of heavy and transition metals in biological samples by chelation ion chromatography. *Journal of Liquid Chromatography & Related Technologies* **1999**, *23* (13), 2033-2045.

(12) Gao, P. F.; Zhang, X. W.; Kuang, H. Z.; Li, Q. Q.; Li, Y. Study on Simultaneous Determination of Ni, Pb, and Cd by Ion Chromatography. *IOP Conference Series: Earth and Environmental Science* **2018**, *146*.

(13) Huang, C.; Hu, B. Silica-coated magnetic nanoparticles modified with y-mercaptopropyltrimethoxysilane for fast and selective solid phase extraction of trace amounts of Cd, Cu, Hg, and Pb in environmental and biological samples prior to their determination by inductively coupled plasma mass spectrometry. *Spectrochimica Acta Part B: Atomic Spectroscopy* **2008**, *63* (3), 437-444.

(14) Suleiman, J. S.; Hu, B.; Huang, C.; Zhang, N. Determination of Cd, Co, Ni, and Pb in biological samples by microcolumn pasked with black stone (Pierre noire) online coupled with ICP-OES. *Journal of Hazardous Materials* **2008**, *157* (2-3), 410-417.

(15) Li, L.; Hu, B.; Xia, L.; Jiang, Z. Determination of trace Cd and Pb in environmental and biological samples by ETV-ICP-MS after single drop microextraction. *Talanta* **2006**, *70* (2), 468-473.

(16) Zhang, N.; Peng, H.; Wang, S.; Hu, B. Fast and selective magnetic solid phase extraction of trace Cd, Mn, and Pb in environmental and biological samples and their determination by ICP-MS. *Microchimica Acta* **2011**, *175*, 121-128.

(17) Kim, H. N.; Ren, W. X.; Kim, J. S.; Yoon, J. Fluorescent and colorimetric sensors for detection of lead, cadmium, and mercury ions. *Chem. Soc. Rev.* **2012**, *41*, 3210-3244.

(18) Lee, Y.; Huang, C. Colorimetric Assay of Lead Ions in Biological Samples Using a Nanogold-Based Membrane. *ACS Appl. Mater. Interfaces* **2011**, *3* (7), 2747-2754.

(19) Shahat, A.; Ali, E. A.; El Shahat, M. F. Colorimetric determination of some toxic metal ions in post mortem biological samples. *Sensors and Actuators B: Chemical* **2015**, *221*, 1027-1034.

(20) Stosnach, H. Environmental trace-Element Analysis Using a Benchtop Total reflection X-Ray Fluorescence Spectrometer. *Analytical Sciences* **2005**, *21*, 873-876.

(21) Woelfl, S.; Mages, M.; Torres, P. Trace metal concentrations in single specimens of the intestinal broad flatworm *(Diphyllobothrium latum)*, copared to their fish host *(Oncorhynchus mykiss)* measured by total reflection X-ray fluorescence spectrometry. *Spectrochimica Acta Part B* **2008**, *63*, 1450-1454.

(22) Mages, M.; Woelfl, S.; Ovari, M.; Tumpling Jr., W. V.; Encina, F. the use of a portable total reflection X-ray fluorescence spectrometer for trace element determination in freshwater microcrustaceans *(Daphnia)*. *Spectrochimica Acta Part B* **2004**, *59*, 1265-1272.

(23) Vieira, D. R.; Castro, J. T.; Lemos, V. A. Determination of lead and manganese in biological samples and sediment using slurry sampling and flame atomic absorption spectrometry. *J AOAC Int* **2011**, *94* (2), 645-649.

(24) Shah, F.; Kazi, T. G.; Ullah, N.; Afridi, H. I. Determination of Lead in Biological Samples of Children with Different Physiological Consequences Using Cloud Point Extraction Method. *Biological Trace Element Research* **2013**, *153*, 134-140.

(25) Afkhami, A.; Saber-Tehrani, M.; Bagheri, H.; Madrakian, T. Flame atomic absorption spectrometric determination of trace amounts of Pb(II) and Cr(III) in biological, food, and environmental samples after preconcentrations by modified nano-alumina. *Microchimica Acta* **2011**, *172*, 125-136.

(26) Borges, D. L. G.; Furtado da Silva, A.; Welz, B.; Curtius, A. J.; Heitmann, U. Determination of lead in biological samples by high-resolution continuum source graphite furnace atomic absorption spectrometry with direct solid sampling. *Journal of Analytical Atomic Spectrometry* **2006**, *21* (8), 763-769.

(27) Sardans, J.; Montes, F.; Penuelas, J. Determination of As, Cd, Cu, Hg, and Pb in biological samples by modren electrothermal atomic absorption spectrometry. *Spectrochimica Acta Part B: Atomic Spectroscopy* **2010**, *65* (2), 97-112.

(28) Urucu, O. A.; Donmez, S.; Yetimoglu, E. K. Solidified floating organic drop microextraction for the detection of trace amount of lead in various samples by electrothermal atomic absorption spectrometry. *Journal of Analytical Methods in Chemistry* **2017**. DOI: 10.1155/2017/6268975.

(29) Chen, L.; Wang, Z.; Pei, J.; Huang, X. highly permeable monolith-based multichannel in-tip microextraction apparatus for simultaneous field sample preparation of pesticides and heavy metal ions in environmental waters. *Analytical Chemistry* **2020**, *92*, 2251-2257.

(30) Järup, L. Hazards of heavy metal contamination. *British Medical Bulletin* **2003**, *68*, 167-182. DOI: 10.1093/bmb/ldg032.

(31) Tchounwou, P. B.; Yedjou, C. G.; Patolla, A. K.; Sutton, D. J. Heavy metals toxicity and the environment. *EXS* **2012**, *101*, 133-164.

(32) Martin, S.; Griswold, W. Human Health Effects of Heavy Metals. *Environmental Science and Technology Briefs for Citizens* **2009**, (15).

(33) Goering, P. L.; Waalkes, M. P.; Klaassen, C. D. Toxicology fo Cadmium. *Handbook of Experimental Toxicology* **1995**, *115*, 189-214.

(34) Waalkes, M. P.; Goering, P. L. Metallothionein and Other Cadmium-Binding Proteins: Recent Developments. *Chemical Research in Toxicology* **1990**, *3* (4), 281-288.

(35) Ulrich, K.; Jakob, U. The role of thiols in antioxidant systems. *Free Radic Biol Med* **2019**, *140*, 14-27. DOI: 10.1016/j.freeradbiomed.2019.05.035.

(36) Abdallah, A. B.; El-kholany, M. R.; Molouk, A. F. S.; Ali, T. A.; El-Shafei, A. A.; Khalifa, M. E. Selective and sensitive electrochemical sensors based on an ion imprinting polymer and graphene oxide for the detection of ultra-trace Cd(II) in biological samples. *RSC Adv.* **2021**, *11*, 30771-30780.

(37) Zheng, F.; Hu, B. Preparation of a high pH-resistant AAPTS-silica coating and its application to capillary microextraction (CME) of CU, ZN, Ni, Hg, and Cd from biological samples followed by on-line ICP-MS detection. *Analytica Chicmia Acta* **2007**, *605* (1), 1-10.

(38) Xia, L.; Hu, B.; Jiang, Z.; Wu, Y.; Liang, Y. Single-Drop Microextraction combined with Low-Temperature Electrothermal Vaporization ICPMS for the determination of Trace Be, Co, Pd, and Cd in Biological Samples. *Analytical Chemistry* **2004**, *76* (10), 2910-2915.

(39) Mages, M.; Bandow, N.; Kuster, E.; Brack, W.; von Tumpling, W. Zinc and cadmium accumulation in single zebrafish (*Danio reriro)* embryos- A total reflection X-ray fluorescence spectrometry application. *Spectrochimica Acta Part B* **2008**, *63*, 1443-1449.

(40) Xiang, G.; Wen, S.; Wu, X.; Jiang, X.; He, L.; Liu, Y. Selective cloud point extraction for the determination of cadmium in food samples by flame atomic absorption spectrometry. *Food Chemistry* **2012**, *132*, 532-536.

(41) Flores, E. M.; Paniz, J. N. G.; Martina, A. F.; Dressler, V. L.; Muller, E. I.; Ben de Costa, A. Cadmium determination in biological samples by solid sampling flame atomic absorption spectrometry. *Spectrochimica Acta Part B: Atomic Spectroscopy* **2002**, *57* (12), 2187-2193.

(42) Aranda, P. R.; Gil, R. A.; Moyano, S.; De Vito, I.; Martinez, L. D. Cloud point extraction for ultra-trace Cd determination in microwave-digested biological samples by ETAAS. *Talanta* **2008**, *77* (2), 663-666.

(43) Zhao, B.; He, M.; Chen, B.; Hu, B. Novel ion imprinted magnetic mesoporous silica for selective magnetic solid phase extraction of trace Cd followed by graphite furnace atomic absorption spectrometry detection. *Spectrochimica Acta Part B* **2015**, *107*, 115-124.

(44) A., A.-W.; Ball, P.; Clegg, B.; Emsley, J.; Leach, M.; Moran, J.; Scerri, E.; Sella, A.; Stewart, P. *30-Second Elements*; Sterling Publishing Company, 2013.

(45) Sugiyama, M.; Wang, X. W.; Costa, M. Comparison of DNA lesions and cytotoxicity induced by calcium chromate in human, mouse, and hamster cell lines. *Cancer Res* **1986**, *46* (9), 4547-4551.

(46) OSHA. Health Effects of Hexavalent Chromium. OSHA, Ed.; www.osha.gov, 2006.

(47) Public Health Statement: Chromium. Services, D. o. H. a. H., Registry, P. H. S. A. f. T. S. a. D., Eds.; 2012.

(48) Case Studies in Environmental Medicine (CSEM) Chromium Toxicity. Service, U. S. D. o. H. a. H., Registry, A. f. T. S. a. D., Medicine, D. o. T. a. E., Branch, E. M. a. E. S., Eds.; 2011.

(49) Prabhakaran, D. C.; Ramamurthy, P. C.; Sivry, Y.; Subramanian, S. Electrochemical detection of Cr(VI) and Cr(III) ions present in aqueous solutions using bio-modified carbon paste electrode: a voltammetric study. *International Journal of Environmental Analytical Chemistry* **2020**. DOI: 10.1080/03067319.2020.1748610.

(50) Ganeshjeevan, R.; Chandrasekar, R.; Yuvaraj, S.; Radhakrishnan, G. Determination of hexavalent chromium by on-line dialysis ion chromatography in a matrix of strong colourants and trivalent chromium. *Journal of Chromatography A* **2003**, *988* (1), 151-159.

(51) Wang, H.; Du, X.; Wang, M.; Wang, T.; Yang, H.; Wang, B.; Zhu, M.; Wang, Y.; Jia, G.; Feng, W. Using ion-pair reversed-phase HPLC ICP-MS to simultaneously determine Cr(III) and Cr(VI) in urine of chromate workers. *Talanta* **2010**, *81* (4-5), 1856-1860.

(52) Wu, Y.; Hu, B.; Hu, W.; Jiang, Z.; Li, B. A novel capillary microextraction on ordered mesoporous titania coating combined with electrothermal vaporization inductively coupled plasma mass spectrometry for the determination of V, Cr, and Cu in environmental and biological samples. *Journal of Mass Spectrometry* **2007**, *42* (4), 467-475.

(53) Leese, E.; Morton, J.; Gardiner, P. H. E.; Carlon, V. A. Development of a method for the simultaneous detection of Cr(III) and Cr(VI) in exhaled breath condensate samples using uLC-ICP-MS. *J. Anal. At. Spectrom.* **2016**, *31*, 924-933.

(54) Guo, J.; Huo, D.; Yang, M.; Hou, C.; Li, J.; Fa, H.; Luo, H.; Yang, P. Colorimetric detection of Cr (VI) based on the leaching of gold nanoparticles using a paper-based sensor. *Talanta* **2016**, *161*, 819-825.

(55) Zhou, Y.; Li, Y.; Tian, X.; Zhang, Y.; Yang, L.; Zhang, J.; Wang, X.; Lu, S.; Ren, H.; Liu, Z. Enhanced ultrasensitive detection of Cr(III) using 5-thio-2-nitrobenzoic acid (TNBA) and horseradish peroxidase (HRP) dually modified gold nanoparticles (AuNPs). *Sensors and Actuators B: Chemical* **2012**, *161* (1), 1108-1113.

(56) Chandra, R.; Manna, A. K.; Rout, K.; Mondal, J.; Patra, G. K. A dipodal molecular probe for naked eye detection of trivalent cations (Al^{3+}, Fe^{3+}, Cr^{3+}) in aqueous medium and its

applications in real sample analysis and molecular logic gates. *RSC Adv.* **2018**, *8*, 35946-35958.

(57) De La Calle, I.; Costas, M.; Cabaleiro, N.; Lavilla, I.; Bendicho, C. use of high-intensity sonication for pre-treatment of biological tissues prior to multielemental analysis by total reflection X-ray fluorescence spectrometry. *Spectrochimica Acta Part B* **2012**, *67*, 43-49.

(58) Sun, Z.; Liang, P. Determination of Cr(III) and total chromium in water samples by cloud point extraction and flame absorption spectrometry. *Microchimica Acta* **2008**, *162*, 121-125.

(59) Kazi, T. G.; Afridi, H. I.; Kazi, N.; Jamali, M. K.; Arain, M. B.; Jalbani, N.; Kandhro, G. A. Copper, Chromium, Manganese, Iron, Nickel, and Zinc levels in Biological Samples of Diabetes Mellitus Patients. *Biological Trace Element Research* **2008**, *122*, 1-18.

(60) Virgilio, A.; Nobrega, J. A.; Rego, J. F.; Neto, j. A. G. Evaluation of solid sampling high-resolution continuum source graphite furnace atomic absorption spectrometry for direct determination of chromium in medicinal plants. In *Spectrochimica Acta Part B*, 2012; Vol. 78, pp 58-61.

(61) Martins, P.; Pozebon, D.; Dressler, V., L.; Kemieciki, G. A. Determination of trace elements in biological materials using tetramethylammonium hydroxide for sample preparation. *Analytica Chimica Acta* **2002**, *470*, 195-204.

(62) Lancashire, R. J. *21.12A Copper Metal*; Department of Education Open Textbook, 2021.

(63) Using Copper Sulfate to Control Algae in Water Supply Impoundments. Resources, A. D. o. t. D. o. E. a. N., Ed.; Illinois State Water Survey, 2011.

(64) Royer, A.; Sharman, T. *Copper Toxicity*; StatPearls, 2021.

(65) Romero-Cano, L. A.; Zarate-Guzman, A. I.; Carrasco-Marin, F.; Conzalez-Gutierrez, L. V. Electrochemical detection of copper in water using carbon paste electrode prepared from bio-template (grapefruit peels) functionalized with carboxyl groups. *Journal of Electroanalytical Chemistry* **2019**, *15*, 22-29.

(66) Fredrikson, M.; Carlsson, N.; Sandberg, A. Simultaneous and Sensitive Analysis of Cu, Ni, Zn, Co, Mn and Fe in Food and Biological Samples Ion Chromatography. *Journal of Agricultural and Food Chemistry* **2002**, *50* (1), 59-65.

(67) Ong, C. N.; Ong, H. Y.; Chua, L. H. Determination of copper and zinc in serum and whole blood by ion chromatography. *Analytical Biochemistry* **1988**, *173* (1), 64-69.

(68) Khalil, M. M. H.; Shahat, A.; Radwan, A.; El-Shahet, M. F. Colorimetric determination of Cu(II) ions in biological samples using metal-organic framework as scaffold. *Sensors and Actuators B: Chemical* **2016**, *233*, 272-280.

(69) Kubala-Kukus, A.; Braziewicz, J.; Pajek, M. Total reflection X-ray fluorescence studies of trace elements in biomedical samples. *Spectrochimica Acta Part B* **2004**, *59*, 1283-1289.
(70) Ghaedi, M.; Shokrollahi, A.; Ahmadi, F.; Rajabi, H. R.; Soylak, M. Cloud point extraction for the determination of copper, nickel, and cobalt ions in environmental samples by flame atomic absorption spectrometry. *Journal of Hazardous Materials* **2008**, *150* (3), 533-540.

(71) Lemos, V. A.; Novaes, G. S.; de Carvalho, A. L.; Gama, E. M.; Santos, A. G. Determination of copper in biological samples by flame atomic absorption spectrometry after precipitation with Me-BTAP. *Environmental Monitoring and Assessment* **2009**, *148*, 245-253.

(72) Souza, S. d. O.; Francois, L. L.; Borges, A. R.; Vale, M. G. R.; Araujo, R. G. O. Determination of copper and mercury in phosphate fertilizers employing direct solid sampling analysis and high resolution continuum source graphite furnace atomic absorption spectrometry. In *Spectrochimica Acta Part B*, 2015; Vol. 114, pp 58-64.

(73) Public Health Statement: Zinc. Services, D. o. H. a. H., Registry, P. H. S. A. f. T. S. a. D., Eds.; 2005.

(74) Fosmire, G. J. Zinc toxicity. *Am J Clin Nutr* **1990**, *51* (2), 225-227. DOI: 10.1093/ajcn/51.2.225.

(75) Agnew, U. M.; Slesinger, T. L. *Zinc Toxicity*; NCBI National Library of Medicine, National Institutes of Health, 2022.

(76) Nemiroski, A.; Christodouleas, D. C.; Hennek, J. W.; Whitesides, G. M. Universal mobile electrochemical detector designed for use in resource-limited applications. *PNAS* **2014**, *111* (33), 11984-11989.

(77) Puente, C.; Gomez, I.; Kharisov, B.; Lopez, I. Selective colorimetric sensing of Zn(II) ions using green-synthesized silver nanoparticles: *Ficus benjamina* extract as reducing and stabilizing agent. *Materials Research Bulletin* **2019**, *112*, 1-8.

(78) Lee, S.; Nam, Y.; Lee, H.; Lee, Y.; Lee, K. Highly selective colorimetric detection of Zn(II) ions using label-free silver nanoparticles. *Sensors and Actuactors B: Chemical* **2016**, *237*, 643-651.

(79) Filgueiras, A. V.; Capelo, J. L.; Lavilla, I.; Bendicho, C. Comparison of ultrasound-assisted extraction and microwave-assisted digestion for determination of magnesium, manganese and zinc in plant samples by flame atomic absorption spectrometry. *Talanta* **2000**, *53* (2), 433-441.

(80) Dutra, R. L.; Cantos, G. A.; Carasek, E. Analysis of zinc in biological samples by flame atomic absorption spectrometry. *Biological Trace Element Research* **2006**, *111* (265). DOI: https://doi.org/10.1385/BTER:111:1:265.

(81) Briceno, J.; Belarra, M. A.; De Schamphelaere, K. A. C.; Vamblaere, S.; Janssen, C. R.; Vanhaecke, F.; Resano, M. Direct determination of Zn in individual *Daphnia magna* specimens by means of solid sampling high-resolution continuum source graphite furnace atomic absorption spectrometry. . In *J. Anal. At. Spectrom.*, 2010; Vol. 25, pp 503-510.

(82) Belarra, M. A.; Crespo, C.; Martinez-Garbayo, M. P.; Resano, M. Direct determination of cobalt and zinc in samples of different volatility by means of solid sampling-graphite furnace atomic absorption spectrometry. *Spectrochimica Acta Part B* **2003**, *58*, 1847-1858.

(83) Agency for Toxic Substances and Disease Registry Case Studies in Environmental Medicines (CSEM). Branch, U. S. D. o. H. a. H. S. A. f. T. S. a. D. R. D. o. T. a. E. M. E. M. a. E. S., Ed.; 2008.

(84) Public Health Statement: Copper. Services, D. o. H. a. H., Registry, A. f. T. S. a. D., Eds.; 2004.

(85) Administration, U. S. F. a. D. CFR- Code of Federal Regulations Title 21: Food for Human Consumption. Services, U. S. D. o. H. a. H., Ed.; 2022; Vol. 21.

(86) *Chromium*. 2022. https://www.hsph.harvard.edu/nutritionsource/chromium/#:~:text=%5B2%5D%20An%20Adequate%20Intake%20(,and%2020%20micrograms%20daily%2C%20respectively. (accessed 2022 April 29).

(87) Organization, W. H. Exposure to Cadmium: A major public health concern. Department of Public Health, E. a. S. D. o. H., Organization, W. H., Eds.; 2019; Vol. 2022.

(88) Riskobewertung, B. f. *Propose maximum levels for the addition of chromium to foods including food supplments*. German Federal Institute for Risk Assessment, 2021. (accessed 2022 April 29).

(89) UK, C. *Copper in Human Health*. Copper Development Association Inc., 2015. https://www.copper.org/consumers/health/cu_health_uk.html#:~:text=The%20World%20Health%20Organization%20(WHO,10mg%2Fday%20for%20adult%20females. (accessed 2022 April 29).

(90) Vilagines, R.; Leroy, P. [Lead in drinking water, determination of its concentration and effects of new recommendations of the World Health Organization (WHO) on public and private networks management]. *Bull Acad Natl Med* **1995**, *179* (7), 1393-1408.

(91) Simon-Hettich, B.; Wibbertmann, A.; Wagner, D.; Tomaska, L.; Malcolm, H. *Zinc*. 2001. https://apps.who.int/iris/handle/10665/42337 (accessed 2022 April 29).

(92) Pearson, T. H.; Ihda, A. J. Chemistry and the Spectrum before Bunsen and Kirchhoff. *Journal of Chemical Education* **1951**, (May), 267-271.

(93) Tyson, J. F.; Haswell, S. J.; Blankley, M.; Henson, A.; Thompson, K. C.; Septon, J. C.; Rains, T. C.; Ohls, K.; Sommer, D.; North, M. R.; et al. *Atomic Absorption Spectrometry: Theory, Design and Applications*; Elsevier, 1991.

(94) Alkemade, C. T. J.; Milatz, J. M. W. Double Beam Method of Spectral Selection with Flames. *Appl. Sci. Research* **1955**, *46* (8).

(95) Jackson, K. W.; Holcombe, J. A.; Gilmutdinov, A. K.; Rademeyer, C. J.; Harnly, J. M.; Styris, D. L.; Sturgeon, R. E. *Electrothermal Atomization for Analytical Atomic Spectrometry*; John Wiley & Sons LTD, 1999.

(96) Zawisza, B.; Pytlakowska, K.; Feist, B.; Polowniak, M.; Kita, A.; Sitko, R. Determination of rare earth elements by spectroscopic techniques: a review. In *J. Anal. At. Spectrom.*, 2011; Vol. 26, p 2373.

(97) Gao, Y.; Shi, Z.; Long, Z.; Wu, P.; Zheng, C.; Hou, X. Determination and speciation of mercury in environmental and biological samples by analytical atomic spectrometry. In *Microchemical Journal*, 2012; Vol. 103, pp 1-14.

(98) Technologies, A. *Analytical Methods for Graphite Tube Atomizers - A user's guide*; 2012.

(99) Krawczyk, M. Determination of macro and trace elements in multivitamin dietary supplements by high resolution continuum source graphite furnace atomic absorption with slurry sampling. In *Journal of Pharmaceutical and Biomedical Analysis*, 2014; Vol. 88, pp 377-384.

(100) Moreira, F. R.; Mello, M. G.; Campos, R. C. Different platform and tube geometries and atomization temperature in graphite furnace atomic absorption spectrometry: Cadmium determination in whole blood as a case study. In *Spectrochimica Acta Part B*, 2007; Vol. 62, pp 1273-1277.

(101) Hage, D. S.; Carr, J. D. *Analytical Chemistry and Quantitative Analysis.*; Pearson Education, 2012.

(102) Skoog, D. A.; Holler, F. J.; Crouch, S. R. *Principles of Instrumental Analysis*; Brooks Cole, Belmont,, 2007.

(103) Beaty, R. D.; Kerber, J. D. *Concepts, Instrumentation and Techniques in Atomic Absorption Spectrophotometry.*; The Perkin-Elmer Corporation, 1993.

(104) Willoughby, C. E.; Ponzin, D.; Ferrari, S.; Lobo, A.; Landau, K.; Omidi, Y. Anatomy and physiology of the human eye: effects of mucopolysaccharidoses disease on structure and function - a review. *Clinical and Experimental Ophthalmology* **2010**, *38*, 2-11. DOI: 10.1111/j.1442-9071.2010.02363.x.

(105) Ray, N. J. Biophysical chemistry of the ageing eye lens. *Biophys Rev.* **2015**, *7*, 353-368.

(106) Dahm, R. Nuclear degradation in the lens, circa 1897-1899. *The scientist* **2009**, *23*.

(107) Rabl, C. Uber den Bau und die Entwicklung der Linse. *Z. Wiss. Zool.* **1899**, *67*, 1-138.

(108) Sharma, K. K.; Santhoshkumar, P. Lens aging: Effects of crystallins. *Biochimica et Biophysica Acta* **2009**, *1790*.

(109) Langford-Smith, A.; Tilakaratna, V.; Lythgoe, P. R.; Clark, S. J.; nishop, P. N.; Day, A. J. Age and smoking related changes in metal ion levels in human lens: implications for cataract formation. *PLoSONE* **2016**, *11* (1). DOI: 10.1371/journal.pone.0147576.

(110) Michael, R.; Bron, A. J. The ageing lens and cataract: a model of normal and pathological ageing. *Philos Trans R Soc Lond B Biol Sci* **2011**, *366* (1568), 1278-1292. DOI: 10.1098/rstb.2010.0300.

(111) Rui, H.; Artigas, P.; Roux, B. The selectivity of the Na^+/K^+ pump is controlled by binding site protonation and self-correcting occlusion. *eLife* **2016**. DOI: 10.7554/eLife.16616.

(112) Quintanar, L.; Dominquez-Calva, J. A.; Serebryany, E.; Rivillas-Acevedo, L.; Haase-Pettingell, C.; Amero, C.; King, J. A. Copper and Zinc ions specifically promote nonamyloid aggregation of the highly stable human y-D Crystallin. *ACS Chem. Biol.* **2016**, *11*, 263-272.

(113) A., S.; Trusdale, A. W. Elemental analysis in normal and cataractous human lens tissue. *Biochem. Biophys. Res. Commun.* **1971**, *10*, 1488-1496.

(114) Oerdoegh, M.; Racz, P. Investigations on inorganic elements in human lenses of normal and senile cataract character. *Journal of Radioanalytical Chemistry* **1977**, *37* (1).

(115) Lakomaa, E. L.; Eklund, P. Trace element analysis of human cataractous lenses by neutron activation analysis and atomic absorption spectrometry with special references to pseudo-exfoliation. *Ophthalmic Res.* **1978**, *10*, 302-306.

(116) Erie, J. C.; Butz, J. A.; Good, J. A.; Erie, E. A.; Burritt, M. F.; Cameron, J. D. Heavy metal concentrations in human eyes. *Am J Ophthalmol* **2005**, *139* (5), 888-893. DOI: 10.1016/j.ajo.2004.12.007.

(117) Schmeling, M.; Gaynes, B.; Tidow-Kebritchi, S. Heavy metal analysis in lens and aqueous humor of cataract patients by total-reflection X-ray fluorescence spectrometry. *Powder Diff.* **2014**, *29* (155-158).

(118) Yildirim, Z.; Yildirim, F.; Ucgun, N. I.; Kilic, N. The Evaluation of the Oxidative Stress Parameters in Nondiabetic and Diabetic Senile Cataract Patients. *Biological trace element research* **2008**, *128* (2), 135-143. DOI: 10.1007/s12011-008-8258-9.

(119) Cekiç, O.; Bardak, Y.; Totan, Y.; Kavakli, S.; Akyol, O.; Ozdemir, O.; Karel, F. Nickel, chromium, manganese, iron and aluminum levels in human cataractous and normal lenses. *Ophthalmic Res* **1999**, *31* (5), 332-336. DOI: 10.1159/000055555.

(120) Gündüz, G.; Gündüz, F.; Yücel, I.; Sentürk, U. K. Levels of zinc and magnesium in senile and diabetic senile cataractous lenses. *Biol Trace Elem Res* **2003**, *95* (2), 107-112. DOI: 10.1385/BTER:95:2:107.

(121) Shukla, N.; Moitra, J. K.; Trivedi, R. C. Determination of lead, zinc, potassium, calcium, copper and sodium in human cataract lenses. *Sci Total Environ* **1996**, *181* (2), 161-165. DOI: 10.1016/0048-9697(95)05006-x.

(122) Aydin, E.; Cumurcu, T.; Özugurlu, F.; Özyurt, H.; Sahinoglu, S.; Mendil, D.; Hasdemir, E. Levels of Iron, Zinc, and Copper in Aqueous Humor, Lens, and Serum in Nondiabetic and Diabetic Patients: Their Relation to Cataract. *Biological trace element research.* **2005**, *108* (1-3), 033-042. DOI: 10.1385/bter:108:1-3:033.

(123) Cekic, O. Effect of cigarette smoking on copper, lead, and cadmium accumulation in human lens. *Br J Ophthalmol* **1998**, *82* (2), 186-188. DOI: 10.1136/bjo.82.2.186.

(124) Reifman, D. L. Calumet Industrial Corridor. Development, D. o. P. a., Ed.; City of Chicago: 2016.

(125) Nevers, M. B.; Whitman, R. I.; Gerovac, P. J. History and Environmental Setting of the Grand Calumet River. *Proceedings of the Indiana Academy of Science* **2000**, *108*, 3-10.

(126) Cordova, T. Calumet River Communities Planning Framework: A guide for Equitable Development. UIC: Great Cities Institute: Chicago, 2019.

(127) Hazardous, toxic, and radioactive waste (htrw)phase I environmental site assessment river riparian connectivity & habitat - section 506 project Cook County, Illinois. Engineers, U. A. C. o., Ed.; Chicago, 2015.

(128) *Summary of the Clean Water Act*. Environmental Protection Agency, https://www.epa.gov/laws-regulations/summary-clean-water-act#:~:text=The%20Clean%20Water%20Act%20(CWA,quality%20standards%20for%20surface%20waters.&text=Under%20the%20CWA%2C%20EPA%20has,setting%20wastewater%20standards%20for%20industry.) (accessed 2022 June 20).

(129) *Key Concepts Module 2: Use*. Environmental Protection Agency, 2022. https://www.epa.gov/wqs-tech/key-concepts-module-2-use (accessed 2022 June 20).

(130) Lokeshwari, H.; Chandrappa, G. T. Impact of heavy metal contamination of Bellandur Lake on soil and cultivated vegetation. *Current Science* **2006**, *91* (5), 622-627.

(131) Zhang, B.; Wu, D.; Zhang, L.; Jiao, Q.; Li, Q. Application of hyperspectral remote sensing for environment monitoring in mining areas. *Environ. Earth Sci* **2012**, *65*, 649-658.

(132) Fernandez-Turiel, J. L.; Lopez-Soler, A.; Llorens, J. F.; Querol, X.; Acenolaza, P.; Durand, F.; Lopez, J. P.; Medina, M. E.; Rossi, J. N.; Toselli, A. J.; et al. Environmental monitoring using surface water, river sediments, and vegetation: A case study in the Famatina Range, Lo Rioja, NW Argentina. *Environment International* **1995**, *21* (6), 807-820.

(133) Peer, W. A.; Baxter, I. R.; Richards, E. L.; Freeman, J. L.; Murphy, A. S. *Phytoremediation and hyperaccumulator plants*; Springer, 2005. DOI: 10.1007/4735_100.

(134) DalCorso, G.; Fasani, E.; Manara, A.; Visioli, G.; Furini, A. Heavy Metal Pollutions: State of the Art and Innovation in Phytoremediation. *Int J Mol Sci* **2019**, *20* (14). DOI: 10.3390/ijms20143412.

(135) Wilson, C.; Weng, Q. Assessing Surface Water Quality and Its Relation with Urban Land Cover Changes in the Lake Calumet Area, Greater Chicago. *Environmental Management* **2010**, *45*, 1096-1111.

(136) A summary of selected background conditions for inoganics in soil. IEPA, Ed.; 1994.

(137) Gonzalez, L. M. H.; Rivera, V. A.; Phillips, C. B.; Haug, L. A.; Hatch, S. L.; Yeager, L. E.; Chang, H.; Alvarez, J.; Gnaedinger, K. J.; Miller, W. M.; et al. Characterization of soil profiles and elemental concentrations reveal deposition of heavy metals and phosphorus in a Chicago-area nature preserve, Gensburg Markham Prairie. *Journal of Soils and Sediments* **2019**, *19*, 3817-3821.

(138) Haque, E.; Thorne, P. S.; Nghiem, A. A.; Yip, C. S.; Bostick, B. C. Lead (Pb) concentrations and speciation in residential soils from an urban community impacted by multiple legacy sources. *Journal of Hazardous Materials* **2021**, *416*.

(139) Ingersoll, C. G.; MacDonald, D. D.; Brumbaugh, W. G.; Johnson, B. T.; Kemble, N. E.; Kunz, J. L.; May, T. W.; Wang, N.; Smith, J. R.; Sparks, D. W.; et al. Toxicity assessment of sediments from the Grand Calumet River and Indiana Harbor Canal in Northwestern Indiana, USA. *Arch Environ Contam Toxicol* **2002**, *43* (2), 156-167. DOI: 10.1007/s00244-001-0051-0.

(140) Shafer, J. M.; Wehrmann, A. H.; Schulmeister, M. K.; Schock, S. C. A plan for the comprehensive evaluation of the occurrence, transport, and Fate of Ground-Water contaminants in the Lake Calumet area of Southeast Chicago. Center, H. W. R. a. I., Ed.; Champaign, IL, 1988.

(141) Perkey, D. W.; Wadman, H. M. Identification of Sediment Sourves to Calumet River through Geochemical Fingerprinting. Chappell, M. A., Seiter, J. M., Eds.; Engineer Research and Development Center, 2017.

(142) Service, U. S. D. o. H. a. H. S. P. H. Lake Calumet Cluster Site, Chicago, Cook County, Illinois. Registry, A. f. T. S. a. D., Ed.; 2009.

(143) Coorporation, S. *Atomic Absorption Spectrometers: AA-7000 Series*. 2014. www.shimadzu.com/an/ (accessed 2022 April 13).

(144) Acar, O. Determination of cadmium an dlead in biological samples by Zeeman ETAAS using various chemical modifiers. *Talanta* **2001**, *55*, 613-622.

(145) Cassella, R. J.; Brum, D. M.; Lima, C. F.; Fonseca, T. C. O. Stabilization of aviation gasoline as detergent emulsion for lead determination by electrothermal atomic absorption spectrometry. In *Fuel Processing Technology*, 2011; Vol. 92, pp 933-938.

(146) Cabon, J. Y.; A.L., B. Determination of lead in seawater by electrothermal atomic absorption spectrometry with transversely heated furnace by using oxalic acid or Pd/Mg as modifiers. *Spectrochimica Acta B* **1996**, *51*, 1245-1251.

(147) Byrne, J. P.; Chakrabarti, C. L.; Gilchrist, G. F. R.; Lamoureux, M. M.; Bertels, P. Chemical Modification by Ascorbic Acid and Oxalic Acid in Graphite Furnace Atomic Absorption Spectrometry. *Anal. Chem.* **1993**, *65*, 1267-1272.

(148) Szkoda, J.; Zmudzki, J. Determination of lead and cadmium in biological material by graphite furnace atomic absorption spectrometry method. *Bulletin - Veterinary Institute in Pulawy* **2005**, *49*, 89-92.

(149) Blake, C.; Bourqui, B. Determination of Lead and Cadmium in Food Products by Graphite Furnace Atomic Absorption Spectroscopy. *Atomic Spectroscopy* **1998**, *19* (6), 207-213.

(150) Ong, K. Determination of Lead and Cadmium in Foods by Graphite Furnace Atomic Absorption Spectroscopy. In *Atomic Absorption*, PerkinElmer: Waltham, MA, 2014.

(151) Danzer, K. Selectivity and specificity in analytical chemistry. General considerations and attempt of a definition and quantification. *Fresenius J. Anal Chem* **2001**, *369*, 397-402.

(152) Guidance for the Validation of Analytical Methodology and Calibration of Equipment used for Testing of Illicit Drugs in Seized Materials and Biological Specimens. Crime, U. N. o. o. D. a., Ed.; United Nations: Vienna, 2009.

(153) Bioanalytical Method Validation Guidance for Industry. Services, U. S. D. o. H. a. H., Administration, F. a. D., (CDER), C. f. D. E. a. R., (CVM), C. f. V. M., Eds.; Bioanalytical Method Validation: 2018.

(154) Şengül, Ü. Comparing determination methods of detection and quantification limits for aflatoxin analysis in hazelnut. *J Food Drug Anal* **2016**, *24* (1), 56-62. DOI: 10.1016/j.jfda.2015.04.009.

(155) Uhrovčík, J. Strategy for determination of LOD and LOQ values--some basic aspects. *Talanta* **2014**, *119*, 178-180. DOI: 10.1016/j.talanta.2013.10.061.

(156) Taleuzzaman, M. Limit of Blank (LOB), Limit of Detection (LOD) and Limit of Quantification (LOQ). *Organic and Medicinal ChemistryIJ* **2018**, *7* (5).

(157) Kingston, H. M.; Jassie, L. B. *Introduction to microwave sample preparation: Theory and practice.*; American Chemical Society, 1988.

(158) Robles, L. C.; Aller, A. J. Determination of cadmium in biological and environmental samples by slurry electrothermal atomic absorption spectrometry. *Talanta* **1995**, *42*, 1731-1744.

(159) Cal-Prieto, M. J.; Felipe-Sotelo, M.; Carlosena, A.; Andrade, J. M.; Lopez-Mahia, P.; Muniategui, S.; Prada, D. Slurry sampling for direct analysis of solid materials by electrothermal atomic absorption spectrometry (ETAAS). A literature review from 1990-2000. *Talanta* **2002**, *56*, 1-51.

(160) Tsalev, D. L.; Slaveykova, V. I.; Lampugnani, L.; D'Ulivo, A.; Georgieva, R. Permanten modification in electrothermal atomic absorption spectrometry-advances, anticipations and reality. *Spectrochimica Acta Part B* **2000**, *55*, 473-490.

(161) Volynsky, A. B. Mechanisms of action of platinum group modifiers in electrothermal atomic absorption spectrometry. *Spectrochimica Acta Part B* **2000**, *55*, 103-150.

(162) Slavin, W.; Carnrick, G. R.; Manning, D. C. Magnesium Nitrate as a Matrix Modifier in the Stabilized Temperature Platform Furnace. *Anal. Chem.* **1982**, *54*, 621-624.

(163) Ajtony, Z.; Bencs, L.; Haraszi, R.; Szigeti, J.; Szoboszlai, N. Study on the simultaneous determination of some essential and toxic trace elements in honey by multi-element graphite furnace atomic absorption spectrometry. In *Talanta*, 2007; Vol. 71, pp 683-690.

(164) de Oliveira, E. Sample preparation for atomic spectroscopy: evolution and future trends. *J. Braz. Chem. Soc.* **2003**, *14* (2), 174-182.

(165) Zacharia, A. N.; Zhuravlev, A. S.; Chebotarev, A. N.; Arabadig, M. V. Direct determination of lead in wine materials by atomic absorption spectrometry using an

electrothermal atomizer with a graphite filter-insert. In *Journal of Applied Spectroscopy*, 2013; Vol. 79, pp 949-954.

(166) Damin, I. C. F.; Dessuy, M. B.; Castilhos, T. S.; Silva, M. M.; Vale, M. G. R.; Welz, B.; Katskov, D. A. Comparison of direct sampling and emulsion analysis using a filter furnace for the determination of lead in crude oil by graphite furnace atomic absorption spectrometry. In *Spectrochimcia Acta Part B*, 2009; Vol. 64, pp 530-536.

(167) Egger, L.; Ménard, O.; Abbühl, L.; Duerr, D.; Stoffers, H.; Berthoud, H.; Meola, M.; Badertscher, R.; Blaser, C.; Dupont, D.; et al. Higher microbial diversity in raw than in pasteurized milk Raclette-type cheese enhances peptide and metabolite diversity after in vitro digestion. *Food Chem* **2021**, *340*, 128154. DOI: 10.1016/j.foodchem.2020.128154.

(168) Paz de Mattos, J. C.; Nunes, A. M.; Martins, A. F.; Dressler, V. L.; Marlon de Moraes Flores, E. Influence of citric acid as chemical modifier for lead determination in dietary calcium supplement samples by graphite furnace atomic absorption spectrometry. **2005**, *60*, 687-692.

(169) Afridi, H. I.; Kazi, T. G.; Jamali, M. K.; Kazi, G. H.; Arian, M. B.; Jalbani, N.; Shar, G. Q. Analysis of Heavy Metals in Scalp Hair Samples of Hypertensive Patients by Conventional and Microwave Digestion Methods. *Spectroscopy Letters* **2006**. DOI: 10.1080/00387010500531266.

(170) Dogan, S.; Kaya, F. N. D. Determination of zinc and lead in human hair by atomic absorption spectrometry after digestion with tetramethylammonium hydroxide and conventional methods. *Trace Elements and Electrolytes* **2010**, *27* (3), 110-114.

(171) Ribeiro, A. S.; Curtius, A. J.; Pozeban, D. Determination of As, Cd, Ni and Pb in human hair by electrothermal atomic absorption spectrometry after sample treatment with tetramethylammonium hydroxide. In *Microchemical Journal*, 2000; Vol. 64, pp 105-110.

(172) Gedye, R. N.; Smith, F. E.; Westaway, K. C. The rapid synthesis of organic compounds in microwave ovens. *Can. J. Chem.* **1988**, *66*, 17-35.

(173) Kappe, C. O.; Stadler, A. *Microwaves in Organic and Medicinal Chemistry*; Wiley-VCH, 2005.

(174) Pereira, L. S. F.; Iop, G. D.; Flores, E. M. M.; Burrow, R. A.; Mellos, P. A.; Duarte, F. A. Strategies for the determination of trace and toxic elements in pitch: Evaluation of combustion and wet digestion methods for sample preparations. In *Fuel*, 2016; Vol. 136, pp 175-179.

(175) McCarthy, H. T.; Ellis, C. P. Comparison of Microwave Digestion with Conventional Wet Ashing and Dry Ashing Digestion for Analysis of Lead, Cadmium, Chromium, Copper, and Zinc in Shellfish by Flame Atomic Absorption Scpectroscopy. *Journal of Association of Official Analytical Chemists* **1991**, *74* (3), 566-569.

(176) Cocchi, M.; Franchini, G.; Manzini, D.; Manfredini, M.; Marchetti, A.; Ulrici, A. A chemometric approach to the comparison of different sample treatments for metals determination by atomic absorption spectroscopy in Aceto Balsamico Tradizionale di Modena. *J. Argic. Food. Chem.* **2004**, *52*, 4047-4056.

(177) Demura, R.; Tsukada, S.; Yamamtoto, I. Rapid determination of trace Metals in Foods by Using the Microwave Oven-Digestion Method. II. Determination of zinc, copper, manganese, lead and cadmium. *Eisei Kagaku* **1985**, *31* (6).

(178) Dong-mei, W.; Yu, C.; Zheng-jun, G.; Ying, L. Determination of Lead in Lipstick by Microwave Digestion and FAAS. *2010 International Conference on Challenges in Environmental Science and Computer Engineering* **2010**, 297-298. DOI: 10.1109/CESCE.2010.137.

(179) Afridi, H. I.; Kazi, T. G.; Talpur, F. N.; Brabazon, D.; Naher, S. Estimation of toxic elements in the samples of different cigarettes and their impact on human health of Irish hypertensive consumers. *Clinica Chimica Acta.* **2013**, *426* (51-57).

(180) Tuzen, M. Determination of heavy metals in fish samples of the middle Black Sea (Turkey) gy graphite furnace atomic absorption spectrometry. *Food Chemistry* **2003**, *80* (1), 119-123.

(181) Uluozlu, O. D.; Tuzen, M.; Mendil, D.; Soylak, M. Trace metal content in nine species of fish from the Black and Aegan Seas, Turkey. *Food Chemistry* **2007**, *104* (2), 835-840.

(182) Wright, R. J.; Stuczynski, T. Atomic Absorption and Flame Emission Spectrometry. In *Methods of Soil Analysis Part 3*, Soil Science Society of America and American Society of Agronomy, 1996; pp 65-90.

(183) Acar, O. Determination of Cadmium, Chromium, Copper and Lead in Sediments and Soil Samples by Electrothermal Atomic Absorption Spectrometry Using Zirconium Containing Chemical Modifiers. *Analytical Sciences* **2006**, *22*, 731-735.

(184) Mahan, K. I.; Foderaro, T. A.; Garza, T. L.; Martinez, R. M.; Maroney, G. A.; Trivisonno, M. R.; Willging, E. M. Micrwoave Digestion Technique in the Sequential and extraction of Calcium, Iron, Chromium, Manganese, Lead and Zinc in Sediments. *Anal. Chem.* **1987**, *59*, 938-945.

(185) Matousek, J. P. Interferences in Electrochemical Atomic Absorption Spectrometry. Their Elimination and Control. *Prog. Anal. At. Spectrosc.* **1981**, *4*.

(186) Krasowski, J. A.; Copeland, T. R. Matrix Interferences in Furnace Atomic Absorption Spectrometry. *Analytical Chemistry* **1979**, *5* (11), 1843-1849.

(187) Huang, S.; Shih, K. Direct determination of zinc in seawater by graphite furnace atomic absorption spectrometry. *Spectrochimica Acta* **1995**, *50B* (8), 837-846.

(188) Davis, A. C.; P., C. J. C.; Jones, B. T. Direct determination of cadmium in urine by tungsten-coil inductively coupled plasma atomic emission spectrometry using palladium as permanent modifier. In *Talanta*, 2007; Vol. 71, pp 1144-1149.

(189) da Silva, J. B. B.; Borges, D. L. G.; Andreia, M.; da Veiga, M. S.; Curtius, A. J.; Welz, B. Determination of cadmium in biological samples solubilized with tetramethylammonium hydroxide by electrothermal atomic absorption spectrometry, using ruthenium as permanent modifier. *Talanta* **2003**, *60*, 977-982.

(190) Magnusson, B.; Ornemark, U. *Eurachem Guide: The Fitness for Purpose of Analytical Methods*; 2014.

(191) Chang, J. R.; Koo, E.; Argon, E.; Hallak, J.; Clemons, T.; Azar, D.; Sperduto, R. D.; Ferris III, F. L.; Chew, E. Y. Risk Factors Associated with Incident Cataracts and Cataract Surgery in the Age-Related Eye Disease Study (AREDS). *Ophthalmology* **2011**, *118* (2113-2119).

(192) Landsteiner, A.; Yendell, S.; Lindgren, P.; Olson, L.; Williams, A. Adult Blood Lead Levels in Minnesota: Rates and Trends, 2005-2012. *Minn Med* **2016**, *99* (2), 47-50.

(193) Cekic, O. Copper, lead, cadmium and calcium in cataractous lenses. *Ophthalmic Res* **1998**, *30* (1), 49-53. DOI: 10.1159/000055454.

(194) Arendsen, L. P.; Thakar, R.; Sultan, A. H. The use of Copper as an Antimicrobial Agent in Health Care, Including Obstetrics and Gynecology. *Clinical Microbiology Reviews* **2019**, *32* (4).

(195) Hussain, S.; Khan, M.; Sheikh, T. M. M.; Mumtaz, M. Z.; Chohan, T. A.; Shamim, S.; Liu, Y. Zinc Essentiality, Toxicity, and Its Bacterial Bioremediation: A Comprehensive Insight. *Front Microbiol* **2022**, *13*, 900740. DOI: 10.3389/fmicb.2022.900740.

(196) Smith, D. *Chicago Rail and Port, LLC*. Inland Rivers, Ports and Terminals, Inc., 2020. https://www.irpt.net/chicago-port-railroad-company/ (accessed 2022 October 7).

(197) Chicago, M. W. R. D. o. G. *Calumet Reclamation Plant*. 2019. https://mwrd.org/sites/default/files/documents/Fact_Sheet_Calumet.pdf (accessed 2022).

(198) Rahman, I. A.; Ismail, J.; Osman, H. Effect of nitric acid digestion on organic materials and silica in rice husk. *J. Mater. Chem.* **1997**, *7* (8), 1505-1509.

(199) Roy, M.; McDonald, L. M. Metal uptake in plants and health risk assessments in metal-contaminated smelter soils. *Land Degradation and Development* **2015**, *26*, 785-792.

(200) Jolly, Y. N.; Islam, A.; Akbar, S. Transfer of metals from soil to vegetables and possible health risk assessment. *SpringerPlus* **2013**, *2*.

(201) Ali, M. H. H.; Al-Qahtani, K. M. Assessment of some heavy metals in vegetables, cereals and fruits in Saudi Arabian markets. *The Egyptian Journal of Aquatic Research* **2012**, *38* (1), 31-37.

(202) Stojic, N.; Pucarevic, M.; Stojic, G. Railway transportation as a source of soil pollution. *Transportation Research Part D* **2017**, *57*, 124-129.

(203) Levengood, J. M.; Heske, E. J.; Wilkins, P. M.; Scott, J. W. Polyaromatic hydrocarbons and elements in sediments associated with a suburban railway. *Environ. Monit. Assess.* **2015**, *187*. DOI: 10.1007/s10661-015-4757-2.

(204) Rachwal, M.; Magiera, T.; Wawer, M. Coke industry and steel metallurgy as the source of soil contamination by technogenic magnetic particles, heavy metals and polycyclic aromatic hydrocarbons. *Chemospher* **2015**, *138*, 863-873.

(205) Hu, J.; Chen, W.; Zhao, Z.; Lu, R.; Cui, M.; Dai, W.; Ma, W.; Feng, X.; Wan, X.; Wang, N. Source tracing of potentially toxic elements in soils around a typical coking plant in an industrial area in northern China. *Science of the Total Environment* **2022**, *807*.

(206) Bastian, R. K. The biosolids treatment, beneficial use, and disposal in the USA. *Eur. Water Pollut. Control* **1997**, *7* (2), 62-79.

(207) Walter, I.; Martinez, F.; Cala, V. Heavy metal speciation and phytotoxic effects of three representative sewage sludges for agricultural uses. *Environmental Pollution* **2006**, *139*, 507-514.

(208) Gardiner, D. T.; Miller, R. W.; Badamchian, B.; Azzari, A. s.; Sisson, D. R. Effects of repeated sewage sludge application on plant accumulation of heavy metals. *Agriculture, Ecosystem and Environment* **1995**, *55*, 1-6.

(209) Agency, U. S. E. P. *Lake Calumet Cluster Chicago, IL*. https://cumulis.epa.gov/supercpad/SiteProfiles/index.cfm?fuseaction=second.Cleanup&id=0500078#bkground (accessed 2022 September 20).

(210) Bhatti, H. N.; Nasir, A. W.; Hanif, M. A. Efficacy of *Daucus carota* L. waste biomass for the removal of chromium from aqueous solutions. *Desalination* **2010**, *253* (1-3), 78-87.

(211) Lilli, M. A.; Syranidou, E.; Palliou, A.; Nikolaidis, N. P.; Karatzas, G.; Kalogerakis, N. Assessing the impact of geogenic chromium uptake by carrots (*Daucus carota)* grown in Asopos river basin. *Environmental Research* **2017**, *152*, 96-101.

(212) Abedin, Z. 2007 Annual Summary Report Water Quality within the Waterways system of the Metropolitan Water Reclamation District of Greater Chicago. Department, R. a. D., Ed.; Metropolitan Water Reclamation District of Greater Chicago: 2008.

(213) Services, U. S. D. o. H. a. H. Analysis of Outdoor Air Contaminants. Registry, A. f. T. S. a. D., Ed.; Agency for Toxic Substances and Disease Registry: Atlanta, Georgia, 2022.

(214) Vaiskunaite, R.; Jasiuniene, V. The analysis of heavy metal pollutants emitted by railway transport. *Transport* **2020**, *35* (2), 213-223.

VITA

Dr. Michelle Gende started her academic career at Winona State University and majored in Chemistry and minored in Biochemistry. She continued her academic career by obtaining a master's degree in Bioanalytical Chemistry from North Dakota State University. While at North Dakota State University she worked under Dr. Guodong Liu in research pertaining to nanoparticle-powered chemiluminescent lateral flow biosensors for early diagnosis of pancreatic cancer. She started her doctoral candidacy at Loyola University Chicago in the Fall of 2017.